The Canadian Mineralogist
Vol. 43, pp. 1839-1894 (2005)

U^{6+} MINERALS AND INORGANIC COMPOUNDS: INSIGHTS INTO AN EXPANDED STRUCTURAL HIERARCHY OF CRYSTAL STRUCTURES

PETER C. BURNS[§]

Department of Civil Engineering and Geological Sciences, 156 Fitzpatrick Hall, University of Notre Dame, Notre Dame, Indiana 46556, U.S.A., and Chemistry Division, Argonne National Laboratory, 9700 South Cass, Argonne, Illinois 60439, U.S.A.

ABSTRACT

The crystal structures of uranyl minerals and inorganic uranyl compounds are important for understanding the genesis of U deposits, the interaction of U mine and mill tailings with the environment, transport of actinides in soils and the vadose zone, the performance of geological repositories for nuclear waste, and for the development of advanced materials with novel applications. Over the past decade, the number of inorganic uranyl compounds (including minerals) with known structures has more than doubled, and reconsideration of the structural hierarchy of uranyl compounds is warranted. Here, 368 inorganic crystal structures that contain essential U^{6+} are considered (of which 89 are minerals). They are arranged on the basis of the topological details of their structural units, which are formed by the polymerization of polyhedra containing higher-valence cations. Overarching structural categories correspond to those based upon isolated polyhedra (8), finite clusters (43), chains (57), sheets (204), and frameworks (56) of polyhedra. Within these categories, structures are organized and compared upon the basis of either their graphical representations, or in the case of sheets involving sharing of edges of polyhedra, upon the topological arrangement of anions within the sheets.

Keywords: uranium, actinide, crystal structure, structural hierarchy, nuclear waste.

SOMMAIRE

Les structures cristallines des minéraux et des composés inorganiques uranylés revêtent une grande importance pour bien comprendre la genèse des gisements d'uranium, l'interaction de haldes et des déchêts de mines avec l'environnement, le transfert des actinides dans les sols et la zone vadose, et l'efficacité des sites d'enfouissement des déchêts nucléaires, et pour développer de matériaux nouveaux ayant des applications de haute technologie. Au cours de la dernière décennie, le nombre de composés inorganiques contenant le groupe uranyle (y inclus les minéraux) dont la structure est connue a plus que doublé, et une reconsidération de la hiérarchie structurale des composés uranylés est appropriée. Ici, 368 structures de cristaux inorganiques contenant le U^{6+} comme composant essentiel (dont 89 sont des minéraux) sont passées en revue. Elles sont regroupées sur la base de détails topologiques de leurs unités structurales, formées par la polymérisation de polyèdres contenant des cations de valence élevée. Les catégories structurales générales correspondent à celles fondées sur les polyèdres isolés (8), regroupements finis (43), chaînes (57), feuillets (204), et trames (56) de polyèdres. A l'intérieur de ces catégories, les structures sont organisées et comparées en fonction de soit leurs représentations graphiques, ou bien dans le cas de feuillets impliquant le partage d'arêtes de polyèdres, en fonction de l'agencement topologique des anions dans ces feuillets.

(Traduit par la Rédaction)

Mots-clés: uranium, actinide, structure cristalline, hiérarchie structurale, déchêts nucléaires.

§ *E-mail address*: pburns@ndu.edu

Introduction

Crystals containing U^{6+} have been the focus of extensive research over several decades. The first crystal structures of inorganic U^{6+} (uranyl) compounds appeared in the literature several decades ago (*e.g.*, Evans 1963), and by 1996, about 180 structures were known (Burns *et al.* 1996). The introduction of CCD-based detectors of X-rays to mineralogy (Burns 1998a) greatly extended the reach of single-crystal X-ray diffraction into the study of complex U^{6+} compounds. Today, at least 368 structures of inorganic uranyl compounds are known, of which 89 correspond to minerals. These materials exhibit fascinating and complex atomic arrangements, owing to the myriad of possible types of connections between uranyl polyhedra and other uranyl polyhedra, as well as polyhedra containing other higher-valence cations. Current research concerning uranyl compounds is driven by the search for novel solids with important materials properties (*e.g.*, Locock & Burns 2002a, Krivovichev *et al.* 2002a, Krivovichev & Burns 2002a, Almond *et al.* 2002a, Burns *et al.* 2005, Krivovichev *et al.* 2005a,b), and their importance in the environment (*e.g.*, Li & Burns 2001a, Burns *et al.* 2000, 2004a, Hughes Kubatko *et al.* 2003). Knowledge of the structures of uranyl minerals is important for understanding the genesis of U deposits (Frondel 1958), and uranyl minerals exhibit substantial structural and chemical diversity, reflecting geochemical conditions dominant during their formation.

Uranyl minerals and compounds are of considerable environmental importance. They are significant for understanding water–rock interactions in U-rich rocks (Frondel 1958). Uranyl minerals exert an impact on the mobility of actinides in contaminated soils (*e.g.*, Buck *et al.* 1996, Roh *et al.* 2000) and in vadose-zone sediments polluted with actinides, such as the Hanford and Savanna River sites in the U.S.A. (*e.g.*, Yamakawa & Traina 2001). Precipitation of uranyl phosphate minerals in the vadose zone of contaminated sites by the addition of phosphate has been proposed as a means to mitigate U^{6+} plumes in groundwater (Fuller *et al.* 2002). Uranyl minerals can be bio-precipitated (Macaskie *et al.* 2000), and potentially provide sources of phosphate for biological consumption, as well as redox-active U to serve as an electron acceptor needed for metabolism of bacteria. Uranyl minerals are important products of alteration of nuclear waste forms under simulated conditions of geological repositories, such as those expected in the proposed repository at Yucca Mountain, Nevada (*e.g.*, Finch *et al.* 1999a, Finn *et al.* 1996, Wronkiewicz *et al.* 1996).

About 200 uranyl minerals have been described from nature. They usually occur in the oxidized zones of U deposits, where it is common for several uranyl mineral species to coexist, commonly in intimate intergrowths. In many cases, uranyl minerals are secondary and result from the alteration of UO_{2+x}, but they are primary minerals in some occurrences. Owing to their structural and chemical complexities, and the experimental difficulties associated with their characterization, understanding of uranyl minerals as a whole lags behind the current level of understanding of most major mineral groups. The structures are fully characterized for less than 50% of described uranyl minerals, and many aspects of their chemical composition, stability and occurrence still require study.

Burns *et al.* (1996) presented a structural hierarchy of 180 inorganic synthetic and natural uranyl phases. Burns (1999a) expanded the hierarchy in the case of minerals only. It is based upon the polymerization of those polyhedra that contain higher-valence cations. Low-valence cations, including H atoms and H bonds, were ignored for the purpose of erecting the hierarchy.

Here I provide a revised and greatly expanded hierarchy of 368 structures of inorganic uranyl compounds (including 89 minerals). The volume of known structures mandates a concise description of structures. Illustrations of all of the structural units are provided, and formulae and crystallographic parameters are given in the tables for each of the 368 structures. I hope that the reader will gain an appreciation of the complex beauty of this chemical class of compounds, and that the structural hierarchy will provide a basis for further studies in actinide crystal chemistry.

I am delighted that this contribution appears in the 50th Anniversary edition of *The Canadian Mineralogist*, not only because it is one of the premier mineralogical journals in the world, but also because of the tremendous impact that the Mineralogical Association of Canada has had on my continuing education and career.

Coordination Polyhedra

Almost all U^{6+} in crystal structures is present as an approximately linear UO_2^{2+} uranyl ion. The formal valence of the uranyl ion is 2+, so it must be coordinated by anions in a stable crystal structure. The uranyl ion is typically coordinated by four, five or six ligands, arranged at the equatorial vertices of square, pentagonal and hexagonal bipyramids, respectively (Fig. 1). The bipyramids are capped by the O atoms of the uranyl ions.

Burns *et al.* (1997a) provided U^{6+}–O bond-length and uranyl ion bond-angle data for ~100 crystal structures. Only well-refined structures analyzed by single-crystal X-ray diffraction, with final *R* indices less than 7%, were included. The bond and angle distributions for uranyl polyhedra have been revised to incorporate data for structures reported since 1997, using the same criteria adopted by Burns *et al.* (1997a). A total of 222 structures have been included. The U^{6+}–ϕ (ϕ: O, OH, H_2O) bond-length distributions for $^{[6]}U^{6+}$, $^{[7]}U^{6+}$ and $^{[8]}U^{6+}$ are provided in Figure 2.

Consider first the case of $^{[7]}U^{6+}$ (U^{6+} coordinated by seven atoms, including the uranyl ion); the distribution of U^{6+}–O bond lengths in 270 polyhedra containing $^{[7]}U^{6+}$ in 143 structures is presented in Figure 2b. The distribution is bimodal, as each polyhedron contains a uranyl ion. The average U^{6+}–O_{Ur} (*Ur*: uranyl) bond-length is 1.793 Å, with a standard deviation of 0.035 Å, whereas for the U^{6+}–O_{eq} bonds, the average is 2.368 Å with a standard deviation of 0.100 Å. The distributions of both the U^{6+}–O_{Ur} and U^{6+}–O_{eq} bonds are rather regular.

The bond-length distribution for $^{[8]}U^{6+}$ is shown in Figure 2a. Although the sample size is smaller than that of $^{[7]}U^{6+}$, it is still apparent that all $^{[8]}U^{6+}$ polyhedra in well-refined structures contain a uranyl ion, and the average U^{6+}–O_{Ur} bond length for 35 polyhedra in 32 structures is 1.783 Å, with a standard deviation of 0.030 Å. The distribution for the U^{6+}–O_{eq} bonds is rather irregular, with an average of 2.460 Å and a standard deviation of 0.107 Å. There are few $^{[8]}$U–O_{eq} bonds less than ~2.4 Å, causing the asymmetric distribution of bond lengths apparent in Figure 2a. This feature presumably is related to the geometrical limitations of packing six coplanar O atoms around a single uranyl ion.

The bond-length distribution for $^{[6]}U^{6+}$ is shown in Figure 2c. As discussed in detail by Burns *et al*. (1997a), not every $^{[6]}U^{6+}$ polyhedron in well-refined structures has an associated uranyl ion. Several reported structures contain $^{[6]}U^{6+}$ in octahedral or distorted octahedral coordination, thus there are three modes in the bond-length distribution for $^{[6]}U^{6+}$ that correspond to U^{6+}–O_{Ur} and U^{6+}–O_{eq} bond lengths of uranyl square bipyramids, and the more regular bond-lengths of octahedral coordination (centered at ~2.1 Å). Considering only the 54 uranyl square bipyramids in 47 well-refined structures, the average U^{6+}–O_{Ur} bond-length is 1.816 Å, with a corresponding standard deviation of 0.050 Å, and the U^{6+}–O_{eq} bond-length is 2.264 Å, standard deviation 0.064 Å.

Using the bond-valence parameters provided by Burns *et al*. (1997a), the typical bond-valences of the U^{6+}–O_{Ur} and U^{6+}–O_{eq} bonds of each coordination polyhedron are: $^{[6]}U^{6+}$–O_{Ur} = 1.59 valence units (*vu*), $^{[6]}U^{6+}$–O_{eq} = 0.71 *vu,* $^{[7]}U^{6+}$–O_{Ur} = 1.64 *vu*, $^{[7]}U^{6+}$–O_{eq} = 0.53 *vu,* $^{[8]}U^{6+}$–O_{Ur} = 1.67 *vu*, $^{[8]}U^{6+}$–O_{eq} = 0.44 *vu* (Fig. 3). These values are consistent with extensive linkage of uranyl polyhedra through equatorial ligands, either with other uranyl polyhedra or other polyhedra containing higher-valence cations. The bond-valences incident upon the O_{Ur} atoms, due to the bond to U^{6+} alone, range from 1.59 to 1.67 *vu*. Thus, the apical (uranyl) vertices of the uranyl bipyramids are seldom shared with polyhedra containing higher-valence cations, as this would overbond the O position. The two-dimensional polymerization of uranyl polyhedra mandated by the distribution of bond strengths within the polyhedra favors the formation of sheets of polyhedra.

In some cases, the solid state and solution chemistry of actinyl ions involves significant cation–cation interactions in which an O atom of an actinyl ion is also an equatorial ligand of a neighboring polyhedron (Krot & Grigoriev 2004). The cation–cation designation arises from the formal valences of the actinyl ions, both of which are cations. Such interactions are relatively common for Np^{5+}, but are rather unusual in the case of U^{6+} (Sullens *et al*. 2004), presumably owing to the fact that the bonding requirements of the O atoms of the uranyl ions are nearly met by the bonds within the uranyl ion alone. To date, there are five inorganic uranyl compounds that exhibit cation–cation interactions (1.4% of known structures), and each of these structures is composed of a framework of polyhedra.

Structural Hierarchy of Uranyl Phases

Structural hierarchies are a means to organize a wealth of complex and strikingly different structures into a cohesive framework. They provide considerable insight into the crystal chemistry of the focus compounds, as the hierarchical arrangement is usually based upon structural connectivity. Structural hierarchies permit recognition of structural trends within large groups of compounds that are generally obscured by the complexity of the class of compounds. They can be the basis for understanding the linkages between mineral occurrences and underlying mineral structures, especially in low-temperature geochemical environments that present complex assemblages of hydrous minerals. However, consideration of minerals alone in the development of a structural hierarchy is akin to viewing a ballet with tunnel vision, as minerals represent only the subset of a chemical class that is stable over geological times under geochemical conditions. As such, the structural hierarchy presented herein includes all inorganic compounds that contain U^{6+} as a necessary structural constituent.

Following the approach of Burns *et al*. (1996) and Burns (1999a), structures of uranyl compounds are arranged here on the basis of their structural units consisting of those cation-centered polyhedra of higher bond-valence. Structures naturally fall into five categories corresponding to isolated polyhedra, finite clusters of polyhedra, chains of polyhedra, sheets of polyhedra, and frameworks of polyhedra. In each case the structural unit is illustrated, and pertinent crystallographic information is provided in the Tables.

In most cases, assignment of a structure to one of the five classes is straightforward. In a few structures, sheets of polyhedra are linked together by sharing anions, forming a framework, or the sheets are linked through uranyl ions located in interlayer positions, which also results in a framework. Such structures usually contain sheets that are similar or identical to the sheets that occur isolated in other structures; as such,

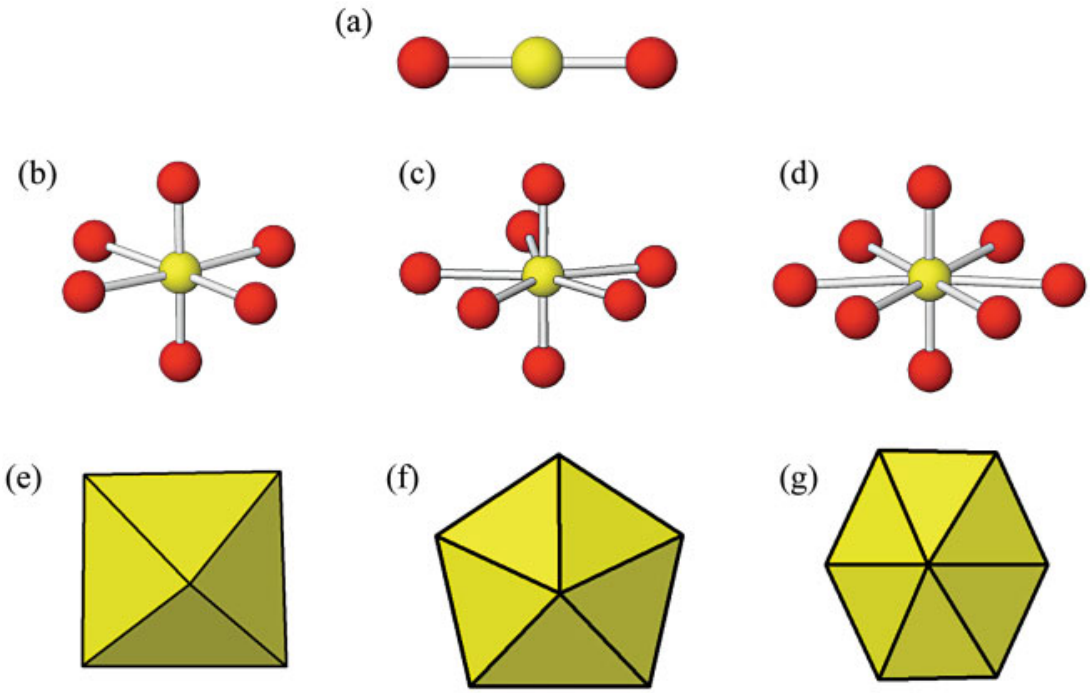

FIG. 1. Uranyl coordination polyhedra in uranyl compounds. Shown are (a) the $(UO_2)^{2+}$ uranyl ion, (b) uranyl square bipyramid, (c) uranyl pentagonal bipyramid, (d) uranyl hexagonal bipyramid, (e) uranyl square bipyramid, (f) uranyl pentagonal bipyramid, (g) uranyl hexagonal bipyramid.

they typically will be grouped with those structures despite their three-dimensional connectivity.

In many cases, the chemical formulae used in the text and tables have been re-arranged from those given by the original authors to emphasize structural features and to facilitate comparisons. In Tables that list clusters and chains, structures based upon similar structural units are grouped, and double lines are used to separate those that have different graphical representations. In Table 4 (see below), structures based upon sheets with identical graphical representations are grouped, and those involving different graphs are separated by double lines. In Tables 5 through 8 (see below), all of which list structures that contain sheets of polyhedra, double lines separate structures with different anion-topologies, and dotted lines separate structures with distinct sheets, but the same underlying anion-topology.

STRUCTURES CONTAINING ISOLATED POLYHEDRA

Eight structures contain isolated U^{6+} polyhedra (Table 1). In these structures, there are no direct linkages between the U^{6+} polyhedra; linkages all take place through low-valence cations. In the structures of $Ca_3[UO_6]$, $Sr_3[UO_6]$, $K_2Li_4[UO_6]$ and $Li_6[UO_6]$, the U^{6+} cation is octahedrally coordinated, with no uranyl ion present. The structure of $Cs_2[(UO_2)Cl_4]$ contains *Ur*Cl_4 square bipyramids, with Cl atoms at the equatorial positions. The structure of $[(UO_2)Cl_2(H_2O)_3]$ has a *Ur*$(H_2O,Cl)_5$ polyhedron, with two equatorial Cl atoms. The structures of $[(UO_2)(H_2O)_5](ClO_4)_2$ and $[(UO_2)(H_2O)_5](ClO_4)_2 \bullet 2H_2O$ each contain isolated *Ur*$(H_2O)_5$ pentagonal bipyramids, as well as isolated perchlorate tetrahedra.

STRUCTURES CONTAINING FINITE CLUSTERS OF POLYHEDRA

There are 43 compounds based upon finite clusters of polyhedra of higher bond-valence, which represents a significant growth from the 22 structures in this class reviewed by Burns *et al.* (1996). Of the 21 new structures reported since 1996, only two correspond to minerals, and only seven of the total in this class are minerals. The structures are arranged in Table 2 on the basis of their graphs; those with identical graphs are grouped together, regardless of the chemical identities of the constituents of the clusters.

Graphical representations of crystal structures are a powerful approach to reducing structural complexity for the establishment of underlying relationships amongst groups of structures. In the case of uranyl compounds,

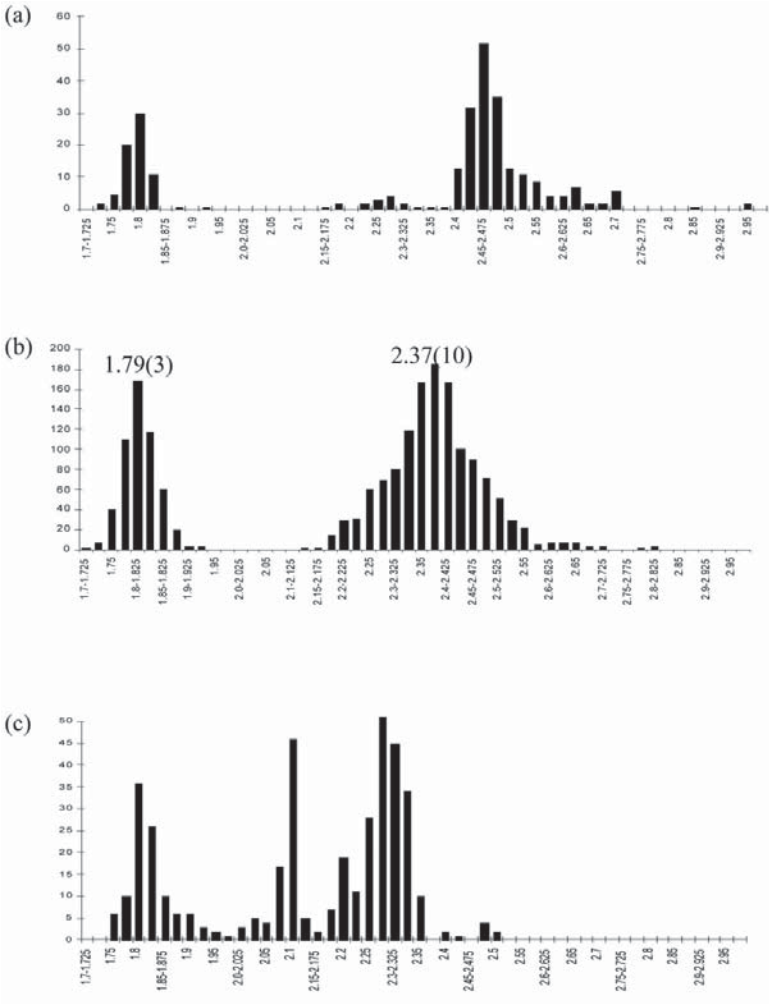

FIG. 2. Bond-length distributions in uranium-bearing polyhedra in well-refined structures. (a) Uranyl hexagonal bipyramids, (b) uranyl pentagonal bipyramids, (c) uranyl square bipyramids and other six-coordinated U^{6+} polyhedra.

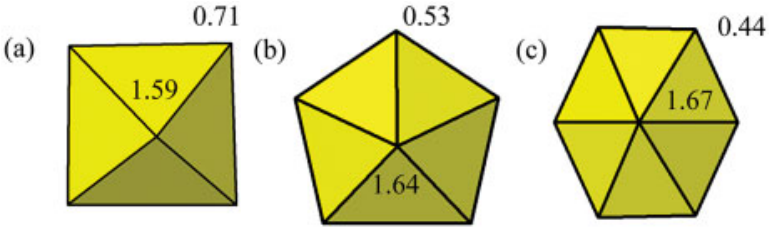

FIG. 3. Uranyl polyhedra and the corresponding average bond-valence (in valence units, *vu*) incident upon each vertex owing to the U^{6+}–O bond within the polyhedron.

TABLE 1. STRUCTURES CONTAINING ISOLATED POLYHEDRA

Name	Formula	S. G.	*a* (Å)	*b* (Å)	*c* (Å)	β (°)	Ref.
	$Ca_3[UO_6]$	$P2_1/n$	5.7292	5.962	8.2991	90.56	1
	$Sr_3[UO_6]$	$P2_1/n$	6.0126	6.2138	8.6139	90.239	2
	$K_2Li_4[UO_6]$	$P\bar{3}m$	6.1927		5.3376		3
	$Li_6[UO_6]$	$R\bar{3}$	8.3807		7.3834		4
	$Cs_2[(UO_2)Cl_4]$	Cm	12.005	7.697	5.850	100.00	5
	$[(UO_2)Cl_2(H_2O)_3]$	$Pnma$	12.738	10.495	5.547		6
	$[(UO_2)(H_2O)_5](ClO_4)_2$	$P2_1/n$	5.2935	16.4543	14.8018	99.847	7
	$[(UO_2)(H_2O)_5](ClO_4)_2 \cdot 2H_2O$	$Pbcn$	9.209	10.679	14.457		7

References: (1) van Duivenboden & Ijdo (1986), (2) Ijdo (1993a), (3) Wolf & Hoppe (1987), (4) Wolf & Hoppe (1985), (5) Tutov *et al.* (1991), (6) Debets (1968), (7) Fischer (2003).

this approach works best where most of the connections between polyhedra containing higher-valence cations occur through the sharing of vertices. The graph is obtained from the structure by representing each distinct type of polyhedron with a colored circle, and the number of vertices shared between adjacent polyhedra are shown by connectors between the colored circles. Throughout this paper, black circles are used to represent uranyl polyhedra, and white circles represent tetrahedra or triangles containing higher-valence cations. Consider for example the clusters shown in Figures 4c and 4i. The graph corresponding to the cluster in Figure 4c has two black circles and eight white circles, which corresponds to the number of uranyl polyhedra and tetrahedra in the corresponding cluster. It is also immediately apparent that there are two types of white circles, those that are connected to two black circles, and those that are linked to only one black circle. These white circles correspond to the two- and one-connected tetrahedra of the cluster, respectively. The graph also indicates that all linkages between the polyhedra in the cluster arise by the sharing of single vertices only (the linkages are indicated by single connectors in the graph). In contrast, the graph corresponding to the cluster shown in Figure 4i has three types of white circles, those that are connected to a single black circle by a single connector, those that are connected to two black circles by single connectors, and those that are connected to a single black circle by two connectors. The presence of two connectors in the cases of two of the white circles indicates that an edge is shared between the uranyl polyhedron and the corresponding tetrahedron.

Uranyl carbonate minerals that crystallize from alkaline solutions contain the uranyl tricarbonate cluster, $[(UO_2)(CO_3)_3]^{4-}$ (Fig. 4a). A uranyl hexagonal bipyramid shares three edges with carbonate triangles, and all equatorial anions of the bipyramids constitute ligands of the carbonate groups. This cluster is known from seven mineral structures as well as 10 synthetic compounds (Table 2). In each case, independent uranyl tricarbonate clusters are linked only through bonds to low-valence cations, including H. A topologically identical cluster containing nitrate triangles instead of carbonate is found in the structures of $Rb[(UO_2)(NO_3)_3]$ and $K[(UO_2)(NO_3)_3]$.

A uranyl square bipyramid shares each equatorial vertex with a different tetrahedron in the cluster with composition $[(UO_2)(XO_4)_4]$ shown in Figure 4b. This cluster was recently found in three compounds (Table 2), with the *X* cation being Mo^{6+} in two structures and Cr^{6+} in the third case. A more complex uranyl molybdate cluster composed of two uranyl pentagonal bipyramids and eight MoO_4 tetrahedra is known from $Na_6[(UO_2)(MoO_4)_4]$ and $Na_3Tl_3[(UO_2)(MoO_4)_4]$ (Fig. 4c, Table 2). Each equatorial ligand of each uranyl pentagonal bipyramid is shared with a tetrahedron, and two tetrahedra provide a bridge between the uranyl pentagonal bipyramids.

Remarkable clusters of uranyl pentagonal bipyramids and sulfate tetrahedra occur in $Na_6[(UO_2)(SO_4)_4](H_2O)_2$, $Na_{10}[(UO_2)(SO_4)_4](SO_4)_2(H_2O)_3$, and $KNa_5[(UO_2)(SO_4)_4](H_2O)$ (Fig. 4d). One sulfate tetrahedron shares an edge with the bipyramid, a connectivity that had not been previously observed in a hydrous uranyl sulfate. Three additional sulfate tetrahedra are linked to the other three equatorial vertices of the bipyramid. The sharing of edges between polyhedra containing U^{6+} and S^{6+} cations presumably entails significant cation–cation repulsion. However, crystals of these compounds several millimeters in maximum dimension were grown at 70°C in uranyl sulfate solutions, which implies cluster stability, even in solutions (*e.g.*, Burns & Hayden 2002).

Six uranyl nitrates contain isolated clusters with uranyl polyhedra and nitrate triangles. The cluster in Figure 4e has a uranyl hexagonal bipyramid that shares two of its *trans* equatorial edges with nitrate triangles, and the remaining two vertices of the bipyramid are shared with two different nitrate triangles. This cluster is the basis of the structure of $Rb_2[(UO_2)(NO_3)_4]$,

TABLE 2. STRUCTURES BASED UPON FINITE CLUSTERS

Name	Fig.	Formula	S. G.	*a* (Å)	*b* (Å)	*c* (Å)	β (°)	Ref.
Liebigite	4a	$Ca_2[(UO_2)(CO_3)_3](H_2O)_{11}$	*Bba*2	16.699	17.557	13.697		1
Schröckingerite	4a	$NaCa_3[(UO)_2(CO_3)_3](SO_4)F(H_2O)_{10}$	$P\bar{1}$	9.634	9.635	14.391	92.33	2
Bayleyite	4a	$Mg_2[(UO_2)(CO_3)_3](H_2O)_{18}$	$P2_1/a$	26.560	15.256	6.505	92.90	3
Swartzite	4a	$CaMg[(UO_2)(CO_3)_3](H_2O)_{12}$	$P2_1/m$	11.080	14.634	6.439	99.43	4
Andersonite	4a	$Na_2Ca[(UO_2)(CO_3)_3](H_2O)_5$	$R\bar{3}m$	17.904		23.753		5
Grimselite	4a	$K_3Na[(UO_2)(CO_3)_3](H_2O)$	$P\bar{6}2c$	9.302		8.260		6
Čejkaite	4a	$Na_4[(UO_2)(CO_3)_3]$	$P\bar{1}$	9.291	9.292	12.895	90.82	7
	4a	$Rb_6Na_2[(UO_2)(CO_3)_3]_2(H_2O)$	$P\bar{6}2c$	9.4316		8.3595		8
	4a	$Cs_4[(UO_2)(CO_3)_3](H_2O)_6$	$P2_1/n$	18.723	9.647	11.297	96.84	9
	4a	$Sr_2[(UO_2)(CO_3)_3](H_2O)_8$	$P2_1/c$	11.379	11.446	25.653	93.40	10
	4a	$(NH_4)_4[(UO_2)(CO_3)_3]$	$C2/c$	10.679	9.373	12.850	96.43	11
	4a	$Rb[(UO_2)(NO_3)_3]$	$R\bar{3}c$	9.384		18.899		12
	4a	$Na_4[(UO_2)(CO_3)_3]$	$P\bar{3}c1$	9.342		12.824		13
	4a	$Ca_5[(UO_2)(CO_3)_3]_2(NO_3)_2(H_2O)_{10}$	$P2_1/n$	6.5729	16.517	15.195	90.494	14
	4a	$Ca_6[(UO_2)(CO_3)_3]_2Cl_4(H_2O)_{19}$	*P*4/*mbm*	16.744		8.136		14
	4a	$Ca_{12}[(UO_2)(CO_3)_3]_4Cl_8(H_2O)_{47}$	$Fd\bar{3}$	27.489				14
	4a	$Cs_4[(UO_2)(CO_3)_3]$	$C2/c$	11.513	9.6037	12.9177	93.767	15
	4a	$K[(UO_2)(NO_3)_3]$	$C2/c$	13.487	9.5843	7.9564	116.124	16
	4a	$K_2Ca_3[(UO_2)(CO_3)_3]_2(H_2O)_6$	*Pnnm*	17.015	18.048	18.394		17
	4b	$Cs_6[(UO_2)(MoO_4)_4]$	$P\bar{1}$	11.613	12.545	14.466	95.281	18
	4b	$Rb_6[(UO_2)(MoO_4)_4]$	$C2/c$	17.312	11.5285	13.916	127.634	19
	4b	$K_8[(UO_2)(CrO_4)_4](NO_3)_2$	$P\bar{1}$	7.0397	9.7341	9.7568	97.992	20
	4c	$Na_6[(UO_2)(MoO_4)_4]$	$P\bar{1}$	7.096	9.566	13.415	86.62	21
	4c	$Na_3Tl_3[(UO_2)(MoO_4)_4]$	*Pbcn*	20.582	7.4391	26.2514		22
	4d	$Na_6[(UO_2)(SO_4)_4](H_2O)_2$	$P\bar{1}$	5.5503	11.2456	14.256	92.583	23
	4d	$Na_{10}[(UO_2)(SO_4)_4](SO_4)_2(H_2O)_3$	*Cc*	9.3072	28.706	9.6152	93.401	24
	4d	$KNa_5[(UO_2)(SO_4)_4](H_2O)$	$C2/c$	16.917	5.5999	35.340	90.437	25
	4e	$Rb_2[(UO_2)(NO_3)_4]$	$P2_1/c$	6.42	7.82	12.79	108.68	26
	4f	$[(UO_2)(NO_3)_2](H_2O)_6$	$Cmc2_1$	13.197	8.035	11.467		27
	4f	$[(UO_2)(NO_3)_2](H_2O)_2$	$P2_1/c$	14.124	8.432	7.028	108.0	28
	4f	$[(UO_2)(NO_3)_2](H_2O)_3$	$P\bar{1}$	7.0359	7.1730	10.084	82.041	29
	4g	$[(UO_2)(NO_3)_2(H_2O)_2](H_2O)$	$P2_1/c$	7.1797	8.954	14.301	99.104	30
	4h	$[(UO_2)_2(OH)_2(NO_3)_2](H_2O)_4$	$P\bar{1}$	8.622	8.628	10.393	105.56	31
	4i	$K_4[(UO_2)(SO_4)_3]$	*Pnma*	13.053	23.200	9.379		32
	4j	$[(UO_2)_4Cl_2O_2(OH)_2(H_2O)_6](H_2O)_4$	$P2_1/n$	11.645	10.101	10.206	105.77	33
	4j	$Rb_4[(UO_2)_4O_2Cl_8(H_2O)_2](H_2O)_2$	$P2_1/c$	8.540	8.096	21.735	111.74	34
	4j	$K_2[(UO_2)_4Cl_4O_2(OH)_2(H_2O)_4](H_2O)_2$	$P\bar{1}$	12.15	12.33	8.026	96.30	35
	4j	$Cs_{0.9}[(UO_2)OCl_{0.9}]$	$P2_1/m$	8.734	4.118	7.718	105.26	36
	4k	$[(UO_2)_3O(OH)_3(H_2O)_6](NO_3)(H_2O)_4$	$P\bar{1}$	8.026	11.276	12.346	99.39	37
	4l	$K_8[(UO_2)_2O_6]$	$P\bar{1}$	6.4738	9.6979	6.3438	102.30	38
	4m	$[(UO_2)(OH)Cl(H_2O)_2]$	$P2_1/n$	17.743	6.136	10.725	95.52	39
	4n	$K_6[(UO_2)B_{16}O_{24}(OH)_8](H_2O)_{12}$	$P2_1/n$	12.024	26.45	12.543	94.74	40
	4o	$[(UO_2)(ClO_4)_2(H_2O)_3]$	$P2_1/c$	5.4544	18.1109	10.3246	90.016	41

References: (1) Mereiter (1982a), (2) Mereiter (1986a), (3) Mayer & Mereiter (1986), (4) Mereiter (1986b), (5) Mereiter (1986c), (6) Li & Burns (2001b), (7) Ondruš *et al.* (2003), (8) Hughes Kubatko & Burns (2003), (9) Mereiter (1988), (10) Mereiter (1986d), (11) Serezhkin *et al.* (1983), (12) Zalkin *et al.* (1989), (13) Li *et al.* (2001a), (14) Li & Burns (2002), (15) Krivovichev & Burns (2004a), (16) Krivovichev & Burns (2004b), (17) Hughes Kubatko & Burns (2004), (18) Krivovichev & Burns (2002b), (19) Krivovichev & Burns (2002a), (20) Krivovichev & Burns (2003c), (21) Krivovichev & Burns (2001a), (22) Krivovichev & Burns (2003b), (23) Hayden & Burns (2002a), (24) Burns & Hayden (2002), (25) Hayden & Burns (2002b), (26) Kapshukov *et al.* (1971), (27) Taylor & Mueller (1965), (28) Mueller *et al.* (1971), (29) Hughes & Burns (2003b), (30) Shuvalov & Burns (2003), (31) Perrin (1976), (32) Mikhailov *et al.* (1977), (33) Åberg (1976), (34) Perrin (1977), (35) Perrin & Le Marouille (1977), (36) Allpress & Wadsley (1964), (37) Åberg (1978), (38) Wolf & Hoppe (1986), (39) Åberg (1969), (40) Behm (1985), (41) Fischer (2003).

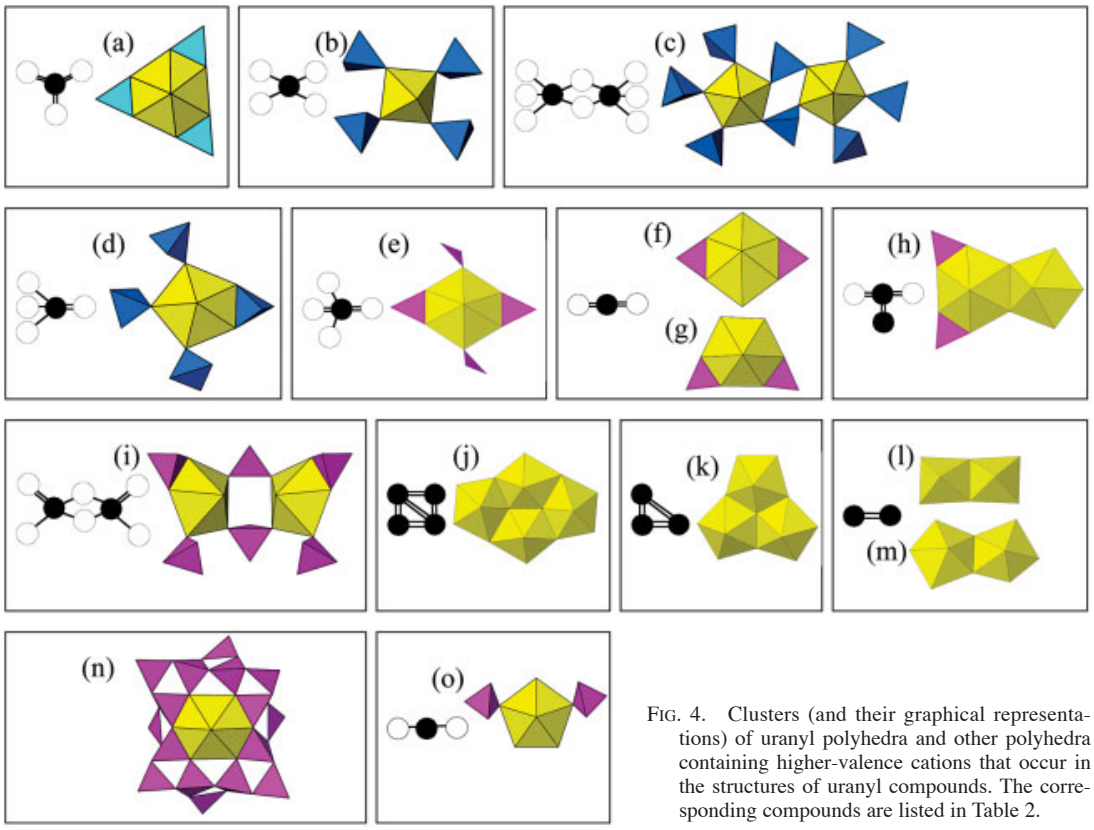

FIG. 4. Clusters (and their graphical representations) of uranyl polyhedra and other polyhedra containing higher-valence cations that occur in the structures of uranyl compounds. The corresponding compounds are listed in Table 2.

which is the only structure known in which nitrate triangles are linked to uranyl polyhedra by sharing only a single vertex; in all other cases, edges are shared between uranyl and nitrate polyhedra. Two clusters that are graphical isomers contain a single uranyl hexagonal bipyramid that shares two equatorial edges with nitrate triangles (Figs. 4f, g). The former is found in the structure of $[(UO_2)(NO_3)_2](H_2O)_6$, $[(UO_2)(NO_3)_2](H_2O)_2$ and $[(UO_2)(NO_3)_2](H_2O)_3$, the latter is found in $[(UO_2)(NO_3)_2(H_2O)_2](H_2O)$. In a more complex cluster found in $[(UO_2)_2(OH)_2(NO_3)_2](H_2O)_4$, a uranyl hexagonal bipyramid shares an equatorial edge with a uranyl pentagonal bipyramid, as well as two equatorial edges with nitrate triangles (Fig. 4h). In all but $Rb_2[(UO_2)(NO_3)_4]$, the uranyl nitrate clusters are linked only though H bonds.

The structure of the anhydrous compound $K_4[(UO_2)(SO_4)_3]$ possesses a remarkable cluster (Fig. 4i), in which two uranyl pentagonal bipyramids are bridged by sharing vertices with two sulfate tetrahedra, and each bipyramid also shares an additional vertex with another sulfate tetrahedron, and an edge with a fourth sulfate tetrahedron. This is the only example of an anhydrous phase in which a sulfate tetrahedron shares an edge with a uranyl bipyramid. This phase was grown at elevated temperature, and its stability under ambient conditions is uncertain.

Four clusters contain only uranyl bipyramids that share equatorial edges (Figs. 4j, k, l, m). Two are simple dimers of either square bipyramids or pentagonal bipyramids (Figs. 4l, m). One is a trimer of uranyl pentagonal bipyramids (Fig. 4k), and one contains four uranyl pentagonal bipyramids that share edges (Fig. 4j). The latter two clusters each contain oxygen atoms that are common to three uranyl polyhedra.

The uranyl borate cluster shown in Figure 4n was synthesized by aging a boron-rich solution at room temperature (Behm 1985). The cluster contains 16 borate triangles and tetrahedra that surround a uranyl hexagonal bipyramid; four of the borate polyhedra share edges with the uranyl bipyramid, and four additional borate polyhedra share a single vertex with the bipyramid.

The cluster shown in Figure 4o contains a uranyl pentagonal bipyramid that shares two vertices with perchlorate tetrahedra. The remaining equatorial vertices of the bipyramid are H_2O groups, and the clusters are linked through H bonding only.

Structures Containing Infinite Chains of Polyhedra

Burns *et al*. (1996) listed 19 uranyl compounds with structures based upon infinite chains of polyhedra of higher bond-valence, of which five correspond to minerals. Currently, 57 such structures are known, of which 10 are minerals (Table 3). The remarkable expansion of this structural class is largely attributable to research focused on understanding linkages between uranyl polyhedra and tetrahedra containing Mo^{6+}, S^{6+} or Cr^{6+}, as well as various polyhedra containing cations with stereoactive lone-electron pairs such as Se^{4+} and I^{5+}, which occur in 16 of the new structures. Thirty-nine structures containing uranyl polyhedra and any of the lone-pair stereoactive cations Te^{4+}, Se^{4+} and I^{5+} are known; remarkably, 41% of these contain infinite chains, whereas only 16% of all inorganic uranyl compounds with known structures are based upon chains. Presumably, the irregular polyhedra surrounding lone-pair stereoactive cations, and the existence of the lone pair of electrons rather than an additional ligand, somewhat favor polymerization in one dimension only.

Chains of polyhedra in uranyl compounds are arranged in Figure 5 on the basis of their graphs, with chains dominated by the sharing of only vertices between polyhedra provided first, followed by chains that also involve sharing of polyhedron edges. Crystallographic parameters of corresponding structures are given in Table 3.

The simple chain of uranyl square bipyramids that share vertices shown in Figure 5a occurs in $Na_4[(UO_2)O_3]$, $Ca_2[(UO_2)O_3]$, $Sr_2[(UO_2)O_3]$ and $Li_4[(UO_2)O_3]$. Each of the structures is anhydrous, and linkages between the chains involve lower-valence cations only.

The chains illustrated in Figures 5b through 5f are graphical isomers. The chains contain either uranyl square bipyramids or pentagonal bipyramids, and each is four-connected within the chain, as illustrated in the corresponding graph. Bipyramids are linked through either tetrahedra or pyramids, each of which is two-connected within the chain. Chain 5b contains either arsenate, molybdate, or phosphate tetrahedra. Chains 5c, 5d, and 5f have lone-pair stereoactive Se^{4+} or Te^{4+}, as reflected by the one-sided pyramidal coordination polyhedra about these cations. The structures corresponding to each chain are listed in Table 3.

The chains of uranyl pentagonal bipyramids and tetrahedra (or SeO_3 pyramids) shown in Figures 5g, 5h and 5i correspond to an identical graph, and are known from seven compounds (Table 3). Uranyl pentagonal bipyramids are bridged through two tetrahedra by the sharing of vertices, such that four equatorial vertices of the bipyramids are also tetrahedral vertices of bridging (two-connected) tetrahedra. The fifth equatorial vertex of the bipyramid is shared with a non-bridging tetrahedron that decorates the side of the chain.

The chains of uranyl pentagonal bipyramids and tetrahedra shown in Figures 5j, 5k, 5l and 5m, which are known from eight compounds (Table 3), are graphical isomers. Each bipyramid shares equatorial vertices with three tetrahedra, whereas the remaining two equatorial vertices correspond to H_2O groups. Each tetrahedron is linked to three bipyramids, and the chains differ in the details of the orientation of the tetrahedra.

Two chain types have been discovered that contain uranyl pentagonal bipyramids, chromate tetrahedra, and iodate pyramids (Fig. 5n, four structures, Fig. 5o, two structures). In these unusually complex chains, pairs of uranyl pentagonal bipyramids are bridged by sharing vertices with two chromate tetrahedra, and the resulting tetramers of polyhedra are connected into chains by sharing vertices with iodate pyramids. In both chains, the tetrahedra are two-connected, and two vertices of each are terminal. In chain 5o, each bipyramid is linked to two tetrahedra and two pyramids. In the case of chain 5n, iodate pyramids also decorate the chains by sharing a single vertex with the uranyl pentagonal bipyramids, resulting in bipyramids that are five-connected within the chains.

The chains shown in Figures 5p (one structure) and 5q (two structures) combine uranyl pentagonal bipyramids and molybdate tetrahedra. Pairs of bipyramids share a vertex, resulting in dimers, and two tetrahedra bridge the dimers on two sides by sharing vertices with each bipyramid. The resulting tetramers are connected into chains by sharing vertices with four different tetrahedra. Thus, each bipyramid is five-connected within the chain, whereas the tetrahedra are each two-connected.

Two types of chain contain only uranyl polyhedra that share edges. The structures of moctezumite and $[(UO_2)Cl_2H_2O]$ have simple chains of pentagonal bipyramids that share edges (Fig. 5r), whereas studtite has chains of edge-sharing hexagonal bipyramids (Fig. 5s). Studtite is one of only two known peroxide minerals, and it is the only one with a known structure (Burns & Hughes 2003). Each hexagonal bipyramid contains two peroxide groups that constitute edges of the bipyramid; both of the O atoms of the peroxide group are bonded to the central U^{6+} cation. The remaining two vertices of each bipyramid are H_2O groups. Polyhedra are linked by the sharing of peroxide groups, for which the corresponding edges of the bipyramids are ~1.45 Å. Recent studies have shown that this unusual mineral probably grows because of the buildup of peroxide that forms by alpha-radiolysis of water in nature (Hughes Kubatko *et al*. 2003).

The chains shown in Figures 5t and 5u are based upon the same graph. That in Figure 5t is from the structures of parsonsite and hallimondite, and is composed of uranyl pentagonal bipyramids and phosphate or arsenate tetrahedra. Bipyramids share an edge, forming a dimer, and dimers are linked into chains by sharing edges and vertices with tetrahedra. Additional tetrahedra decorate

TABLE 3. STRUCTURES BASED UPON INFINITE CHAINS

Name	Fig.	Formula	S. G.	*a* (Å)	*b* (Å)	*c* (Å)	β (°)	Ref.
	5a	$Na_4[(UO_2)O_3]$	*I*4/*m*	7.5571		4.6411		1
	5a	$Ca_2[(UO_2)O_3]$	$P2_1/c$	7.9137	5.4409	11.4482	108.803	2
	5a	$Sr_2[(UO_2)O_3]$	$P2_1/c$	8.1043	5.6614	11.9185	108.985	2
	5a	$Li_4[(UO_2)O_3]$	*I*4/*m*	6.725		4.451		3
	5a	$Pb_3P[(UO_2)O_3]$	*Pnam*	13.719	12.351	8.213		4
Walpurgite	5b	$Bi_4O_4[(UO_2)(AsO_4)_2](H_2O)_2$	$P\bar{1}$	7.135	10.426	5.494	110.82	5
Orthowalpurgite	5b	$Bi_4O_4[(UO_2)(AsO_4)_2](H_2O)_2$	*Pbcm*	5.492	13.324	20.685		6
Deloryite	5b	$Cu_4[(UO_2)(MoO_4)_2](OH)_6$	*C*2/*m*	19.94	6.116	5.520	104.18	7
	5b	$Cu_2[UO_2(PO_4)_2]$	*C*2/*m*	14.040	5.7595	5..0278	107.24	8
	5b	$Cu_4[(UO_2)(MoO_4)_2](OH)_6$	*B*2/*m*	19.8392	5.5108	6.1009		9
	5b	$Li_2[(UO_2)(MoO_4)_2]$	$P\bar{1}$	5.3455	5.8287	8.2652	100.566	10
	5c	Beta $Tl_2[UO_2(TeO_3)_2]$	$P2_1/n$	5.4766	8.2348	20.849	92.329	11
Derriksite	5d	$Cu_4[(UO_2)(SeO_3)_2](OH)_6$	$Pn2_1m$	5.570	19.088	5.965		12
	5d	$Sr_3[(UO_2)(TeO_3)_2](TeO_3)_2$	*C*2/*c*	20.546	5.6571	13.0979	94.416	11
	5e	$UO_2(H_2AsO_4)_2(H_2O)$	*C*2/*c*	13.164	8.862	9.050	124.41	13
	5f	$[UO_2(HSeO_3)_2(H_2O)]$	*C*2/*c*	9.924	12.546	6.324	98.09	14
	5f	$[(UO_2)(HSeO_3)_2(H_2O)]$	*A*2/*a*	6.354	12.578	9.972	82.35	15
	5g	$Na_4[(UO_2)(CrO_4)_3]$	$P\bar{1}$	7.1548	8.4420	11.5102	79.310	16
	5h	$[(UO_2)(H_2PO_4)_2(H_2O)](H_2O)_2$	$P2_1/c$	11.369	13.899	7.481	113.67	17
	5h	$K_5[(UO_2)(CrO_4)_3](NO_3)(H_2O)_3$	$P2_12_12_1$	6.1112	12.136	27.464		18
	5h	$Mn[(UO_2)(SO_4)_2(H_2O)](H_2O)_4$	$P2_1$	6.506	11.368	8.338	90.79	19
	5h	$Na_{13-x}Tl_{3-3x}[(UO_2)(MoO_4)_3]_4(H_2O)_{6+x}$	*P*2/*c*	19.7942	7.1913	22.8835	97.828	20
	5h	$Na_2[(UO_2)(MoO_4)_2](H_2O)_4$	$P2_12_12_1$	10.7662	11.9621	12.8995		20
Demesmaekerite	5i	$Pb_2Cu_5[(UO_2)(SeO_3)_3]_2(OH)_6(H_2O)_2$	$P\bar{1}$	11.955	10.039	5.639	100.36	21
	5j	$[(UO_2)(CrO_4)(H_2O)_2]\ (H_2O)_{3.5}$	$P2_1/c$	11.179	7.119	26.49	94.19	22
	5j	$[(UO_2)(SO_4)(H_2O)_2](H_2O)_{1.5}$	*C*2/*c*	13.70	10.79	11.91	110.8	23
	5j	$[(UO_2)(SO_4)(H_2O)_2](H_2O)_{0.5}$	$P2_1/a$	16.887	12.492	6.7354	90.88	24
	5j	$[(UO_2)(SO_4)(H_2O)_2]_2(H_2O)_3$	$P2_1ca$	11.227	6.790	21.186		25
	5j	$[(UO_2)(SeO_4)(H_2O)_2](H_2O)_2$	*C*2/*c*	14.653	10.799	12.664	119.95	26
	5k	$(UO_2)(CrO_4)(H_2O)_2$	*C*2/*m*	16.786	22.731	6.9969	90.051	27
	5l	$[(UO_2)(CrO_4)(H_2O)_2](H_2O)$	$P2_1$	9.7206	7.1617	11.0909	92.388	27
	5m	$[(UO_2)(CrO_4)(H_2O)_2]_4(H_2O)_9$	$P2_1/c$	31.397	7.1701	16.2480	97.515	27
	5n	$K_2[UO_2(CrO_4)(IO_3)_2]$	$P2_1/c$	11.1337	7.2884	15.5661	107.977	28
	5n	$Rb_2[UO_2(CrO_4)(IO_3)_2]$	$P2_1/c$	11.3463	7.3263	15.9332	108.173	28
	5n	$Cs_2[UO_2(CrO_4)(IO_3)_2]$	$P2_1/n$	7.3929	8.1346	22.126	90.647	28
	5n	$K_2[UO_2(MoO_4)(IO_3)_2]$	$P2_1/c$	11.3717	17.2903	15.7122	108.167	28
	5o	$Rb[UO_2(CrO_4)(IO_3)(H_2O)]$	$P\bar{1}$	7.3133	8.0561	8.4870	87.075	28
	5o	$Cs_2[(UO_2)(CrO_4)(IO_3)_2]$	$P2_1/n$	7.3929	8.1346	22.126	90.647	29
	5p	$Rb_6[(UO_2)_2O(MoO_4)_4]$	$P\bar{1}$	10.1567	10.1816	13.1129	76.553	30
	5q	$Na_6[(UO_2)_2O(MoO_4)_4]$	$P\bar{1}$	7.637	8.164	8.746	79.36	31
	5q	$K_6[(UO_2)_2O(MoO_4)_4]$	$P\bar{1}$	7.828	7.830	10.302	73.13	31
Moctezumite	5r	$PbTe[(UO_2)O_3]$	$P2_1/c$	7.813	7.061	13.775	93.71	32
	5r	$[(UO_2)Cl_2H_2O]$	$P2_1/m$	5.828	8.534	5.557	97.79	33
Studtite	5s	$[(UO_2)(O_2)(H_2O)_2](H_2O)_2$	*C*2/*c*	14.068	6.721	8.428	123.356	34

TABLE 3. STRUCTURES BASED UPON INFINITE CHAINS

Name	Fig.	Formula	S. G.	*a* (Å)	*b* (Å)	*c* (Å)	β (°)	Ref.
Parsonsite	5t	$Pb_2[(UO_2)(PO_4)_2]$	$P\bar{1}$	6.842	10.383	6.670	98.17	35
Hallimondite	5t	$Pb_2[(UO_2)(AsO_4)_2](H_2O)_n$	$P\bar{1}$	7.1153	10.4780	6.8571	95.711	36
	5u	$Ca[(UO_2)(SeO_3)_2]$	$P\bar{1}$	5.5502	6.6415	11.013	93.342	37
	5u	$Sr[(UO_2)(SeO_3)_2]$	$P\bar{1}$	5.6722	6.7627	11.2622	93.708	38
	5v	$Sr[(UO_2)(SeO_3)_2]\cdot 2H_2O$	$P2_1/c$	7.3067	8.1239	13.651	100.375	37
	5w	$[UO_2(IO_3)_2]$	$P2_1/n$	4.245	16.636	5.284	107.57	39
	5x	$K_2[(UO_2)_3(IO_3)_4O_2]$	$P\bar{1}$	7.0372	7.7727	8.9851	105.668	40
	5x	$Rb_2[(UO_2)_3(IO_3)_4O_2]$	$P\bar{1}$	7.0834	7.8935	9.092	105.110	41
	5x	$Tl_2[(UO_2)_3(IO_3)_4O_2]$	$P\bar{1}$	7.0602	7.9475	9.0175	105.595	41
	5y	$Ba[(UO_2)_2(IO_3)_2O_2](H_2O)$	$P2_1/c$	8.062	6.940	21.67	98.05	41
	5y	$Sr[(UO_2)_2(IO_3)_2O_2](H_2O)$	$P2_1/c$	7.8140	6.9425	21.434	99.324	41
	5y	$Pb[(UO_2)_2(IO_3)_2O_2](H_2O)$	$P2_1/c$	7.8441	6.9328	21.340	99.062	41
Uranopilite	5z	$[(UO_2)_6(SO_4)O_2(OH)_6(H_2O)_6]$	$P\bar{1}$	8.896	14..029	14.339	98.472	42

References: (1) Wolf & Hoppe (1986), (2) Loopstra & Rietveld (1969), (3) Reshetov & Kovba (1966), (4) Sterns *et al.* (1986), (5) Mereiter (1982b), (6) Krause *et al.* (1995), (7) Pushcharovsky *et al.* (1996), (8) Guesdon *et al.* (2002), (9) Tali *et al.* (1993), (10) Krivovichev & Burns (2003d), (11) Almond *et al.* (2002a), (12) Ginderow & Cesbron (1983a), (13) Gesing & Rüscher (2000), (14) Koskenlinna *et al.* (1997), (15) Mistryukov & Michailov (1983), (16) Krivovichev & Burns (2003e), (17) Krogh-Andersen *et al.* (1985), (18) Krivovichev & Burns (2003c), (19) Tabachenko *et al.* (1979), (20) Krivovichev & Burns (2003b), (21) Ginderow & Cesbron (1983b), (22) Serezhkin & Trunov (1981), (23) Brandenburg & Loopstra (1973), (24) van der Putten & Loopstra (1974), (25) Zalkin *et al.* (1978), (26) Serezhkin *et al.* (1981a), (27) Krivovichev & Burns (2003f), (28) Sykora *et al.* (2002a), (29) Sykora *et al.* (2002b), (30) Krivovichev & Burns (2002a), (31) Krivovichev & Burns (2001a), (32) Swihart *et al.* (1993), (33) Taylor & Wilson (1974), (34) Burns & Hughes (2003), (35) Burns (2000), (36) Locock *et al.* (2005), (37) Almond *et al.* (2002b), (38) Almond & Albrecht-Schmitt (2004), (39) Bean *et al.* (2001a), (40) Bean *et al.* (2001b), (41) Bean & Albrecht-Schmitt (2001), (42) Burns (2001a).

the edges of the chains by sharing vertices with the polyhedra. The structures of $Ca[(UO_2)(SeO_3)_2]$ and $Sr[(UO_2)(SeO_3)_2]$ contain chains (Fig. 5u) in which selenite pyramids assume the role of tetrahedra in the parsonsite chain.

The chain shown in Figure 5v is known only from $Sr[(UO_2)(SeO_3)_2](H_2O)_2$, and contains units similar to those in $Ca[(UO_2)(SeO_3)_2]$ and $Sr[(UO_2)(SeO_3)_2]$. These chains have the same dimers of edge-sharing uranyl pentagonal bipyramids, with two selenite pyramids that share edges with the bipyramids, but the linkages of these units into chains differ.

The backbone of the chain found in $UO_2(IO_3)_2$ (Fig. 5w) is composed of uranyl hexagonal bipyramids that share edges, and is thus related to the chains found in studtite (Fig. 5s). In $UO_2(IO_3)_2$, the chains also contain iodate pyramids that are attached to either side by sharing edges with the bipyramids.

The chain shown in Figure 5x occurs in three uranyl iodates, and is unusual in that it is the only chain that contains uranyl ions in two different coordinations. The zig-zag chain is formed by the sharing of edges between uranyl pentagonal bipyramids and square bipyramids, arranged such that there are dimers of pentagonal bipyramids that are bridged by the square bipyramids. Additional rigidity of the chain is provided by iodate pyramids that bridge adjacent dimers of pentagonal bipyramids, and the chain is decorated by iodate pyramids that share only a single vertex with the bipyramids.

The complex chain shown in Figure 5y is known from three uranyl iodates (Table 3). The bulk of the chain is composed of uranyl pentagonal bipyramids that share equatorial edges, resulting in a chain that is two bipyramids wide. Chain rigidity is enhanced by iodate pyramids that bridge between bipyramids, and additional iodate pyramids decorate the chain by sharing single vertices with the bipyramids.

The chain found in uranopilite (Fig. 5z) is the most complex chain found to date in a uranyl mineral. It is composed of uranyl pentagonal bipyramids that are linked by sharing equatorial edges to form six-membered clusters. Within these clusters, two O atoms are bonded to three uranyl ions, and all but four of the equatorial anions that terminate the cluster are H_2O groups. Identical clusters of six bipyramids are linked by sharing vertices with sulfate tetrahedra, such that each tetrahedron is four-connected. Chains are linked

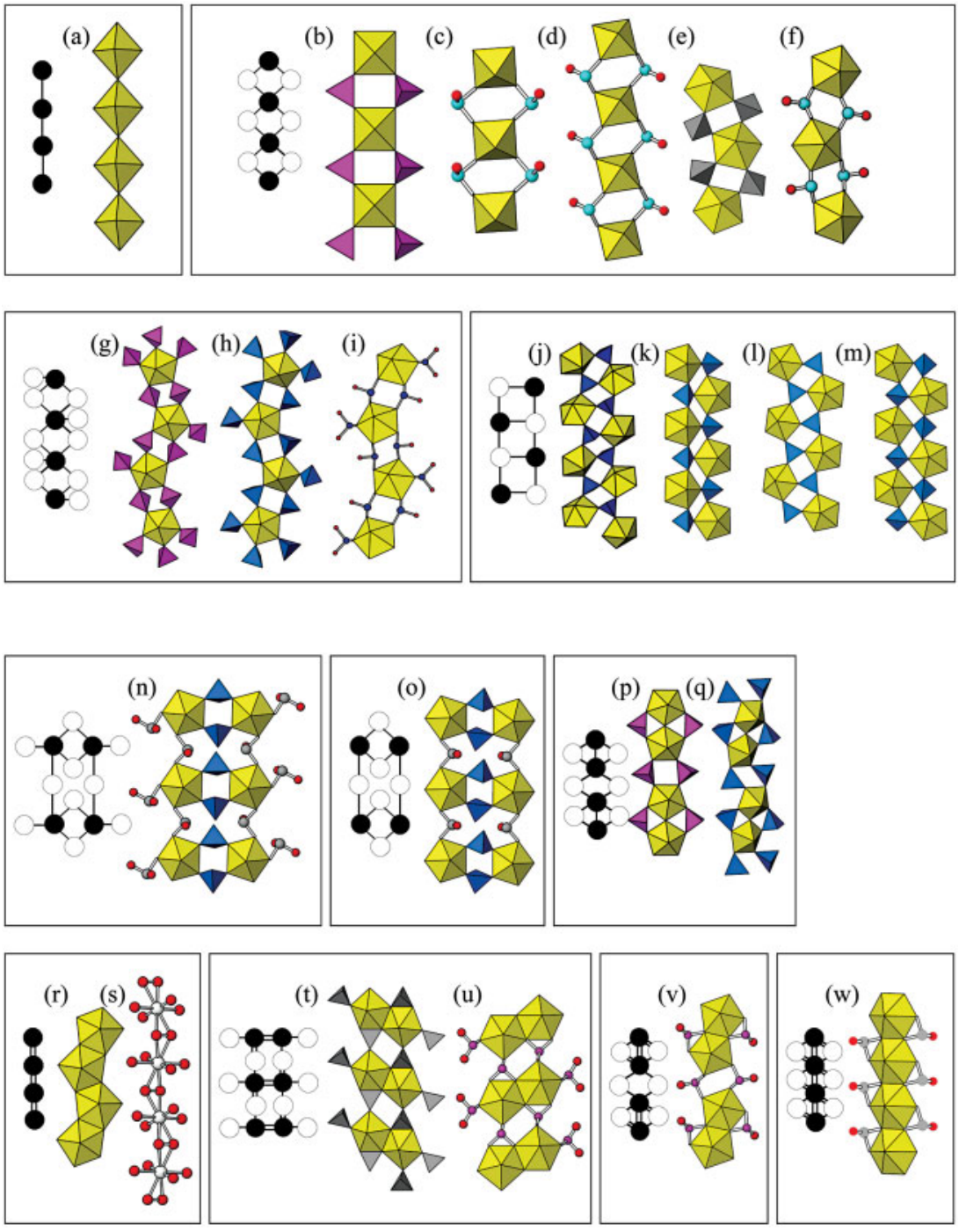
(a)
(b)
(c)
(d)
(e)
(f)
(g)
(h)
(i)
(j)
(k)
(l)
(m)
(n)
(o)
(p)
(q)
(r)
(s)
(t)
(u)
(v)
(w)

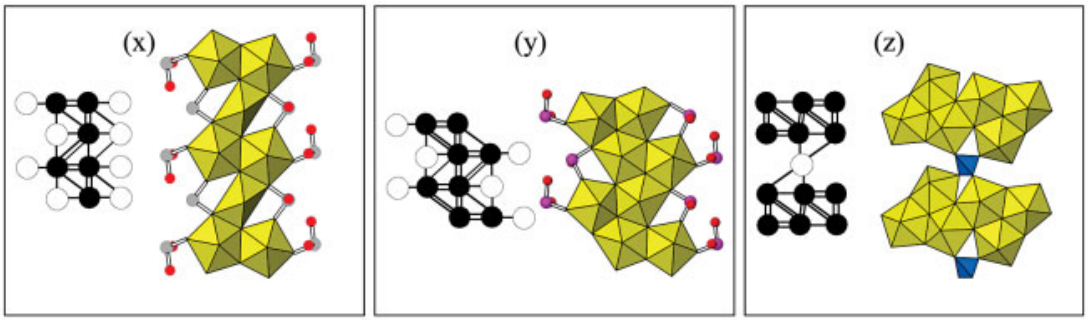

FIG. 5. Chains (and their graphical representations) of uranyl polyhedra and other polyhedra containing higher-valence cations that occur in the structures of uranyl compounds. The corresponding compounds are listed in Table 3.

into the three-dimensional structure by H bonds, both directly between adjacent chains, and to interstitial H_2O groups. Hydrogen bonds also extend between clusters of bipyramids within the same chain.

STRUCTURES WITH INFINITE SHEETS OF POLYHEDRA

Structures containing infinite sheets of polyhedra of higher bond-valence are the most abundant class in uranyl minerals and synthetic inorganic compounds, accounting for 204 of the 368 structures examined herein. The dominance of sheets of polyhedra arises from the uneven distribution of bond strengths within uranyl polyhedra. The bond-valence requirements of the O_{Ur} atoms are nearly satisfied by the bond to the U^{6+} cation alone, thus these O atoms usually do not form bonds to other higher-valence cations. In contrast, the equatorial ligands of the uranyl bipyramids must participate in additional significant bonding for a stable configuration to result. In some cases, equatorial ligands correspond to H_2O groups that are not bonded to additional high-valence cations. However, it is more common for uranyl polyhedra to link to other uranyl polyhedra or other polyhedra of higher bond-valence through the equatorial ligands, which favors the formation of sheets.

Burns *et al*. (1996) and Burns (1999a) grouped sheets on the basis of the topological arrangement of anions within the sheet. In this approach, all anions that are bonded to at least two cations within the sheet are considered, and those separated by less than ~3.5 Å are connected by lines. Removal of all atoms from further consideration results in the sheet anion-topology, which, when projected onto a plane, is a two-dimensional tiling of space that represents the topological arrangement of anions within the sheet from which it was derived. The utility of this approach is that sheets of polyhedra that bear little immediate resemblance commonly have the same underlying sheet anion-topology. The sheet anion-topology is a representation of an approximate closest packing of anions, with smaller cations populating interstitial positions to produce the observed sheets. As shown by Miller *et al*. (1996) and Burns (1999a), the sheet anion-topologies can be assessed as stacking sequences of a small number of distinct chains of polygons, which provides a useful means of comparison of the topologies as well as a short-hand notation. This approach has demonstrated that some of the extraordinarily complex sheets recently found in minerals such as vandendriesscheite and wölsendorfite are composed of modules of simpler sheets found in other minerals or synthetic compounds (Burns 1997, 1999b).

Sheets dominated by the sharing of vertices

The sheet anion-topology approach works well for most sheets that are dominated by the sharing of edges between polyhedra of higher bond-valence. However, sheets connected only by the sharing of vertices between polyhedra correspond to a myriad of complex anion-topologies that defy usefulness. This was not a substantial setback for Burns *et al*. (1996) or Burns (1999a), but the recent discovery of many such sheets in synthetic compounds, especially those containing hexavalent cations in tetrahedral coordination (such as Mo^{6+}, Cr^{6+}, S^{6+}), requires a new approach to their hierarchical organization. To further understanding of the relationships within sheets dominated by vertex sharing, Krivovichev & Burns (2003j) developed a graphical approach for the analysis of such sheets. This approach has considerable merit, as it is generally possible to find parent graphs that may be used to derive the graphs of a diverse range of sheets by simple deletion of vertices and connectors.

Krivovichev (2004) has greatly expanded the treatment of Krivovichev & Burns (2003j) to include a graphical approach to structures containing zero-, one-, and two-dimensional units with corner-sharing between coordination polyhedra. He developed a method of graphical representation of these structures, and intro-

TABLE 4. STRUCTURES CONTAINING SHEETS DOMINATED BY SHARING OF VERTICES

Name	Fig.	Parent	Graph	Formula	S. G.	*a* (Å)	*b* (Å)	*c* (Å)	β (°)	Ref.
	6c	3.6.3.6	L1/2b	$UO_2(IO_3)_2(H_2O)$	*Pbcn*	8.452	7.707	12.271		1
	6d	3.6.3.6	L1/2b	$Cs_2[(UO_2)(SeO_4)_2H_2O]H_2O$	$Pna2_1$	14.367	11.682	7.826		2
	6f	3.6.3.6	L1/2c	$(NH_4)_2[(UO_2)(SO_4)_2(H_2O)](H_2O)$	$P2_1/c$	7.783	7.403	20..918	102.25	3
	6h	3.6.3.6	L1/2d	$Cs_2[(UO_2)(MoO_4)_2]$	*Pbca*	11.762	14.081	14.323		4
	6h	3.6.3.6	L1/2d	$Cs_2[(UO_2)(MoO_4)_2](H_2O)$	$P2_1/c$	8.2222	11.0993	13.9992	95.155	4
	6h	3.6.3.6	L1/2d	$K_2[(UO_2)(MoO_4)_2]$	$P2_1/c$	12.269	13.468	12.857	95.08	5
	6h	3.6.3.6	L1/2d	$Na_2[(UO_2)(MoO_4)_2](H_2O)_4$	$P2_1/n$	8.9023	11.5149	13.8151	107.743	6
	6h	3.6.3.6	L1/2d	$Rb_2[(UO_2)(MoO_4)_2]$	$P2_1/c$	12.302	13.638	13.508	94.975	7
	6h	3.6.3.6	L1/2d	$K_2[(UO_2)(MoO_4)_2](H_2O)$	$P2_1/c$	7.893	10.907	13.558	98.70	8
	6h	3.6.3.6	L1/2d	$Rb_2[(UO_2)(MoO_4)_2](H_2O)$	$P2_1/c$	7.967	10.956	13.679	96.69	9
	6h	3.6.3.6	L1/2d	$Tl_2[(UO_2)(CrO_4)_2]$	$Pca2_1$	10.977	14.004	14.041		10
	6h	3.6.3.6	L1/2d	$Tl_2[(UO_2)(MoO_4)_2]$	$Pca2_1$	10.7034	13.4252	13.9364		10
	6i	3.6.3.6	L1/2d	$K[(UO_2)(HSeO_3)(SeO_3)]$	$P2_1/n$	8.4164	10.1435	9.6913	97.556	11
	6i	3.6.3.6	L1/2d	$Rb[(UO_2)(HSeO_3)(SeO_3)]$	$P2_1/n$	8.4167	10.2581	9.8542	96.825	11
	6i	3.6.3.6	L1/2d	$Cs[(UO_2)(HSeO_3)(SeO_3)]$	$P2_1/n$	13.8529	10.6153	12.5921	101.094	11
	6i	3.6.3.6	L1/2d	$Tl[(UO_2)(HSeO_3)(SeO_3)]$	$P2_1/n$	8.364	10.346	9.834	97.269	11
	6i	3.6.3.6	L1/2d	$(NH_4)_2UO_2(SeO_3)_2(H_2O)_{0.5}$	$P2_1/c$	7.193	10.368	13.823	9.147	12
	6i	3.6.3.6	L1/2d	$(NH_4)[(UO_2)(HSeO_3)(SeO_3)]$	$P2_1/n$	8.348	10.326	9.929	97.06	13
	6i	3.6.3.6	L1/2d	$Na_2[(UO_2)(SeO_4)_2](H_2O)_4$	$P2_1/c$	8.650	11.003	13.879	108.08	14
	6k	3.6.3.6	L1/2e	$Na_2[(UO_2)(MoO_4)_2]$	$P2_12_12_1$	7.2298	11.3240	12.0134		15
	6l	3.6.3.6	L1/2e	$Ag_2(UO_2)(SeO_3)_2$	$P2_1/n$	5.8555	6.5051	21.164	96.796	11
	6n	3.6.3.6	L1/2g	$Mg(UO_2)_3(MoO_4)_4(H_2O)_8$	$Cmc2_1$	17.105	13.786	10.908		16
	6n	3.6.3.6	L1/2g	$Zn(UO_2)_3(MoO_4)_4(H_2O)_8$	$Cmc2_1$	17.056	13.786	10.919		16
	6p	3.6.3.6	L2/3e	$K_2[(UO_2)_2(CrO_4)_3(H_2O)_2](H_2O)_4$	$P2_1/c$	10.7417	14.529	14.1387	108.135	18
	6r	3.6.3.6	L3/5b	$K_4[(UO_2)_3(CrO_4)_5](H_2O)_8$	$P2_1/c$	8.2336	18.8042	21.2413	89.979	18
	6r	3.6.3.6	L3/5b	$Mg_2[(UO_2)_3(CrO_4)_5](H_2O)_{17}$	*Pbca*	19.9206	21.0526	18.4966		19
	6r	3.6.3.6	L3/5b	$Ca_2[(UO_2)_3(CrO_4)_5](H_2O)_{19}$	$P2_1/m$	11.0359	17.5364	11.5056	118.18	19
	6r	3.6.3.6	L3/5b	$Cu_2[(UO_2)_3((S,Cr)O_4)_5](H_2O)_{17}$	*Pbca*	18.0586	19.9898	20.5553		20
	6r	3.6.3.6	L3/5b	$Zn_2[(UO_2)_3(SeO_4)_5](H_2O)_{17}$	*Pbca*	18.4288	19.9793	20.6901		21
	6t	5.3.5.3		β-$Cs_2(UO_2)_2(MoO_4)_3$	$P4_2/n$	10.1367		16.2831		22
	6t	5.3.5.3		$Cs_2[(UO_2)_2(SO_4)_3]$	$P\bar{4}21$	9.62		8.13		23
Meta-uranocircite	6v	4.4.4.4		$Ba[(UO_2)(PO_4)]_2(H_2O)_6$	$P2_1/a$	9.789	9.882	16.868		24
Threadgoldite	6v	4.4.4.4		$Al[(UO_2)(PO_4)]_2(OH)(H_2O)_8$	*C2/c*	20.168	9.847	19.719	110.71	25
Meta-autunite	6v	4.4.4.4		$Ca[(UO_2)(PO_4)]_2(H_2O)_6$	*P4/nmm*	6.96		8.40		26
Autunite	6v	4.4.4.4		$Ca[(UO_2)(PO_4)]_2(H_2O)_{11}$	*Pnma*	14.0135	20.7121	6.9959		27
Saléeite	6v	4.4.4.4		$Mg[(UO_2)(PO_4)]_2(H_2O)_{10}$	$P2_1/c$	6.951	19.947	9.896	135.17	28
Abernathyite	6v	4.4.4.4		$K[(UO_2)(AsO_4)](H_2O)_3$	*P4/ncc*	7.176		18.126		29
Zeunerite	6v	4.4.4.4		$Cu[(UO_2)(AsO_4)_2]_2(H_2O)_{12}$	*P4/nnc*	7.1797		20.857		30
Metazeunerite	6v	4.4.4.4		$Cu[(UO_2)(AsO_4)_2]_2(H_2O)_8$	*P4/n*	7.1094		17.416		30
Torbernite	6v	4.4.4.4		$Cu[(UO_2)(PO_4)_2]_2(H_2O)_{12}$	*P4/nnc*	7.0267		20.807		30
Metatorbernite	6v	4.4.4.4		$Cu[(UO_2)(PO_4)_2]_2(H_2O)_8$	*P4/n*	6.9756		17.349		30
	6v	4.4.4.4		$[(UO_2)H(PO_4)](H_2O)_4$	*P4/ncc*	6.995		17.491		31
	6v	4.4.4.4		$K[(UO_2)(PO_4)](D_2O)_3$	*P4/ncc*	6.99379		17.7839		32
	6v	4.4.4.4		$ND_4[(UO_2)(PO_4)](D_2O)_3$	*P4/ncc*	7.0221		18.0912		33
	6v	4.4.4.4		$NH_4[(UO_2)(AsO_4)](H_2O)_3$	*P4/ncc*	7.189		18.191		29
	6v	4.4.4.4		$KH_3O[(UO_2)(AsO_4)]_2(H_2O)_6$	*P4/ncc*	7.171		18.048		29
	6v	4.4.4.4		$[(UO_2)D(AsO_4)](D_2O)_4$	*P4/ncc*	7.1615		17.6390		34
	6v	4.4.4.4		$Li[(UO_2)(AsO_4)](D_2O)_4$	*P4/n*	7.0969		9.1903		35

TABLE 4. STRUCTURES CONTAINING SHEETS DOMINATED BY SHARING OF VERTICES

Name	Fig.	Parent Graph	Formula	S. G.	*a* (Å)	*b* (Å)	*c* (Å)	β (°)	Ref.
	6w	4.4.4.4	$Li_2[(UO_2)O_2]$	*Pnma*	10.547	6.065	5.134		36
	6w	4.4.4.4	$Ba[(UO_2)O_2]$	*Pbcm*	5.744	8.136	8.237		37
	6w	4.4.4.4	$Sr[(UO_2)O_2]$	*Pbcm*	5.4896	7.9770	8.1297		38
	6w	4.4.4.4	γ-$[(UO_2)(OH)_2]$	$P2_1/c$	5.560	5.522	6.416	112.71	39
	6w	4.4.4.4	β-$[(UO_2)(OH)_2]$	*Pbca*	5.6438	6.2867	9.9372		40
	6w	4.4.4.4	β-$Na_2[(UO_2)O_2]$	*Pccn*	11.708	5.805	5.970		41
	6w	4.4.4.4	$Pb[(UO_2)O_2]$	*Pbcm*	5.536	7.968	8.212		42
	6y	4.4.4.4	$K_4[(UO_2)(PO_4)_2]$	$P4_2/nmc$	6.985		11.865		43
	7a		$Pb(UO_2)(SeO_3)_2$	$Pmc2_1$	11.9911	5.7814	11.2525		11
	7b		$Ba[(UO_2)(SeO_3)_2]$	$P\bar{1}$	7.0523	7.4627	10.0433	108.027	44
	7c		$K[(UO_2)(CrO_4)(OH)](H_2O)_{1.5}$	$P2_1/c$	13.292	9.477	13.137	104.12	45
	7d		$Cs[(UO_2)(PO_3)_3]$	$P2_1/n$	6.988	10.838	13.309	104.25	46
	7e		$(UO_2)H(PO_3)_3$	$P2_1/b$	9.811	20.814	8.6947		47
	7f		$(NH_4)[(UO_2)F(SeO_4)](H_2O)$	*Pnma*	8.450	13.483	13.569		48
	7g		$[Co(H_2O)_6]_3[(UO_2)_5(SO_4)_8(H_2O)](H_2O)_5$	$P2_1/c$	27.1597	9.9858	22.7803	106.52	49

References: (1) Bean *et al.* (2001a), (2) Mikhailov *et al.* (2001a), (3) Niinistö *et al.* (1978), (4) Krivovichev & Burns (2004c), (5) Sadikov *et al.* (1988), (6) Krivovichev & Burns (2003b), (7) Krivovichev & Burns (2002a), (8) Krivovichev *et al.* (2002b), (9) Khrustalev *et al.* (2000), (10) Krivovichev *et al.* (2005c), (11) Almond & Albrecht-Schmitt (2002a), (12) Koskenlinna *et al.* (1997), (13) Koskenlinna & Valkonen (1996), (14) Mikhailov *et al.* (2001b), (15) Krivovichev *et al.* (2002b), (16) Tabachenko *et al.* (1983), (18) Krivovichev & Burns (2003c), (19) Krivovichev & Burns (2003a), (20) Krivovichev & Burns (2004d), (21) Krivovichev & Kahlenberg (2005), (22) Krivovichev *et al.* (2002a), (23) Ross & Evans (1960), (24) Khosrawan-Sazedj (1982a), (25) Khosrawan-Sazedj (1982b), (26) Makarov & Ivanov (1960), (27) Locock & Burns (2003a), (28) Miller & Taylor (1986), (29) Ross & Evans (1964), (30) Locock & Burns (2003b), (31) Fitch *et al.* (1983), (32) Morosin (1978), (33) Fitch & Cole (1991), (34) Fitch & Fender (1983), (35) Fitch *et al.* (1982), (36) Gebert *et al.* (1978), (37) Reis *et al.* (1976), (38) Loopstra & Rietveld (1969), (39) Siegel *et al.* (1972b), (40) Taylor & Bannister (1972), (41) Kovba (1971), (42) Cremers *et al.* (1986), (43) Linde *et al.* (1980), (44) Almond *et al.* (2002b), (45) Serezhkina *et al.* (1990), (46) Linde *et al.* (1978), (47) Sarin *et al.* (1983), (48) Blatov *et al.* (1989), (49) Krivovichev & Burns (2006).

duced short-hand notations for the required graphs. His study included structures in which two adjacent polyhedra share no more than one common vertex, and where there is no linkage between polyhedra of the same type. These criteria match many of the sheets containing uranyl polyhedra that are dominated by vertex sharing (Table 4), and Krivovichev (2004) arranged these structures on the basis of their graphs, together with coverage of non-uranium structures.

Krivovichev (2004) defined the connectedness, **s**, of a polyhedron as the number of adjacent polyhedra with which it shares common corners. Consider the graph shown in Figure 6a. It contains black circles and white circles. Each black circle is connected to six white circles, and white circles are connected to three black circles. The elementary unit of the graph is a rhomb that contains two black and two white circles. The values of **s** at the nodes of the rhomb written in cyclic order are {3.6.3.6}, which may be used to designate the graph. Krivovichev (2004) denoted the {3.6.3.6} graph as a parent graph because a series of graphs may be derived from it, which correspond to known structures, by simply deleting connectors or vertices, together with all of their associated connectors in the case of deleted vertices. In the case of the {3.6.3.6} graph, Krivovichev (2004) found 34 derivative graphs that correspond to known structures, with *M*:*T* ratios of 1:2, 2:3, 4:3, 13:18, 3:8, 5:8, 3:5, and 1:1 (where *M* represents non-tetrahedral polyhedra such as uranyl pentagonal bipyramids, and *T* corresponds to tetrahedra). Krivovichev (2004) provided a designation for the graphs of the general form L *M*/*T c*, where L designates that the graph is a sheet, *M*/*T* gives the ratio of non-tetrahedral polyhedra to tetrahedra, and *c* is an alphabetic designator used to distinguish various graphs with the same *M*/*T* ratio.

Several sheets considered by Krivovichev (2004) and herein have either $Se^{4+}O_3$ or $I^{5+}O_3$ polyhedra. In these cases, the cations contain stereoactive lone pairs of electrons that occur in the position of the fourth vertex of a distorted tetrahedron. For the purposes of

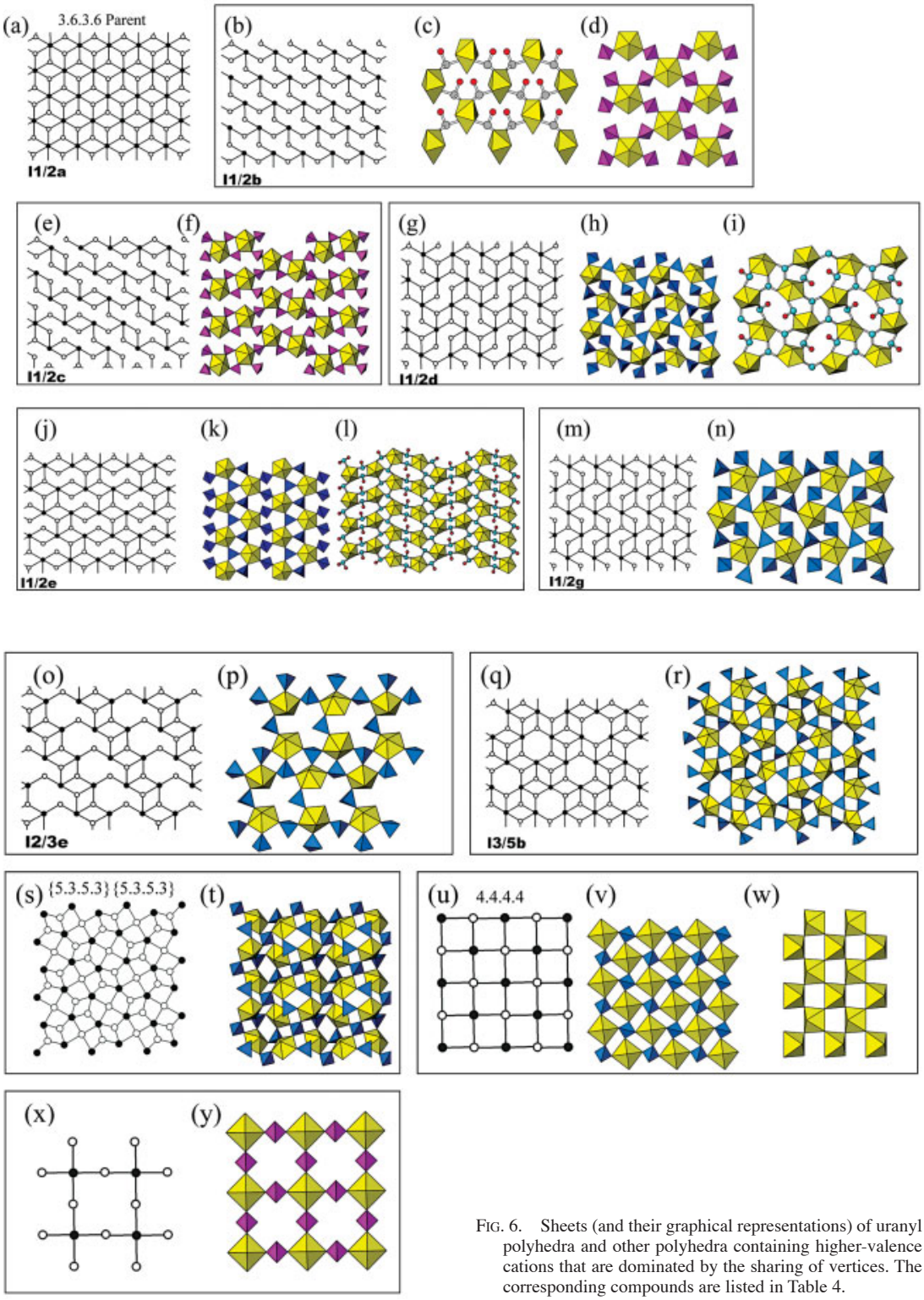

FIG. 6. Sheets (and their graphical representations) of uranyl polyhedra and other polyhedra containing higher-valence cations that are dominated by the sharing of vertices. The corresponding compounds are listed in Table 4.

the current discussion, $Se^{4+}O_3$ and $I^{5+}O_3$ polyhedra are treated as tetrahedra.

Twenty-nine uranyl compounds contain sheets with corresponding graphs that are derived from the {3.6.3.6} parent graph (Table 4). Polyhedral representations of each distinct sheet, together with their corresponding graphs, are shown in Figure 6.

Two sheets are known that correspond to the graph L1/2b (Fig. 6b). The sheet in the structure of $[UO_2(IO_3)_2(H_2O)]$ contains uranyl pentagonal bipyramids and $I^{5+}O_3$ pyramids. The sheet in $Cs_2[(UO_2)(SeO_4)_2(H_2O)](H_2O)$ is composed of uranyl pentagonal bipyramids and selenate tetrahedra. In each case the bipyramids are only connected to four tetrahedra, and the fifth equatorial vertex of the bipyramid is occupied by H_2O. Each tetrahedron is connected to two bipyramids.

The structure of $(NH_4)_2[(UO_2)(SO_4)_2(H_2O)](H_2O)$ contains the sheet shown in Figure 6f, which is based upon the L1/2c graph shown in Figure 6e. The bipyramids share equatorial vertices with four sulfate tetrahedra, and H_2O is present at the fifth equatorial vertex of the bipyramid. As in L1/2b, each tetrahedron is connected to two bipyramids. Sheets based upon graphs L1/2b and L1/2c differ in the orientation of the bipyramids and the unshared equatorial vertices of the bipyramids. Sheets based on L1/2b have all unshared vertices of the bipyramids extending in the same direction, but these vertices alternate in opposite directions in the case of sheets based upon L1/2c (Figs. 6d, f).

Twenty-three structures contain sheets with a *M:T* ratio of 1:2; they contain twice as many tetrahedra as uranyl pentagonal bipyramids. Sixteen correspond to the graph designated L1/2d by Krivovichev (2004) (Table 4). Of these, eight have molybdate tetrahedra (Fig. 6h) and seven contain selenite pyramids or selenate tetrahedra (Fig. 6i), and all but three crystallize in space group $P2_1/c$ or $P2_1/n$. Each uranyl pentagonal bipyramid in the uranyl molybdate and uranyl selenite or selenate sheet shares vertices with five distinct tetrahedra, but tetrahedra are linked either to two or three bipyramids. The connectivity of the tetrahedra traversing around the bipyramids is 2–3–3–2–3 in each case. All known structures containing this sheet have monovalent cations in the interlayer regions, where H_2O also occurs in some cases.

The structures of $Na_2[(UO_2)(MoO_4)_2]$ and $Ag_2[(UO_2)(SeO_3)_2]$ contain sheets based upon the L1/2e graph shown in Figure 6j. Examination of the sheets shown in Figures 6k and 6l shows that each bipyramid is linked to five tetrahedra, and that tetrahedra are connected to either two or three bipyramids. The connectivity of the tetrahedra traversing around the bipyramids is 2–2–3–3–3 in both cases, which differs from L1/2d, for which the connectivity is 2–3–3–2–3.

The isostructural compounds $Mg[(UO_2)_3(MoO_4)_4](H_2O)_8$ and $Zn[(UO_2)_3(MoO_4)_4](H_2O)_8$ contain the uranyl molybdate sheet shown in Figure 6n that is based upon graph L1/2g (Fig. 6m). In these structures, the uranyl dimolybdate sheets are connected through uranyl pentagonal bipyramids located in the interlayer, resulting in frameworks. They are included here as sheets because the fundamental portion of the structure corresponds to a graph whose parent is {3.6.3.6}. Within the sheet, each bipyramid is linked to five tetrahedra, and tetrahedra are either connected to two or three bipyramids. The connectivity of the tetrahedra traversing around the bipyramids is 2–3–3–2–3, which is identical to graph L1/2d. The distinction between sheets based upon graphs L1/2g and L1/2d lies in the specific bipyramids to which each tetrahedron bridges.

The uranyl chromate sheet in the structure of $K_2[(UO_2)_2(CrO_4)_3(H_2O)_2](H_2O)_4$ (Fig. 6p) is the only example of a uranyl compound with a sheet based upon the graph designated L2/3e (Fig. 6o). This is a relatively open sheet in which each bipyramid is linked to four tetrahedra, with the fifth vertex of the bipyramid corresponding to H_2O. Of the four tetrahedra that are linked to any bipyramid, two bridge between two bipyramids and two are connected to three bipyramids.

Five structures contain sheets that are based upon the graph designated L3/5b (Fig. 6q). Each contains a uranyl chromate sheet with a bipyramid-to-tetrahedron ratio of 3:5 (Fig. 6r). All bipyramids share their five equatorial vertices with five tetrahedra, and all five of the tetrahedra are connected to three different bipyramids.

The structures of β-$Cs_2[(UO_2)_2(MoO_4)_3]$ and $Cs_2[(UO_2)_2(SO_4)_3]$ contain identical sheets (Fig. 6t), and are the only known uranyl compounds that are based upon graphs derived from a parent graph with the connectivity {5.3.5.3}{5.3.5.3} (Fig. 6s) (Krivovichev 2004). Each bipyramid in this sheet is linked to five tetrahedra, of which three of the tetrahedra are connected to three bipyramids and two are linked to four bipyramids.

The {4.4.4.4} graph shown in Figure 6u corresponds to the autunite anion-topology of Burns *et al.* (1996). The autunite-type sheet shown in Figure 6v is formed by uranyl square bipyramids and tetrahedra that are connected by sharing vertices, such that each bipyramid is connected to four tetrahedra, and each tetrahedron is linked to four bipyramids. Structures of the autunite and meta-autunite groups contain this sheet, with either phosphate or arsenate tetrahedra. The sheet is based upon the autunite anion-topology that is composed of squares that share vertices and edges (Burns *et al.* 1996). This is a large family of structures, with 17 refined thus far, of which 10 correspond to minerals. The structures vary considerably in the occupation and connectivity of their interlayer constituents (*e.g.*, Locock & Burns 2003a, d). The minerals of this group are commonly associated with uranium deposits containing phosphate, and have a significant impact upon uranium mobility in such situations due to their low solubilities (Murakami *et al.* 1997). Current studies are addressing the possi-

bility that enhanced formation of autunite-group minerals in the subsurface may reduce uranium mobility in the vadose zones of contaminated sites.

The sheet of vertex-sharing uranyl square bipyramids shown in Figure 6w is also based upon the {4.4.4.4} graph presented in Figure 6u. This sheet occurs in seven structures (Table 4). In five cases, the structures are anhydrous, and sheets are connected by bonds to interlayer cations including Li, Ba, Sr, Na and Pb. In γ-$UO_2(OH)_2$ and β-$UO_2(OH)_2$, all of the equatorial vertices of the uranyl square bipyramids are occupied by hydroxyl groups, and linkages between adjacent sheets are assured through H bonds only.

The structure of $K_4[(UO_2)(PO_4)_2]$ contains the unusual sheet of uranyl square bipyramids and phosphate tetrahedra shown in Figure 6y. This sheet can be obtained from the autunite sheet (Fig. 6v) by deleting every second bipyramid. The sheet contains twice as many tetrahedra as bipyramids, each bipyramid is linked through its equatorial vertices to four tetrahedra, but the tetrahedra are only connected to two bipyramids.

Miscellaneous sheets based upon uranyl pentagonal bipyramids and tetrahedra (or $Se^{4+}O_3$ pyramids) dominated by single linkages between polyhedra are shown in Figure 7. The structures of $Pb[(UO_2)(SeO_3)_2]$ and $Ba[(UO_2)(SeO_3)_2]$ contain sheets with identical compositions, but different connections between polyhedra (Figs. 7a, b). In both sheets, each bipyramid is linked to four different SeO_3 pyramids, three by the sharing of a single vertex, and one by sharing an edge. Half of the SeO_3 groups are linked to two bipyramids only by sharing single vertices (designated *A*), whereas the other half are connected to one bipyramid by sharing a vertex, and another by sharing an edge (designated *B*). The distinction between the two sheets lies in the arrangement of these two types of SeO_3 groups. In the sheet shown in Figure 7a, a circuit about any bipyramid involves the sequence *ABAB*, whereas the circuits in the sheet in Figure 7b involve the sequence *AABB*.

The structure of $K[(UO_2)(CrO_4)(OH)](H_2O)_{1.5}$ contains dimers of edge-sharing uranyl pentagonal bipyramids, and all of the equatorial vertices of the bipyramids that are not shared within the dimer are linked to chromate tetrahedra (Fig. 7c). Each tetrahedron is connected to three different dimers of bipyramids.

The structures of $Cs[(UO_2)(PO_3)_3]$ (Fig. 7d) and $[(UO_2)H(PO_3)_3]$ (Fig. 7e) are closely related in that each contains sheets of uranyl pentagonal bipyramids and phosphate tetrahedra, with groups of tetrahedra linked by vertex sharing. In $Cs[(UO_2)(PO_3)_3]$, three phosphate tetrahedra are linked, and non-bridging O atoms are shared with four different bipyramids. All of the equatorial vertices of the bipyramids are shared with tetrahedra. In $[(UO_2)H(PO_3)_3]$, phosphate tetrahedra are linked into dimers and trimers, and only four of the equatorial vertices of the bipyramids are shared with tetrahedra.

The structure of $(NH_4)[(UO_2)F(SeO_4)](H_2O)$ is based upon the uranyl selenate sheet shown in Figure 7f. The sheet contains uranyl pentagonal bipyramids that are linked into chains by the sharing of a single vertex between adjacent bipyramids. According to Blatov *et al.* (1989), the vertices shared between the bipyramids correspond to F, which is uncommon in uranyl compounds. The three equatorial vertices of the bipyramids that are not shared within the chain are linked to selenate tetrahedra. Each selenate tetrahedron is connected to three bipyramids of two chains, resulting in the uranyl selenate sheet. It is interesting to note that this is the only known sheet that involves uranyl pentagonal bipyramids and tetrahedra in which the bipyramids are linked by sharing single vertices.

The structure of $Co(H_2O)_6[(UO_2)_5(SO_4)_8(H_2O)](H_2O)_5$ contains the complex sheet of uranyl pentagonal bipyramids and sulfate tetrahedra shown in Figure 7g. The structure has two types of bipyramids; those that share all five, and those that share only four of their equatorial vertices with sulfate tetrahedra. In the latter case, the fifth equatorial vertex of the bipyramid corresponds to H_2O. There are three types of tetrahedra in the sheet, which share two, three, or four of their vertices with bipyramids. The inclusion of H_2O in an equatorial position of some of the bipyramids, as well as the connection of some sulfate tetrahedra to only two bipyramids, results in small pores within the sheets of polyhedra.

Sheet anion-topologies containing triangles and pentagons

Those structures based upon sheet anion-topologies containing only triangles and pentagons are presented in Table 5 and Figure 8. Only five such topologies have been found in structures, and in all but one case, all of the pentagons of the anion topologies are occupied with uranyl ions, giving uranyl pentagonal bipyramids, whereas the triangles remain vacant. Thus, the sheet anion-topologies in Figure 8 represent five distinct types of sheets composed only of uranyl pentagonal bipyramids.

Protasite anion-topology: The protasite anion-topology (Fig. 8a) is the basis for two distinct types of sheet. Population of each pentagon of the anion topology with a uranyl ion results in the well-known α-U_3O_8-type sheet of edge-sharing uranyl pentagonal bipyramids (Fig. 8b). This sheet is the basis of seven known uranyl oxide hydrate minerals, as well as four synthetic phases. The sheet topology is compatible with a variety of interlayer constituents, including Pb, Na, K, Ca, Sr, Ba and Cs. The net charge of the sheet is variable, as there are four distinct distributions of hydroxyl ions known for this anion topology (Fig. 9).

Three uranyl sulfates are known that contain a sheet based upon the protasite anion-topology (Fig. 8c). In

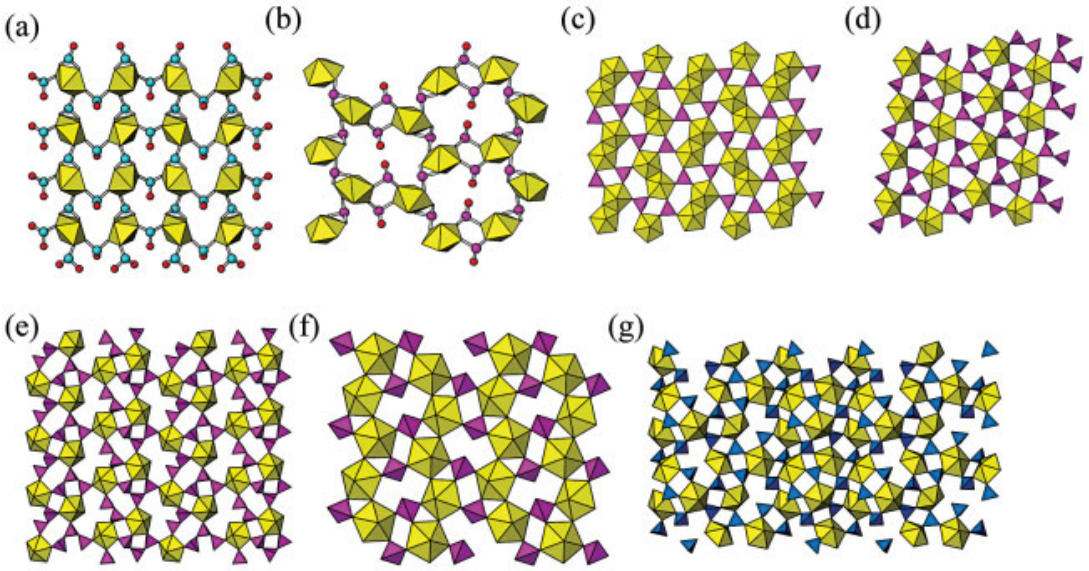

FIG. 7. Miscellaneous sheets of uranyl polyhedra and other polyhedra containing higher-valence cations that are dominated by the sharing of vertices. The corresponding compounds are listed in Table 4.

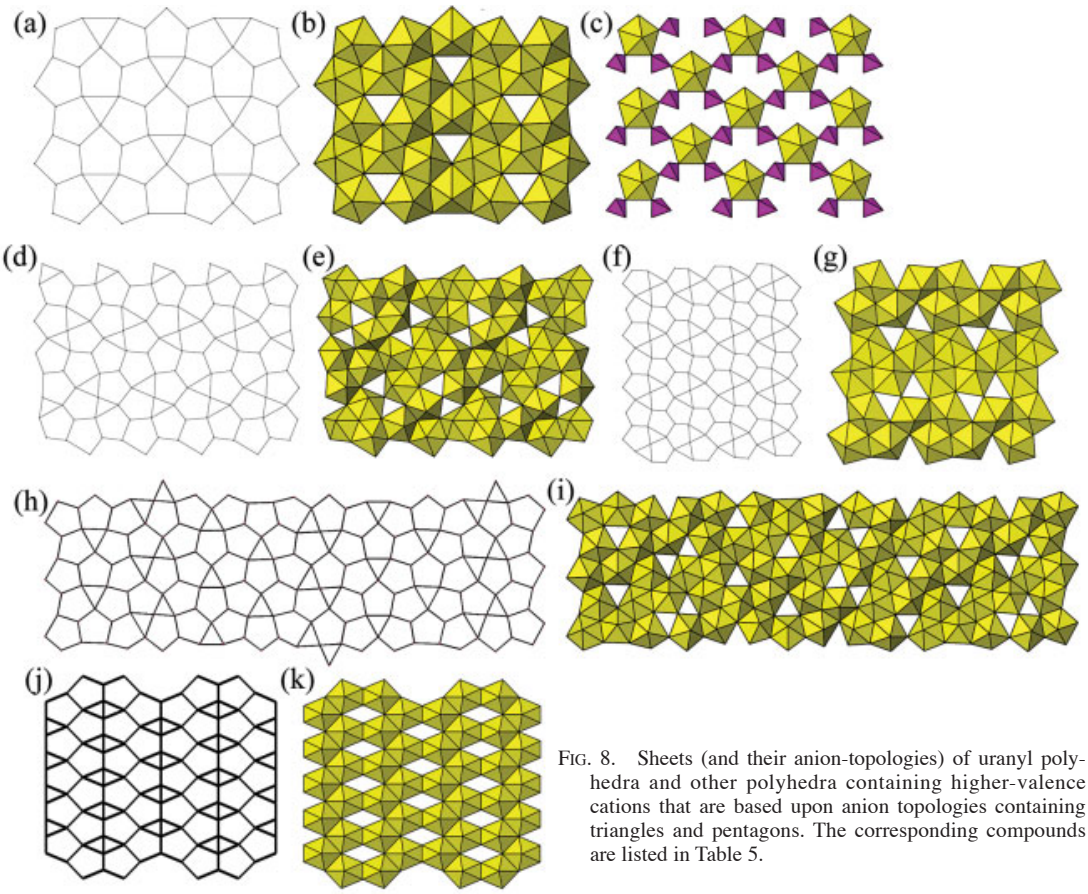

FIG. 8. Sheets (and their anion-topologies) of uranyl polyhedra and other polyhedra containing higher-valence cations that are based upon anion topologies containing triangles and pentagons. The corresponding compounds are listed in Table 5.

this sheet, uranyl pentagonal bipyramids are connected by sharing vertices with sulfate tetrahedra, such that each bipyramid and each tetrahedron is four-connected within the sheet.

$Na[(UO_2)_4O_2(OH)_5](H_2O)_2$ anion-topology: The structure of $Na[(UO_2)_4O_2(OH)_5](H_2O)_2$, which was obtained by mild hydrothermal synthesis, represents the first occurrence of its underlying sheet anion-topology (Fig. 8d). The composition of this sheet is distinct from any known sheet with the protasite anion-topology, despite the fact that it is composed only of uranyl pentagonal bipyramids. The sheet in $Na[(UO_2)_4O_2(OH)_5](H_2O)_2$ is closely related to that of $Ca[(UO_2)_4O_3(OH)_4](H_2O)_2$, as outlined below.

Fourmarierite anion-topology: The fourmarierite anion-topology (Fig. 8f) is the basis of topologically identical sheets found in fourmarierite, schoepite, and metaschoepite. The sheets in each mineral are arrangements of uranyl pentagonal bipyramids; in fourmarierite, the sheets have a net negative charge, whereas those in schoepite and metaschoepite are electroneutral. In fourmarierite, Pb^{2+} cations and H_2O groups occupy interlayer positions, but the interlayers of schoepite and metaschoepite contain only H_2O. In a study of the crystal chemistry of fourmarierite, Li & Burns (2000a) found evidence for significant variability of both the amount of Pb in the interlayer, and the OH content of the sheets. Li & Burns (2000a) also synthesized a crystal intermediate in composition between schoepite and fourmarierite, suggesting that a solid-solution series involving a coupled substitution is possible between these minerals. Li & Burns (2000a) proposed the general formula $Pb_{(1-x)}[(UO_2)_4O_{(3-2x)}(OH)_{(4+2x)}](H_2O)_4$ for fourmarierite.

Vandendriesscheite anion-topology: The vandendriesscheite anion-topology is the most complex topology known that contains only pentagons and triangles (Figs. 8h, i). The sheet is truly extraordinary in that it contains a 41 Å primitive repeat-distance, a reflection of the complex arrangement of pentagons and triangles in its corresponding anion-topology. Notably, there are several simpler topologies that are also based

TABLE 5. STRUCTURES CONTAINING SHEETS BASED UPON ANION TOPOLOGIES CONTAINING TRIANGLES AND PENTAGONS

Name	Fig.	Formula	S. G.	*a* (Å)	*b* (Å)	*c* (Å)	β (°)	Ref.
Protasite	8b	$Ba[(UO_2)_3O_3(OH)_2](H_2O)_3$	*Pn*	12.2949	7.2206	6.9558	90.401	1
Billietite	8b	$Ba[(UO_2)_3O_2(OH)_3]_2(H_2O)_4$	$Pbn2_1$	12.0720	30.167	7.1455		1
Becquerelite	8b	$Ca[(UO_2)_3O_2(OH)_3]_2(H_2O)_8$	$Pn2_1a$	13.8527	12.3929	14.9297		2
	8b	$Sr_{1.27}[(UO_2)_3O_{3.54}(OH)_{1.46}](H_2O)_3$	*P*3	7.020		6.992		2
	8b	$Cs_3[(UO_2)_{12}O_7(OH)_{13}](H_2O)_3$	*R*3	14.124		22.407		3
	8b	$Na_2[(UO_2)_3O_3(OH)_2]$	$P2_1/n$	7.0476	11.4126	12.0274	90.563	4
Richetite	8b	$(Fe,Mg)_xPb_{8.57}[(UO_2)_{18}O_{18}(OH)_{12}]_2(H_2O)_{41}$	*P*1	20.939	12.100	16.345	115.37	5
Agrinierite	8b	$K_2(Ca_{0.65}Sr_{0.35})[(UO_2)_3O_3(OH)_2]_2(H_2O)_5$	*F*2*mm*	14.094	14.127	24.106		6
Masuyite	8b	$Pb[(UO_2)_3O_3(OH)_2](H_2O)_3$	*Pn*	12.241	7.008	6.983	90.40	7
Compreignacite	8b	$K_2[(UO_2)_3O_2(OH)_3]_2(H_2O)_7$	*Pnnm*	14.859	7.175	12.187		8
	8b	α-U_3O_8	*C*2*mm*	6.716	11.960	4.147		9
	8c	$Mg[(UO_2)(SO_4)_2](H_2O)_{11}$	*C*2/*c*	11.334	7.715	21.709	102.22	10
	8c	$[(UO_2)(SO_4)_2]H_2(H_2O)_5$	*C*2/*c*	11.008	8.242	15.619	113.71	11
	8c	$K_2[UO_2(SO_4)_2](H_2O)_2$	*Pnma*	13.806	11.577	7.292		12
	8e	$Na[(UO_2)_4O_2(OH)_5](H_2O)_2$	$P\bar{1}$	8.0746	8.4633	11.2181	87.492	13
Fourmarierite	8g	$Pb[(UO_2)_4O_3(OH)_4](H_2O)_4$	$Bb2_1m$	13.986	16.400	14.293		14
Metaschoepite	8g	$[(UO_2)_4O(OH)_6](H_2O)_5$	*Pbcm*	14.6861	13.9799	16.7063		15
Schoepite	8g	$[(UO_2)_8O_2(OH)_{12}](H_2O)_{12}$	$P2_1ca$	14.337	16.813	14.731		16
Vandendriesscheite	8i	$Pb_{1.57}[(UO_2)_{10}O_6(OH)_{11}](H_2O)_{11}$	*Pbca*	14.116	41.378	14.535		17
	8k	α-$Cs_2[(UO_2)_2O_3]$	*C*2/*m*	14.528	4.2638	7.605	112.	18
	8k	β-$Cs_2[(UO_2)_2O_3]$	*C*2/*m*	14. 615	4.3199	7.465	113.78	18

References: (1) Pagoaga *et al.* (1987), (2) Burns & Li (2002), (3) Hill & Burns (1999), (4) Li & Burns (2001a), (5) Burns (1998b), (6) Cahill & Burns (2000), (7) Burns & Hanchar (1999), (8) Burns (1998c), (9) Loopstra (1977), (10) Serezhkin *et al.* (1981b), (11) Alcock *et al.* (1982), (12) Niinistö *et al.* (1979), (13) Burns & Deely (2002), (14) Piret (1985), (15) Weller *et al.* (2000), (16) Finch *et al.* (1996), (17) Burns (1997), (18) van Egmond (1976b).

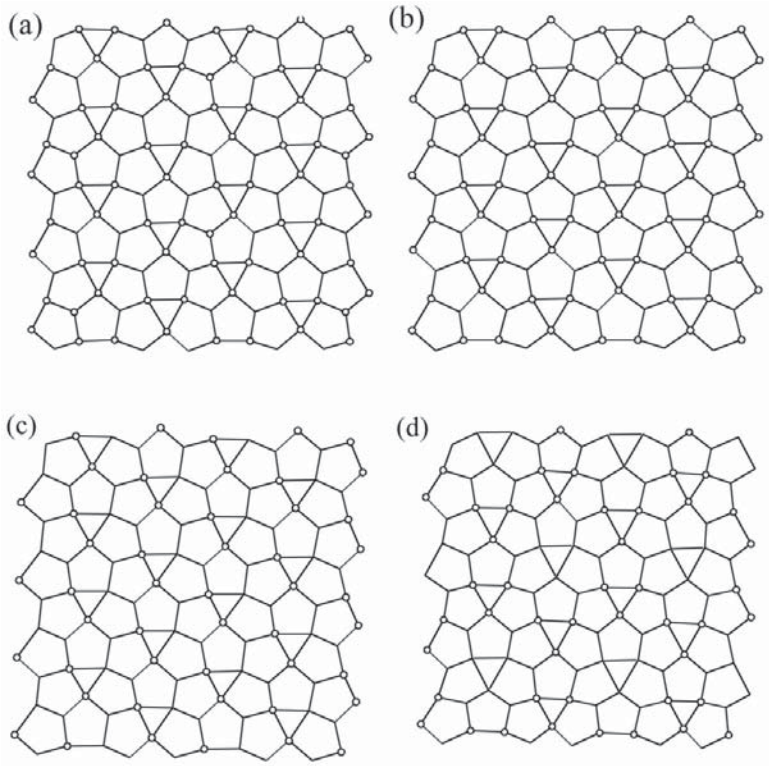

FIG. 9. Observed distributions of OH groups within the protasite anion-topology. The locations of OH groups are indicated by open circles. Vertices in the anion topology that are not marked by circles correspond to O atoms.

upon pentagons and triangles, and factors that result in the stabilization of the complex vandendriesscheite sheet are unclear. However, the sheet is related to a simpler sheet that contains only uranyl pentagonal bipyramids. Using an approach involving stacking sequences of chains of polygons, Burns (1997) showed that the vandendriesscheite anion-topology is built of modules of the much simpler protasite (α-U_3O_8) anion-topology.

$Cs_2[(UO_2)_2O_3]$ anion-topology: The structures of the alpha and beta polymorphs of $Cs_2[(UO_2)_2O_3]$ each possess sheets of uranyl pentagonal bipyramids (Fig. 8k) that are based upon the sheet anion-topology shown in Figure 8j. Each of the pentagons in the anion topology share three of their edges with adjacent pentagons, and all of the pentagons are populated by uranyl ions in the observed sheets. The sheet contains a zig-zag chain of edge-sharing pentagonal bipyramids that is two polyhedra wide (vertical in Fig. 8k), topologically identical to that in the zippeite sheet (see below, Fig. 11v). Unlike in the zippeite sheet, these chains are linked by sharing of edges between bipyramids of adjacent chains. The triangles of the topology are vacant, and the Cs cations are located between the sheets of polyhedra.

The distinction between the various sheets containing only uranyl pentagonal bipyramids is most apparent in the distribution of the triangles within the sheet anion-topology, which remain vacant in the populated sheets. In the case of the protasite anion-topology and derivative sheets, each triangle is isolated from the others and points in the same direction. In $Na[(UO_2)_4O_2(OH)_5](H_2O)_2$, the triangles occur in pairs that share a vertex, resembling bowties, and there are two distinct orientations of bowties. The fourmarierite anion-topology also contains triangle bowties, but differs from $Na[(UO_2)_4O_2(OH)_5](H_2O)_2$ in that each is oriented in the same direction. The vandendriesscheite anion-topology contains both isolated triangles and triangle bowties; all bowties are aligned, whereas the isolated triangles occur in two orientations. The $Cs_2[(UO_2)_2O_3]$ anion-topology contains pairs of triangles that share an edge, giving a flattened rhomb.

The uranyl oxide hydrates based upon sheets of uranyl pentagonal bipyramids are the first minerals

to form where uraninite, UO_{2+x}, is altered in a moist, oxidizing environment (Finch & Ewing 1992). Studies of natural analogues, as well as laboratory-scale simulations, have also demonstrated that several of these minerals form where spent nuclear fuel is altered in an oxidizing environment in the presence of water, similar to conditions expected in the proposed geological repository for nuclear waste at Yucca Mountain, Nevada (*e.g.*, Pearcy *et al.* 1994, Finn *et al.* 1996, Finch *et al.* 1999a). Recently, Burns *et al.* (2004a) showed that Np^{5+} is incorporated into synthetic powders of the Na analogue of compreignacite, which supports the hypothesis that formation of such minerals in a geological repository may impact the future mobilities of key radionuclides.

Sheet anion-topologies containing triangles, squares and pentagons

Seventy-one uranyl compounds are known that contains sheets that are based upon anion topologies containing triangles, squares and pentagons. In all cases at least some of the pentagons are populated by uranyl ions; thus all sheets in this class contain uranyl pentagonal bipyramids. The triangles of the anion topologies are occupied by BO_3 groups in two structures, and by the face of a tetrahedron in many structures. The square sites of the anion topologies provide coordination environments for cations in square pyramidal or octahedral coordination.

Uranophane anion-topology: The uranophane anion-topology is elegant in its simplicity (Fig. 10a). It contains chains of edge-sharing pentagons that are separated by chains of edge-sharing triangles and squares. This anion topology is the basis for a chemically diverse group of compounds that includes the important group of the uranophane minerals. In all but two of the representative structures, the pentagons are all populated by uranyl ions, giving pentagonal bipyramids. In the case of ulrichite, half of the pentagons are populated by Ca, and half of the pentagons contain Na in $Na_{5.5}(UO_2)_3(H_{0.5}PO_4)(PO_4)_3$, but the Na is not considered to be part of the structural unit for the purposes of illustration in Figure 10h. There are 17 structures known that contain sheets based upon the uranophane anion-topology, of which 11 are minerals; they are grouped in Table 10 (see below) according to the specific population of the topology.

In the compounds $Na[(UO_2)(BO_3)]$ and $Li[(UO_2)(BO_3)]$, the triangles of the uranophane anion-topology are populated by BO_3 groups (Fig. 10b). These anhydrous compounds are readily synthesized at elevated temperatures, and contain topologically identical sheets.

The uranophane-group minerals are uranyl silicates that have sheets based upon the uranophane anion-topology. In each case, the triangles of the topology correspond to the faces of silicate tetrahedra, but three graphical isomers of the uranyl silicate sheet are known to occur because of different orientations of the silicate tetrahedra. This may readily be seen by examining the sheets given in Figures 10c–e, with emphasis on the orientation of the apical, non-bridging, O or OH groups of the silicate tetrahedra. The structure of oursinite, which was only recently reported, represents a new graphical isomer. With the exception of kasolite, all of the uranophane-group minerals with known structures contain acid silicate groups, where the hydroxyl group is non-bridging within the sheet.

Studies of natural analogues (Pearcy *et al.* 1994), as well as laboratory simulations (Wronkiewicz *et al.* 1992, 1996, Finch *et al.* 1999a) have shown that alteration of spent nuclear fuel in the proposed geological repository at Yucca Mountain, Nevada, will likely result in the formation of uranophane and boltwoodite. Burns *et al.* (1997b) argued that these minerals may incorporate various radionuclides released from the nuclear waste, and as such, they may have an impact upon rates of radionuclide release from the proposed repository. Using crystals of natural boltwoodite, Burns (1999c) ion-exchanged Cs into interlayer positions of the structure by treating crystals with solutions containing CsCl at elevated temperatures. Notably, ion exchange was accomplished for single crystals that remained intact even following exchange, and ion exchange was demonstrated by structure solution for a treated crystal. This was the first demonstration of ion exchange in a single crystal of a uranyl mineral, and demonstrated that radioactive Cs can be accommodated in the interlayer region of boltwoodite. Recently, Burns *et al.* (2004a) showed that Np^{5+} is incorporated into powders of uranophane synthesized at pH ~5 and 100°C, conditions similar to those expected in the proposed repository at Yucca Mountain where water may first contact the nuclear waste.

The structure of ulrichite was recently revisited by Kolitsch & Giester (2001); this work confirmed many of the earlier-reported aspects of the structure, but provides a new space-group assignment and significantly improved precision of the structural parameters. Ulrichite contains a sheet that is based upon the uranophane anion-topology, with half of the pentagons populated by uranyl ions, and the other half populated by $Ca\phi_8$ polyhedra (Fig. 10f). The triangles of the topology are populated by phosphate tetrahedra.

The structure of umohoite was once considered to contain sheets of uranyl hexagonal bipyramids (Makarov & Anikina 1963). A redetermination of the structure revealed a new uranyl molybdate sheet that is based upon the uranophane anion-topology (Krivovichev & Burns 2000a). Each pentagon in the anion topology is populated by a uranyl ion, giving uranyl pentagonal bipyramids, and the squares of the topology are equatorial vertices of distorted $Mo\phi_5$ polyhedra (Fig. 10g), and the non-sheet ligand is H_2O. The interlayer of the structure contains only H_2O, with the sheets connected by H bonds.

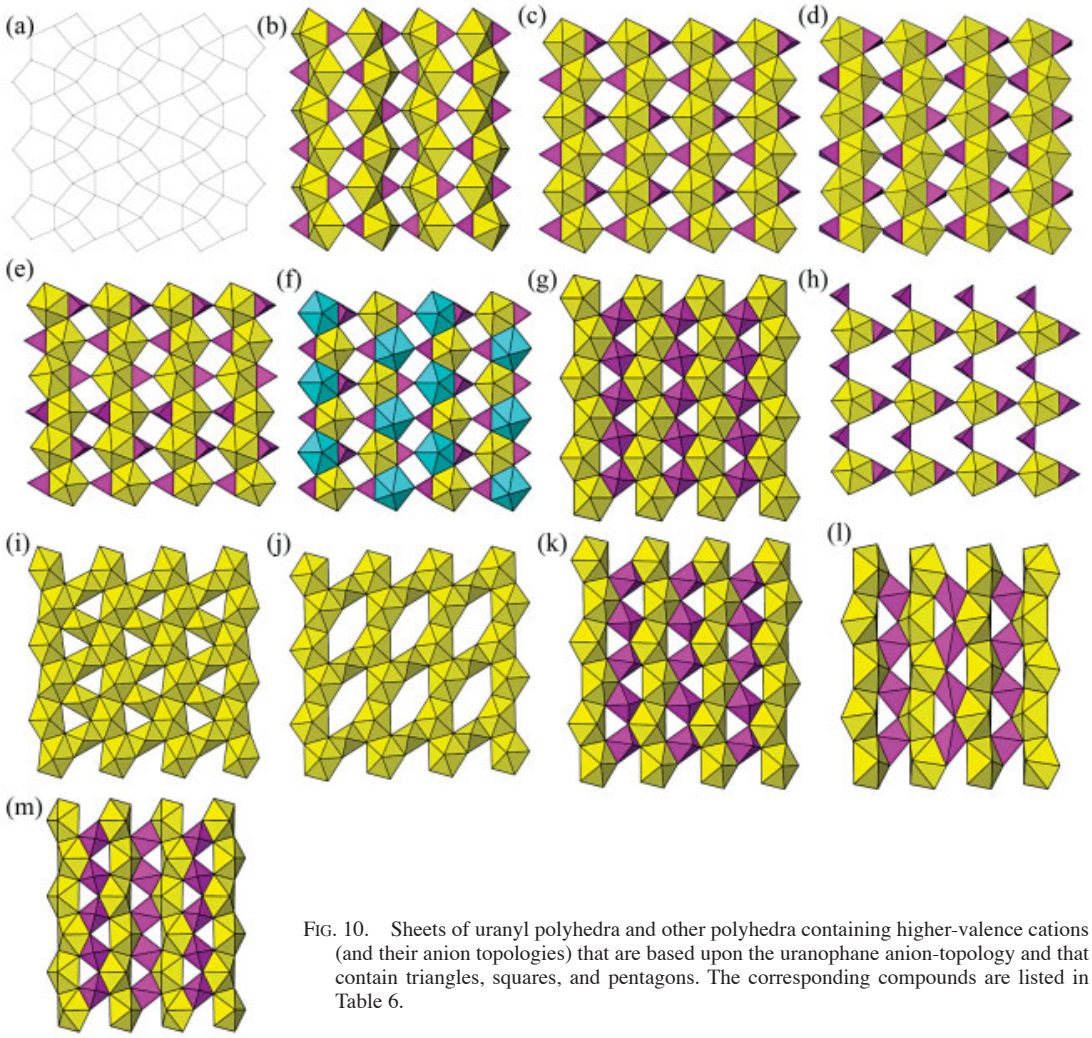

FIG. 10. Sheets of uranyl polyhedra and other polyhedra containing higher-valence cations (and their anion topologies) that are based upon the uranophane anion-topology and that contain triangles, squares, and pentagons. The corresponding compounds are listed in Table 6.

The structures of $K_2[(UO_2)_2O_3]$, $[H_2(UO_2)_3O_4]$, $[(UO_2)(CuO_4)]$, schmitterite, and $K[(UO_2)(NbO_4)]$ all contain sheets based upon the uranophane anion-topology, in which all pentagons are occupied by uranyl ions, and the squares of the topology are occupied by various cations (Figs. 10i–m). In $K_2[(UO_2)_2O_3]$ (Fig. 10i) and $[H_2(UO_2)_3O_4]$ (Fig. 10j), uranyl ions populate the squares of the anion topology, resulting in uranyl square bipyramids, with all squares occupied in $K_2[(UO_2)_2O_3]$ and only half of the squares occupied in $[H_2(UO_2)_3O_4]$. Schmitterite is unusual in that it is the only uranyl tellurite with a structure based upon the uranophane anion-topology (Fig. 10l). Each square contains Te^{4+} in a highly distorted pyramidal geometry owing to the stereoactive lone-electron pair on the cation.

A substantial family of synthetic uranyl phosphate framework structures has recently been discovered that contains sheets based upon the uranophane anion-topology, with the triangles populated by the faces of phosphate tetrahedra. Uranyl polyhedra in the interlayer regions provide direct connections between the sheets, and this family of structures is included with the framework structures discussed below (see below, Figs. 15m–o).

Francevillite anion-topology: The francevillite anion-topology (Fig. 11a) consists of pairs of edge-sharing pentagons and edge-sharing squares as well as triangles. Twelve structures are known in which sheets are based upon this anion topology, of which four are minerals (Table 6). In all of the sheets, each

TABLE 6. STRUCTURES CONTAINING SHEETS BASED UPON ANION TOPOLOGIES WITH TRIANGLES, SQUARES AND PENTAGONS

Name	Fig.	Formula	S. G.	*a* (Å)	*b* (Å)	*c* (Å)	β (°)	Ref.
	10b	$Na[(UO_2)(BO_3)]$	*Pcam*	10.712	5.780	6.862		1
	10b	$Li[(UO_2)(BO_3)]$	$P2_1/c$	5.767	10.574	6.835	105.04	2
α-uranophane	10c	$Ca[(UO_2)(SiO_3OH)]_2(H_2O)_5$	$P2_1$	15.909	7.002	6.665	97.27	3
Boltwoodite	10c	$(K_{0.56}Na_{0.42})[(UO_2)(SiO_3OH)](H_2O)_{1.5}$	$P2_1/m$	7.077	7.060	6.648	104.98	4
	10c	$Cs[(UO_2)(SiO_3OH)]_2$	$P2_1/m$	7.4038	7.0774	6.6566	104.314	5
Cuprosklodowskite	10c	$Cu[(UO_2)(SiO_3OH)]_2(H_2O)_6$	*P*1	7.052	9.267	6.655	89.84	6
Sklodowskite	10c	$Mg[(UO_2)(SiO_3OH)]_2(H_2O)_6$	*C*2/*m*	17.382	7.047	6.610	105.9	7
Kasolite	10c	$Pb[(UO_2)(SiO_4)](H_2O)$	$P2_1/c$	6.704	6.932	13.252	104.22	8
	10c	$Mg[(UO_2)(AsO_4)]_2(H_2O)_4$	*C*2/*m*	18.207	7.062	6.661	99.65	9
Oursinite	10d	$Co[(UO_2)(SiO_3OH)]_2(H_2O)_6$	*Cmca*	7.0494	17.550	12.734		10
β-uranophane	10e	$Ca[(UO_2)(SiO_3OH)]_2(H_2O)_5$	$P2_1/a$	13.966	15.443	6.632	91.38	11
Ulrichite	10f	$CaCu(UO_2)(PO_4)_2{\cdot}4H_2O$	$P2_1/c$	12.784	6.996	13.007	91.92	12
Umohoite	10g	$[(UO_2)MoO_4(H_2O)](H_2O)$	$P\bar{1}$	6.375	7.529	14.628	85.95	13
	10h	$Na_{5.5}(UO_2)_3(H_{0.5}PO_4)(PO_4)_3$	*P*1	6.675	6.922	10.732	82.29	14
	10i	$K_2[(UO_2)_2O_3]$	$P2_1$	6.931	7.690	6.984	109.69	15
	10j	$[H_2(UO_2)_3O_4]$	$P\bar{1}$	6.802	7.417	5.556	125.5	16
	10k	$[(UO_2)(CuO_4)]$	$P\bar{1}$	6.516	7.614	5.615	125.18	17
Schmitterite	10l	$[(UO_2)(TeO_3)]$	$Pca2_1$	10.161	5.363	7.862		18
	10m	$K[(UO_2)(NbO_4)]$	*Pcab*	7.579	11.321	15.259		19
Francevillite	11b	$Ba_{0.96}Pb_{0.04}[(UO_2)_2(V_2O_8)](H_2O)_5$	*Pcan*	10.419	8.510	16.763		20
Curienite	11b	$Pb[(UO_2)_2(V_2O_8)](H_2O)_5$	*Pcan*	10.40	8.45	16.34		21
Uranosphaerite	11b	$[Bi(UO_2)O_2OH]$	$P2_1/n$	7.559	7.811	7.693	92.88	22
	11b	$K_2[(UO_2)_2(V_2O_8)]$	$P2_1/a$	10.47	8.41	6.59	103.8	23
Sengierite	11b	$Cu_2[(UO_2)_2(V_2O_8)](OH)_2(H_2O)_6$	$P2_1/a$	10.599	8.093	10.085	103.42	24
	11b	$Ni[(UO_2)_2(V_2O_8)](H_2O)_4$	*Pnam*	10.60	8.25	15.12		25
	11b	$Cs_2[(UO_2)_2(V_2O_8)]$	$P2_1/a$	10.521	8.4369	7.308	106.08	26
	11b	$Cs_2[(UO_2)_2(Nb_2O_8)]$	$P2_1/c$	7.430	8.700	10.668	105.08	27
	11b	$K_2[(UO_2)_2(Cr_2O_8)]$	$P2_1/c$	6.5483	8.3548	10.4200	105.040	28
	11b	$Rb_2[(UO_2)_2(Cr_2O_8)]$	$P2_1/c$	6.8677	8.3599	10.4625	106.004	28
	11b	$Cs_2[(UO_2)_2(Cr_2O_8)]$	$P2_1/c$	7.2643	8.3803	10.5100	106.399	28
	11b	$Mg_2[(UO_2)_2(Cr_2O_8)](H_2O)_4$	*Pnam*	10.5825	15.1337	8.1425		28
	11d	$\beta\text{-}U_3O_8$	*Cmcm*	7.069	11.445	8.303		29
Wyartite	11d	$CaU^{5+}(UO_2)_2(CO_3)O_4(OH)(H_2O)_7$	$P2_12_12_1$	11.271	7.105	20.807		30
Ianthinite	11d	$[U_2^{4+}(UO_2)_4O_6(OH)_4(H_2O)_4](H_2O)_5$	$P2_1ca$	7.178	11.473	30.39		31
Spriggite	11d	$Pb_3[(UO_2)_6O_8(OH)_2](H_2O)_3$	*C*2/*c*	28.355	11.990	13.998	104.248	32
Iriginite	11f	$[(UO_2)Mo_2O_7(H_2O)_2](H_2O)$	*Pbcm*	6.705	12.731	11.524		33
	11f	$[(UO_2)Mo_2O_7(H_2O)_2]$	C2/*c*	35.071	6.717	11.513	90.069	34
	11f	$[Ca(UO_2)(Mo_4O_7)_2]$	$P2_1/n$	6.651	8.236	11.447	90.44	35
Sayrite	11h	$Pb_2[(UO_2)_5O_6(OH)_2](H_2O)_4$	$P2_1/c$	10.704	6.960	14.533	116.81	36
	11h	$K_2[(UO_2)_5O_8](UO_2)_2$	*Pbam*	6.945	19.533	7.215		37
	11j	$[Pb_3(UO_2)_{11}O_{14}]$	*Pmmn*	28.459	8.3790	6.7650		38
	11j	$[Sr_3(UO_2)_{11}O_{14}]$	*Pmmn*	28.508	8.3806	6.7333		39
	11l	$Sr_{2.82}(H_2O)_2[(UO_2)_4O_{3.82}(OH)_{3.18}]_2$	*Pnam*	12.314	12.961	8.404		40
Curite	11l	$Pb_3[(UO_2)_8O_8(OH)_6](H_2O)_3$	*Pnam*	12.551	13.003	8.390		41
	11n	$K_5[(UO_2)_{10}O_8(OH)_9](H_2O)$	*Pn*	13.179	20.895	13.431	106.32	42
	11p	$Ca[(UO_2)_4O_3(OH)_4](H_2O)_2$	$P\bar{1}$	8.0556	8.4214	10.958	87.922	43

TABLE 6. STRUCTURES CONTAINING SHEETS BASED UPON ANION TOPOLOGIES WITH TRIANGLES, SQUARES AND PENTAGONS

Name	Fig.	Formula	S. G.	*a* (Å)	*b* (Å)	*c* (Å)	β (°)	Ref.
	11r	$Cs_4[(UO_2)_5O_7]$	*Pbcn*	18.776	7.070	14.958		44
Vandenbrandeite	11t	$[(UO_2)Cu(OH)_4]$	$P\bar{1}$	7.855	5.449	6.089	101.90	45
Zippeite	11v	$K_3(H_2O)_3[(UO_2)_4(SO_4)_2O_3(OH)]$	*C*2	8.7524	13.9197	17.6972	104.178	46
"Na zippeite"	11v	$Na_5(H_2O)_{12}[(UO_2)_8(SO_4)_4O_5(OH)_3]$	$P2_1/n$	17.6425	14.6272	17.6922	104.461	46
"Mg zippeite"	11v	$Mg(H_2O)_{3.5}[(UO_2)_2(SO_4)O_2]$	*C*2/*m*	8.6514	14.1938	17.7211	104.131	46
"Zn zippeite"	11v	$Zn(H_2O)_{3.5}[(UO_2)_2(SO_4)O_2]$	*C*2/*m*	8.6437	14.1664	17.701	104.041	46
"Co zippeite"	11v	$Co(H_2O)_{3.5}[(UO_2)_2(SO_4)O_2]$	*C*2/*m*	8.650	14.252	17.742	104.092	46
Marecottite	11v	$Mg_3(H_2O)_{18}[(UO_2)_4O_3(OH)(SO_4)_2]_2(H_2O)_{10}$	$P\bar{1}$	10.815	11.249	13.851	72.412	47
	11v	$(NH_4)_4(H_2O)[(UO_2)_2(SO_4)O_2]_2$	*C*2/*m*	8.6987	14.166	17.847	104.117	46
	11v	$(NH_4)_2[(UO_2)_2(SO_4)O_2]$	*Cmca*	14.2520	8.7748	17.1863		46
	11v	$Mg_2(H_2O)_{11}[(UO_2)_2(SO_4)O_2]_2$	$P2_1/c$	8.6457	17.2004	18.4642	102.119	46
	11x	$K_2(UO_2)_2(WO_5)O$	$P2_1/n$	8.083	28.724	9.012	102.14	48
	11x	$Rb_2(UO_2)_2(WO_5)O$	$P2_1/n$	8.234	28.740	9.378	104.59	48
	11x	$Tl_2[(UO_2)_2O(MoO_5)]$	$P2_1/n$	8.2527	28.5081	9.1555	104.122	49
	11z	$K_6(UO_2)_5(VO_4)_2O_5$	$P2_1/c$	6.856	24.797	7.135	98.79	50
	11z	$Na_6(UO_2)_5(VO_4)_2O_5$	$P2_1/c$	12.584	24.360	7.050	100.61	50
	11z	α-$Rb_6U_5V_2O_{23}$	*C*2/*c*	24.887	7.099	14.376	103.92	51
	11z	β-$Rb_6U_5V_2O_{23}$	$P2_1/n$	7.1635	14.079	24.965	90.23	51
	11ab	$K_8(UO_2)_8(MoO_5)_3O_6$	*P*4/*n*	23.488		6.7857		52
	11ad	$[Mg(UO_2)(B_2O_5)]$	*Pcam*	9.747	7.315	7.911		53
Wölsendorfite	11af	$Pb_{0.16}Ba_{0.36}[(UO_2)_{14}O_{19}(OH)_4](H_2O)_{12}$	*Cmcm*	14.131	13.885	55.969		54
	11ah	$Cs_4[(UO_2)_3O(MoO_4)_2(MoO_5)]$	*P*1	7.510	7.897	9.774	81.269	55
	11aj	$Ag_{10}[(UO_2)_8O_8(Mo_5O_{20})]$	*C*2/*c*	24.672	23.401	6.7932	94.985	56
	11aj	$Na_{10}[(UO_2)_8O_8(Mo_5O_{20})]$	*C*2/*c*	24.359	23.506	6.8028	94.85	56
	11al	$K_2(UO_2)_2(MoO_4)O_2$	$P2_1/c$	8.250	15.337	8.351	104.75	57

References: (1) Gasperin (1988), (2) Gasperin (1990), (3) Ginderow (1988), (4) Burns (1998d), (5) Burns (1999c), (6) Rosenzweig & Ryan (1975), (7) Ryan & Rosenzweig (1977), (8) Rosenzweig & Ryan (1977a), (9) Bachet *et al.* (1991), (10) Kubatko & Burns (2006), (11) Viswanathan & Harneit (1986), (12) Kolitsch & Giester (2001), (13) Krivovichev & Burns (2000a), (14) Gorbunova *et al.* (1980), (15) Sainc (1989), (16) Siegel *et al.* (1972a), (17) Dickens *et al.* (1993), (18) Meunier & Galy (1973), (19) Gasperin (1987b), (20) Mereiter (1986e), (21) Borène & Cesbron (1971), (22) Hughes *et al.* (2003), (23) Appleman & Evans (1965), (24) Piret *et al.* (1980), (25) Borène & Cesbron (1970), (26) Dickens *et al.* (1992), (27) Gasperin (1987c), (28) Locock *et al.* (2004), (29) Loopstra (1970), (30) Burns & Finch (1999), (31) Burns *et al.* (1997c), (32) Brugger *et al.* (2004), (33) Krivovichev & Burns (2000b), (34) Krivovichev & Burns (2002c), (35) Lee & Jaulmes (1987); Marsh (1988), (36) Piret *et al.* (1983), (37) Kovba (1972), (38) Ijdo (1993b), (39) Cordfunke *et al.* (1991), (40) Burns & Hill (2000a), (41) Li & Burns (2000b), (42) Burns & Hill (2000b), (43) Glatz *et al.* (2002), (44) van Egmond (1976a), (45) Rosenzweig & Ryan (1977b), (46) Burns *et al.* (2003), (47) Brugger *et al.* (2003), (48) Obbade *et al.* (2003c), (49) Krivovichev & Burns (2003g), (50) Dion *et al.* (2000), (51) Obbade *et al.* (2003a), (52) Obbade *et al.* (2003b), (53) Gasperin (1987a), (54) Burns (1999b), (55) Krivovichev & Burns (2002b), (56) Krivovichev & Burns (2003h), (57) Obbade *et al.* (2003b).

of the pentagons of the anion topology is populated by uranyl ions, giving uranyl pentagonal bipyramids. The francevillite group of minerals, as well as synthetic uranyl vanadates, involves population of the squares of the anion topology by VO_5 square pyramids, resulting in dimers of edge-sharing pyramids. Within each dimer, the apical vertices of the two adjacent square pyramids point in opposite directions. One structure is known that contains NbO_5 square pyramids. Recently, five structures have been reported with the francevillite-type sheet in which the squares are populated by CrO_5 square pyramids (Locock *et al.* 2004). These structures are remarkable in that they contain pentavalent chromium, which is uncommon in crystal structures. In each case, low-valence cations in the interlayers of the structures,

which also contain H_2O groups in some cases, provide linkages between the sheets.

β-U_3O_8 anion-topology: The β-U_3O_8 anion-topology (Fig. 11c) is the basis of the structure of β-U_3O_8, which contains U in multiple valence states, and three minerals. This topology is similar to the uranophane anion-topology in that both contain identical chains of edge-sharing pentagons, as well as chains of edge-sharing triangles and squares. The distinction is that pentagons of adjacent chains share vertices only in the β-U_3O_8 anion-topology, which also contains more triangles. In the case of the sheet in β-U_3O_8, all of the pentagons and squares of the anion topology are populated by U. Wyartite is the only mineral known to contain pentavalent uranium, although several synthetic compounds contain uranium in this valence state (Burns & Finch 1999). The sheet of uranyl polyhedra in wyartite is closely related to that in β-U_3O_8, but one of the U polyhedra contains pentavalent U, and the CO_3 group shares an edge with one U polyhedron such that it extends into the interlayer. The sheets are linked through bonds to Ca in the interlayer, as well as by a network of H bonds. The structures of ianthinite and spriggite each have sheets of uranyl pentagonal and square bipyramids that are topologically identical to those in β-U_3O_8; in spriggite, all of the U is hexavalent, whereas the U in the structure of ianthinite has multiple valence states. On the basis of an imprecise refinement of the structure, Burns *et al.* (1997c) reported that ianthinite probably contains both U^{6+} and U^{4+}, but the subsequent discovery of wyartite suggests that ianthinite also may contain pentavalent U.

Iriginite anion-topology: Iriginite, as well as two synthetic uranyl molybdates, contain sheets based upon the iriginite anion-topology, shown in Figure 11e. The sheets are identical in these three structures, and contain uranyl pentagonal bipyramids and distorted $M\phi_6$ octahedra that form dimers by sharing an edge. Uranyl

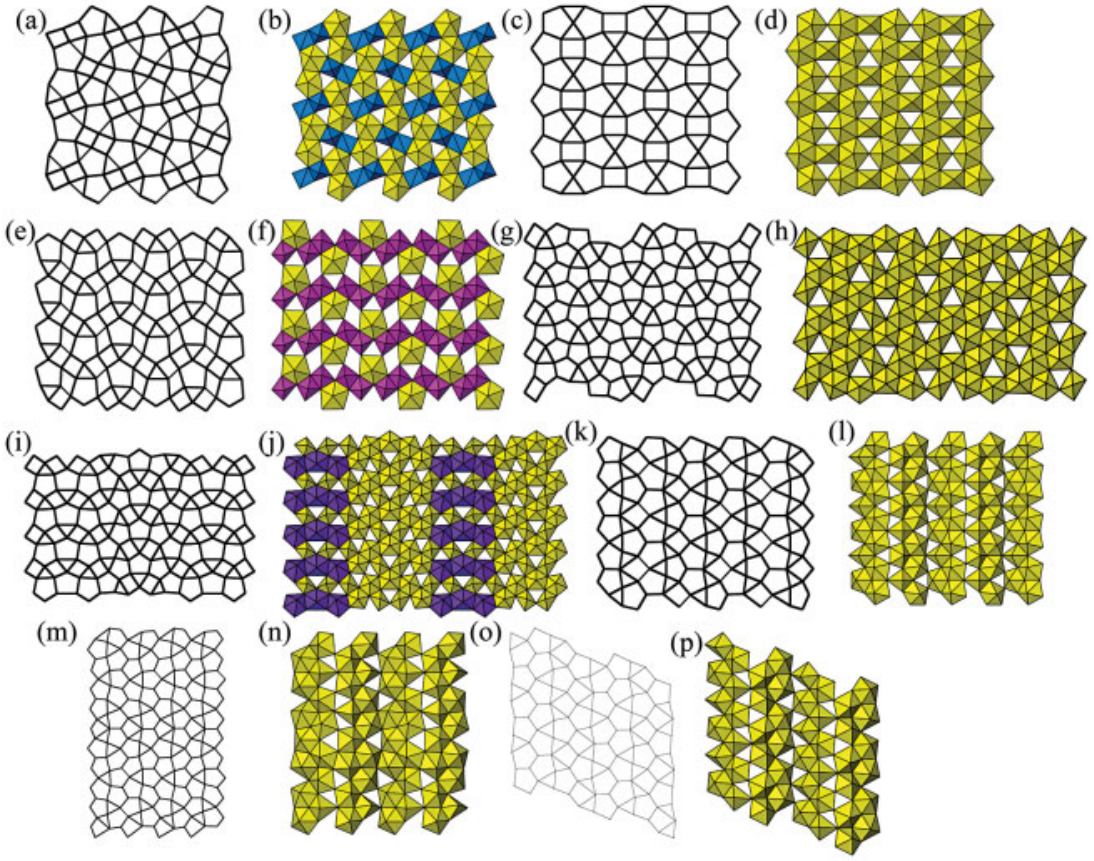

FIG. 11. Sheets of uranyl polyhedra and other polyhedra containing higher-valence cations that are based upon anion topologies and that contain triangles, squares, and pentagons (other than the uranophane anion-topology). The corresponding compounds are listed in Table 6.

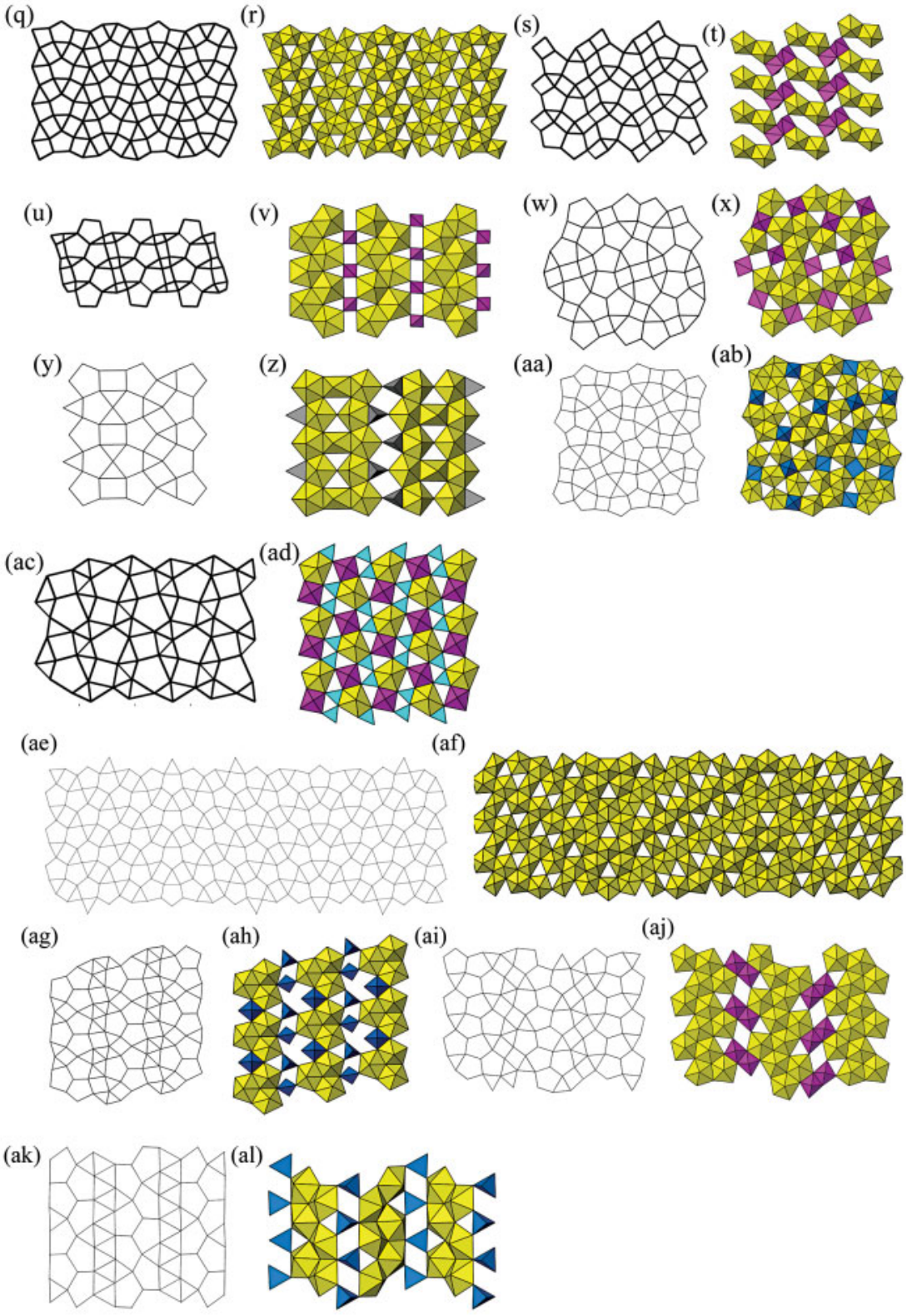
(q)
(r)
(s)
(t)
(u)
(v)
(w)
(x)
(y)
(z)
(aa)
(ab)
(ac)
(ad)
(ae)
(af)
(ag)
(ah)
(ai)
(aj)
(ak)
(al)

pentagonal bipyramids are linked to four different $Mo\phi_6$ octahedra, two by sharing edges and two by sharing only vertices. In the case of $[Ca(UO_2)(Mo_2O_7)_2]$, pentagons of the anion topology are populated by Ca as well as U.

Sayrite anion-topology: Two structures are known that contain sheets of uranyl square and pentagonal bipyramids (Fig. 11h) that are based upon the sayrite anion-topology (Fig. 11g). The squares and pentagons of the anion topology are each populated by uranyl ions; thus the resulting sheet is composed of edge- and vertex-sharing uranyl square and pentagonal bipyramids. The sheet is anhydrous in $K_2[(UO_2)_5O_8](UO_2)_2$, and the interlayer of the structure contains uranyl ions. In the case of the rare mineral sayrite, the sheet contains H present as OH groups, and adjacent sheets are linked by bonds to Pb^{2+} cations and H_2O groups located in the interlayer.

$[Pb_3(UO_2)_{11}O_{14}]$ anion-topology: The isostructural compounds $[Pb_3(UO_2)_{11}O_{14}]$ and $[Sr_3(UO_2)_{11}O_{14}]$ contain complex sheets of uranyl square and pentagonal bipyramids and either $Pb\phi_7$ or $Sr\phi_7$ pentagonal bipyramids (Fig. 11j). In this case, inclusion of Pb and Sr in the structural unit is warranted, as they assume similar structural roles as U. Adjacent sheets are linked directly through the $Pb\phi_7$ or $Sr\phi_7$ polyhedra. These structures are remarkable in the presence of Pb^{2+} and Sr^{2+} within the sheets of uranyl polyhedra, which is not known to occur in any of the structures of uranyl oxide hydrates.

Curite anion-topology: The curite anion-topology (Fig. 11k), which contains pentagons, distorted squares, and triangles, is the basis of sheets of uranyl pentagonal and square bipyramids in curite and its synthetic Sr-substituted analogue. Although the square bipyramid in this sheet is strongly distorted from an ideal geometry, similarly distorted square bipyramids also occur in the structures of $K_5[(UO_2)_{10}O_8(OH)_9](H_2O)$ (Fig. 11n), $Ca[(UO_2)_4O_3(OH)_4](H_2O)_2$ (Fig. 11p), and $Pb_2(H_2O)[(UO_2)_{10}UO_{12}(OH)_6(H_2O)_6]$ (see below, Fig. 15g). Li & Burns (2000b) studied the structures of several crystals of curite, including a synthetic crystal, and found that the Pb sites are partially occupied in each crystal studied. The general formula $Pb_{3+x}(H_2O)_2[(UO_2)_4O_{4+x}(OH)_{3-x}]_2$ was proposed, and Pb variability in the interlayer is accompanied by changes of the hydroxyl content of the sheet of uranyl polyhedra, which provides a charge-balance mechanism. Synthesis and structure determination of the Sr-substituted analogue of curite (Burns & Hill 2000a) demonstrate that the unusual sheet of uranyl polyhedra found in curite is not a result of the distorted coordination environment about the interlayer Pb^{2+} cation caused by a stereoactive lone-electron pair.

$K_5[(UO_2)_{10}O_8(OH)_9](H_2O)$ anion-topology: Burns & Hill (2000b) reported the structure of a new K uranyl oxide hydrate that contains complex sheets of uranyl pentagonal bipyramids and highly distorted uranyl square bipyramids (Fig. 11n). Despite its chemical similarity to compreignacite, this phase has not been found as a mineral. The sheet within its structure consists of double-width chains of bipyramids that share equatorial edges; adjacent chains are connected by the sharing of vertices and edges between bipyramids. The chains are similar to those of the curite-type sheet (Fig. 11l), except that they contain fewer square bipyramids, although these polyhedra are similarly distorted in the two structures.

$Ca[(UO_2)_4O_3(OH)_4](H_2O)_2$ anion-topology: Despite its chemical similarity with becquerelite, the structure of $Ca[(UO_2)_4O_3(OH)_4](H_2O)_2$ is based upon a novel sheet of uranyl pentagonal bipyramids and distorted square bipyramids (Fig. 11p). The sheet contains two distinct double-width chains of bipyramids, one that contains only pentagonal bipyramids, and one that contains equal proportions of square and pentagonal bipyramids. The chains are linked into sheets only by the sharing of vertices between bipyramids. The sheet is similar to the curite-type sheet and the sheet found in $K_5[(UO_2)_{10}O_8(OH)_9](H_2O)$ in the dominance of double-width chains and the presence of highly distorted square bipyramids. $Ca[(UO_2)_4O_3(OH)_4](H_2O)_2$ has not been found in nature, but it is readily synthesized under a variety of conditions, and it commonly occurs with becquerelite in products of synthesis (Glatz *et al.* 2002). Recently, Kubatko *et al.* (2005) determined the heats of formation of several uranyl oxide hydrates using drop-solution calorimetry. Those results demonstrated that $Ca[(UO_2)_4O_3(OH)_4](H_2O)_2$ is unstable in terms of enthalpy relative to the oxides; thus it appears to form metastably in synthesis reactions.

The sheet in $Ca[(UO_2)_4O_3(OH)_4](H_2O)_2$ is closely related to the sheet of uranyl pentagonal bipyramids found in the structure of $Na[(UO_2)_4O_2(OH)_5](H_2O)_2$ (Fig. 8e). The U(3) square bipyramid in $Ca[(UO_2)_4O_3(OH)_4](H_2O)_2$ has only four equatorial ligands; if this were a pentagonal bipyramid, the sheet would be topologically identical to that in $Na[(UO_2)_4O_2(OH)_5](H_2O)_2$. Displacement of a single atom by ~0.6 Å is the topological difference between these two sheets.

$Cs_4[(UO_2)_5O_7]$ anion-topology: The $Cs_4[(UO_2)_5O_7)]$ anion-topology (Fig. 11q) is the basis for the sheet (Fig. 11r) found only in $Cs_4[(UO_2)_5O_7]$. The sheet contains both uranyl square and pentagonal bipyramids that are connected by sharing equatorial edges and vertices. Adjacent sheets are linked through bonds to the Cs cations in the interlayer of the structure.

Vandenbrandeite anion-topology: The vandenbrandeite anion-topology (Fig. 11s) is the basis for one sheet (Fig. 11t) that contains dimers of edge-sharing uranyl pentagonal bipyramids that are linked by dimers of edge-sharing $Cu\phi_5$ square pyramids. The O_{Ur} anions of the pentagonal bipyramids are apical ligands of the $Cu\phi_5$ square pyramids of adjacent sheets.

Zippeite anion-topology: The zippeite anion-topology and corresponding sheet are shown in Figures 11u and 11v. The sheet contains zig-zag chains of edge-

sharing uranyl pentagonal bipyramids, and the chains are connected by the sharing of vertices between the bipyramids and sulfate tetrahedra, such that each sulfate tetrahedron is linked to four different bipyramids. The formulae and crystallographic parameters for zippeite-group compounds are listed in Table 6. Vochten *et al*. (1995) reported the first structure of a zippeite-structure material for the synthetic analogue of zippeite, the K-bearing mineral. Burns *et al*. (2003) presented a revised structure for zippeite, as well as structures for four additional synthetic analogues of zippeite-group minerals and three synthetic phases of the zippeite group. Brugger *et al*. (2003) reported the structure of the new zippeite-group mineral marecottite.

Burns *et al*. (2003) showed that although the uranyl sulfate sheets are topologically identical in each zippeite-group structure studied, the sheets in some are anhydrous, whereas in others they may contain hydroxyl groups located at equatorial vertices of the uranyl pentagonal bipyramids. The interlayer configurations of zippeite-group phases are diverse, and include either monovalent or divalent cations as well as H_2O groups. Burns *et al*. (2003) concluded that the distribution of interlayer constituents can be rationalized on the basis of the bonding requirements of the uranyl sulfate sheets.

$K_2[(UO_2)_2(WO_5)O]$ anion-topology: Three topologically identical sheets (Fig. 11x) have recently been found that are based upon the anion-topology shown in Figure 11w, which contains clusters of eight pentagons linked by edge-sharing (Table 6). Each of these clusters is connected to four identical clusters by sharing one vertex with each, which results in both triangles and squares in the anion topology. All pentagons of the anion topology are populated by uranyl ions in each of the three structures, giving uranyl pentagonal bipyramids, and three out of four of the squares are the bases of square pyramids containing W in two structures, and Mo in the other. One square pyramid shares three of its edges with uranyl bipyramids, whereas the other two share only one edge with a bipyramid, but two of their vertices are shared with other bipyramids. Interlayer cations provide linkage between the sheets.

$K_6[(UO_2)_5(VO_4)_2O_5]$ anion-topology: Topologically and chemically identical uranyl vanadate sheets (Fig. 11z) based upon the same anion-topology (Fig. 11y) have recently been found in four anhydrous compounds (Table 6). The sheet contains three-polyhedron-wide chains of uranyl square and pentagonal bipyramids, identical to those found in the β-U_3O_8-type sheet (Fig. 11d), that are connected into sheets by sharing edges and vertices with VO_4 tetrahedra. Linkages between sheets are provided by monovalent cations located in the interlayer regions of the structures.

$K_8[(UO_2)_8(MoO_5)_3O_6]$ anion-topology: The uranyl molybdate sheet contained in $K_8[(UO_2)_8(MoO_5)_3O_6]$ is shown in Figure 11ab, with its corresponding anion-topology in Figure 11aa. The sheet contains groups of six uranyl pentagonal bipyramids that are linked into a cluster by the sharing of equatorial edges. The resulting clusters are linked into a sheet both by sharing vertices directly between clusters, and by sharing polyhedron edges with MoO_5 groups.

$[Mg(UO_2)(B_2O_5)]$ anion-topology: The $[Mg(UO_2)(B_2O_5)]$ anion-topology, and the corresponding heteropolyhedral sheet, are shown in Figures 11ac and 11ad, respectively. The sheet contains uranyl pentagonal bipyramids that share two equatorial edges with BO_3 groups that are part of B_2O_5 dimers of BO_3 groups. Each bipyramid also shares two equatorial vertices with other BO_3 groups, and MgO_6 octahedra share an equatorial edge of a bipyramid, as well as vertices with two other bipyramids.

Wölsendorfite anion-topology: The structure of wölsendorfite contains an extremely complex sheet of uranyl square and pentagonal bipyramids (Fig. 11af), and has a primitive repeat-distance of 56 Å (Burns 1999b). Wölsendorfite contains the most topologically complex sheet known in any uranyl compound. By considering the sheet anion-topology of wölsendorfite (Fig. 11ae) as a stacking sequence of simpler chains, Burns (1999b) demonstrated that the topology is composed of modules of the simpler protasite (α-U_3O_8) and β-U_3O_8 anion topologies. Sheets are linked through a complex interlayer that contains Pb and Ba cations, as well as H_2O groups.

$Cs_4[(UO_2)_3O(MoO_4)_2(MoO_5)]$ anion-topology: The uranyl molybdate sheet that occurs in the structure of $Cs_4[(UO_2)_3O(MoO_4)_2(MoO_5)]$, and its corresponding anion-topology, are shown in Figures 11ag and 11ah. The uranyl molybdate sheet contains uranyl pentagonal bipyramids, molybdate tetrahedra, and MoO_5 polyhedra. Three bipyramids share edges and a common O atom, resulting in trimers that are linked into chains by the sharing of polyhedron vertices. The MoO_5 polyhedron occupies a pocket in the chain of bipyramids, where it shares two of its edges with bipyramids. The chains of bipyramids and MoO_5 polyhedra are linked into sheets by sharing vertices with tetrahedra, and each tetrahedron is linked to two bipyramids, one from the chain on either side.

$Ag_{10}[(UO_2)_8O_8(Mo_5O_{20})]$ anion-topology: The structures of $Ag_{10}[(UO_2)_8O_8(Mo_5O_{20})]$ and $Na_{10}[(UO_2)_8O_8(Mo_5O_{20})]$ contain the sheet of uranyl pentagonal bipyramids and MoO_6 or WO_6 octahedra shown in Figure 11aj, with the corresponding sheet anion-topology shown in Figure 11ai. The sheet consists of complex chains of edge-sharing uranyl pentagonal bipyramids that are in turn linked through sharing equatorial edges and vertices of the bipyramids with dimers of edge-sharing MoO_6 or WO_6 octahedra. Identical sheets are linked into complex double sheets through a MoO_4 tetrahedron that shares two equatorial vertices with MoO_6 or WO_6 octahedra in the sheet above as well as the sheet below. The unusual linkage of molybdate

and tungstate polyhedra in this structure type results in pentanuclear Mo_5O_{20} and W_5O_{20} clusters.

$K_2(UO_2)_2(MoO_4)O_2$ anion-topology: The structure of $K_2[(UO_2)_2(MoO_4)O_2]$ contains the sheet of uranyl pentagonal bipyramids and molybdate tetrahedra shown in Figure 11al, which is based upon the sheet anion-topology given in Figure 11ak. The sheet contains chains of edge-sharing bipyramids two polyhedra wide that are cross-linked into a sheet by sharing equatorial vertices with molybdate tetrahedra.

Sheet anion-topologies containing triangles, squares, pentagons and hexagons

Twenty uranyl phases, including 17 minerals, contain sheets based upon anion topologies with triangles, squares, pentagons and hexagons (Table 7). These include the large phosphuranylite group of uranyl phosphate minerals, for which several new structures have been described recently.

Phosphuranylite anion-topology: The phosphuranylite anion-topology, shown in Figure 12a, contains pentagons that share edges, resulting in dimers, which are in turn linked into chains by sharing edges with hexagons. These chains are linked through chains of edge-sharing triangles and squares, arranged such that the triangles and squares alternate along the chain length. Several populations of this anion topology are known, but none involves occupancy of the square sites. In most cases, both the pentagons and hexagons are populated by uranyl ions, resulting in chains of edge-sharing pentagonal and hexagonal bipyramids. Population of the triangles of the anion topology by phosphate tetrahedra, such that a face of the tetrahedron corresponds to the triangle of the topology, results in the uranyl phosphate sheets of the phosphuranylite group. Four graphical isomers of this sheet are known; they differ in the orientations of apical (non-sheet) ligands of the phosphate tetrahedra (Figs. 12b–e). For example, consider the orientations of the tetrahedra attached to a single chain of uranyl polyhedra in the phosphuranylite sheet (Fig. 12b). Tetrahedra attached to the chain on either side immediately opposite each other are in the same orientation. Along the side of a chain of uranyl polyhedra, the tetrahedra alternate up and down. In the case of the vanmeersscheite sheet (Fig. 12c), all tetrahedra that share edges with a given chain of uranyl polyhedra are in the same orientation.

The interlayers of the structures of minerals of the phosphuranylite group are complex, and some contain more than one type of cation, as well as H_2O groups. The structures of phosphuranylite and vanmeersscheite are unusual in that both contain uranyl ions in all three common coordinations: square, pentagonal and hexagonal bipyramids. The square bipyramids are located between the sheets in each structure, with the uranyl ions extending roughly parallel to the sheets. In phosphuranylite, all four of the equatorial ligands of the square bipyramid are apical (non-sheet) vertices of the phosphate tetrahedra of sheets on either side. In

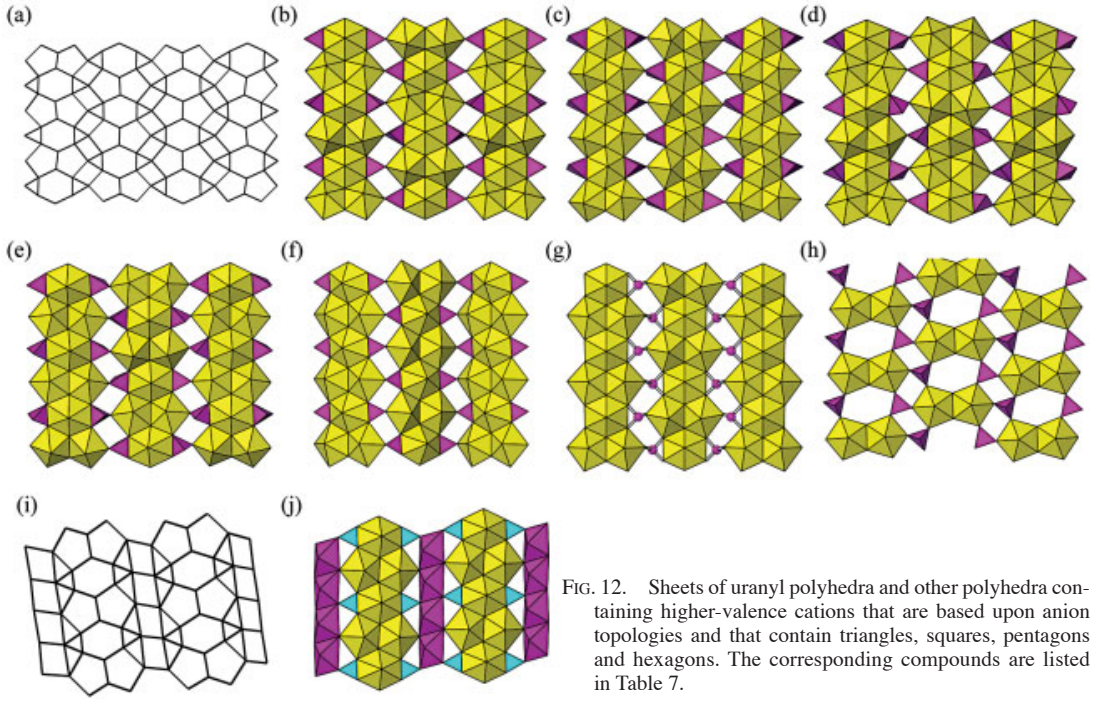

FIG. 12. Sheets of uranyl polyhedra and other polyhedra containing higher-valence cations that are based upon anion topologies and that contain triangles, squares, pentagons and hexagons. The corresponding compounds are listed in Table 7.

TABLE 7. STRUCTURES CONTAINING SHEETS BASED UPON ANION TOPOLOGIES CONTAINING TRIANGLES, SQUARES, PENTAGONS AND HEXAGONS

Name	Fig.	Formula	S. G.	*a* (Å)	*b* (Å)	*c* (Å)	β (°)	Ref.
Phosphuranylite	12b	$KCa(H_3O)_3(UO_2)[(UO_2)_3(PO_4)_2O_2]_2(H_2O)_8$	*Cmcm*	15.899	13.740	17.300		1
Upalite	12b	$Al[(UO_2)_3(PO_4)_2O(OH)](H_2O)_7$	$P2_1/a$	13.704	16.82	9.332	111.5	2
Françoisite-(Nd)	12b	$Nd[(UO_2)_3(PO_4)_2O(OH)](H_2O)_6$	$P2_1/c$	9.298	15.605	13.668	112.77	3
Dewindtite	12b	$Pb_3[H(UO_2)_3O_2(PO_4)_2]_2(H_2O)_{12}$	*Bmmb*	16.031	17.264	13.605		4
Vanmeersscheite	12c	$U(OH)_4[(UO_2)_3(PO_4)_2(OH)_2](H_2O)_4$	$P2_1mn$	17.06	16.76	7.023		5
Dumontite	12c	$Pb_2[(UO_2)_3(PO_4)_2O_2](H_2O)_5$	$P2_1/m$	8.118	16.819	6.983	109.03	6
Hügelite	12c	$Pb_2[(UO_2)_3O_2(AsO_4)_2](H_2O)_5$	$P2_1/m$	31.066	17.303	7.043	96.492	7
Phurcalite	12d	$Ca_2[(UO_2)_3(PO_4)_2(OH)_2](OH)_2(H_2O)_4$	*Pbca*	17.415	16.035	13.598		8
Phuralumite	12d	$Al_2[(UO_2)_3(PO_4)_2(OH)_2](OH)_4(H_2O)_{10}$	$P2_1/a$	13.836	20.918	9.428	112.44	9
Althupite	12d	$AlTh(UO_2)[(UO_2)_3(PO_4)_2O(OH)]_2(OH)_3(H_2O)_{15}$						
			$P\bar{1}$	10.953	18.567	13.504	68.20	10
Bergenite	12e	$Ca_2Ba_4[(UO_2)_3O_2(PO_4)_2]_3(H_2O)_{16}$	$P2_1/c$	10.092	17.245	17.355	113.678	11
Fontanite	12f	$Ca[(UO_2)_3(CO_3)_2O_2](H_2O)_6$	$P2_1/n$	6.968	17.276	15.377	90.064	12
Marthozite	12g	$Cu[(UO_2)_3(SeO_3)_2O_2](H_2O)_8$	$Pbn2_1$	6.9879	16.4537	17.2229		13
Guilleminite	12g	$Ba[(UO_2)_3(SeO_3)_2O_2](H_2O)_3$	$P2_1nm$	7.084	7.293	16.881		14
Larisaite	12g	$Na(H_3O)[(UO_2)_3(SeO_3)_2O_2](H_2O)_4$	$P11m$	6.9806	7.646	17.249	90.039	15
	12g	$Sr[(UO_2)_3(SeO_3)_2O_2](H_2O)_4$	$C2/m$	17.014	7.0637	7.1084	100.544	16
Johannite	12h	$Cu[(UO_2)_2(SO_4)_2(OH)_2](H_2O)_8$	$P\bar{1}$	8.903	9.499	6.812	112.01	17
	12h	$Sr[(UO_2)_2(CrO_4)_2(OH)_2](H_2O)_8$	$P\bar{1}$	8.923	9.965	11.602	99.09	18
Roubaultite	12j	$[Cu_2(UO_2)_3(CO_3)_2O_2(OH)_2](H_2O)_4$	$P\bar{1}$	7.767	6.924	7.850	90.89	19
	12l	$[Ca(UO_2)_2(BO_3)_2]$	$C2$	16.512	8.169	6.582	96.97	20

References: (1) Demartin *et al.* (1991), (2) Piret & Declercq (1983), (3) Piret *et al.* (1988), (4) Piret *et al.* (1990), (5) Piret & Deliens (1982), (6) Piret & Piret-Meunier (1988), (7) Locock & Burns (2003b), (8) Atencio *et al.* (1991), (9) Piret *et al.* (1979), (10) Piret & Deliens (1987), (11) Locock & Burns (2003c), (12) Hughes & Burns (2003a), (13) Cooper & Hawthorne (2001), (14) Cooper & Hawthorne (1995), (15) Chukanov *et al.* (2004), (16) Almond & Albrecht-Schmitt (2004), (17) Mereiter (1982c), (18) Serezhkin *et al.* (1982), (19) Ginderow & Cesbron (1985), (20) Gasperin (1987d).

contrast, the uranyl square bipyramid in the vanmeersscheite interlayer shares vertices with only two phosphate tetrahedra, one from each adjacent sheet. Linkage of the uranyl phosphate sheets through interlayer uranyl polyhedra results in open three-dimensional structures in phosphuranylite and vanmeersscheite.

The structure of hügelite contains sheets that are topologically identical to those in vanmeersscheite and dumontite, but in this case, the triangles of the anion topology are populated by arsenate tetrahedra.

Recent studies of uranyl carbonates have revealed more structural complexity within this chemical class (Li *et al*. 2000, Hughes Kubatko & Burns 2003). Although many uranyl carbonates that form under somewhat alkaline conditions contain the isolated uranyl tricarbonate cluster, minerals formed under neutral to acidic conditions tend to adopt sheet structures. Fontanite is the only uranyl carbonate with a sheet based upon the phosphuranylite anion-topology (Fig. 12f). This sheet contains uranyl pentagonal and hexagonal bipyramids, and the triangles of the anion topology are populated by carbonate triangles, such that the CO_3 group shares an edge with a hexagonal bipyramid and one vertex with a pentagonal bipyramid of an adjacent chain. Calcium cations and H_2O groups located in the interlayer provide linkages between the sheets in fontanite.

Four uranyl selenites, of which three are minerals, contain sheets based upon the phosphuranylite anion-topology. Each sheet has chains of uranyl pentagonal and hexagonal bipyramids linked by bonds to $Se^{4+}O_3$ pyramids with a base of three O atoms and Se^{4+} at the fourth apex of the pyramid (Fig. 12g). The strongly distorted coordination environment about the Se^{4+} cation is due to the presence of a stereoactive lone-pair of electrons on the cation that is directed away from the coordinating anions. In each structure, low-valence cations and H_2O groups provide linkages between the sheets.

Johannite and $Sr[(UO_2)_2(CrO_4)_2(OH)_2](H_2O)_8$ contain sheets based upon the phosphuranylite anion-

topology (Fig. 12h). However, in this case the hexagons of the topology are not occupied; the sheet contains dimers of edge-sharing uranyl pentagonal bipyramids that are linked only by sharing vertices with sulfate or chromate tetrahedra. Edges of the tetrahedra correspond to the hexagons of the anion topology, thus occupancy of the hexagons by uranyl ions would result in short U^{6+}–S^{6+} or U^{6+}–Cr^{6+} interatomic distances.

Roulbaultite anion-topology: The structure of roulbaultite contains the complex sheet shown in Figure 12j, which is based upon the anion topology shown in Figure 12i. This structure has notable similarities to that of fontanite (Fig. 12f). Both contain the same chain of uranyl pentagonal and hexagonal bipyramids, and CO_3 triangles. In fontanite, these chains are linked directly through the sharing of vertices between the CO_3 group of one chain with uranyl pentagonal bipyramids of an adjacent chain. In contrast, the roulbaultite sheet also contains chains formed by the sharing of edges between $Cu\phi_6$ octahedra, and uranyl carbonate chains are separated by chains of octahedra on either side. The uranyl carbonate chains are linked to the chains of octahedra through the sharing of non-chain vertices of the CO_3 triangles, as well as equatorial vertices of uranyl pentagonal bipyramids. Linkages between the sheets in roulbaultite occur by H bonds to interlayer H_2O groups only.

Miscellaneous anion-topologies with hexagons

Twenty-one compounds, of which only one is a mineral, are grouped as miscellaneous sheets with anion topologies containing hexagons (Table 8, Fig. 13). Only six anion topologies are needed to account for all of the 21 structures.

α-UO_3 anion-topology: The simplest anion-topology involves a two-dimensional tiling of space using only hexagons (Fig. 13a), and corresponds to the sheets of uranyl hexagonal bipyramids (Fig. 13b) that are known from 10 structures. The structure of α-UO_3 has sheets constructed from hexagonal bipyramids, but in the reported structure, no uranyl ions are present, and adjacent sheets are linked through the sharing of apical ligands between adjacent sheets. In the structure of α-

TABLE 8. MISCELLANEOUS STRUCTURES CONTAINING SHEETS BASED UPON ANION TOPOLOGIES CONTAINING HEXAGONS

Name	Fig.	Formula	S. G.	*a* (Å)	*b* (Å)	*c* (Å)	α (°)	β (°)	γ (°)	Ref.
	13b	α-UO_3	*C2mm*	3.961	6.860	4.166				1
	13b	α-$[(UO_2)(OH)_2]$	*Cmca*	4.242	10.302	6.868				2
	13b	$Bi_2[(UO_2)O_2]O_2$	*C*2	6.872	4.009	9.690		90.16		3
	13b	$Cs_2(U_2O_7)(D_2O)_{0.444}$	*C*2/*m*	14.5314	4.2739	7.6011		113.02		4
	13b	$Ca[(UO_2)O_2]$	$R\bar{3}m$	6.2683			36.040			5
	13b	α-$Sr[(UO_2)O_2]$	$R\bar{3}m$	6.587			35.30			6
	13b	γ-$Sr[(UO_2)O_2]$	$R\bar{3}m$	6.542			35.54			6
	13b	α-$Cd[(UO_2)O_2]$	$R\bar{3}m$	6.233			36.12			7
	13b	$(Na_2U_2O_7)_{0.5}$	$R\bar{3}m$	6.34			36.11			8
	13b	$K_2U_2O_7$	$R\bar{3}m$	6.99			32.90			9
Rutherfordine	13d	$[UO_2CO_3]$	*Imm*2	4.840	9.273	4.298				10
	13d	$[(UO_2)(SeO_3)]$	$P2_1/m$	5.408	9.278	4.2545		93.45		11
	13f	$K_2[(UO_2)(W_2O_8)]$	*Pmcn*	7.5884	8.6157	13.946				12
	13f	$Na_2[(UO_2)W_2O_8]$	$P\bar{1}$	6.6484	7.5308	8.4869	86.190			13
	13f	α-$Ag_2[(UO_2)W_2O_8]$	$P2_1/c$	8.4263	7.4897	12.927	95.443			13
	13f	β-$Ag_2[(UO_2)W_2O_8]$	*Pnma*	8.6415	7.5610	12.4513				13
	13h	$[(UO_2)(B_2O_3)O]$	*C*2/*c*	12.504	4.183	10.453		122.18		14
	13j	$[(UO_2)TiNb_2O_8]$	*Fddd*	7.28	12.62	16.02				15
	13j	$[(UO_2)\ Nb_3O_8]$	*Fddd*	7.38	12.78	15.96				16
	13j	$Cs[UV_3O_{11}]$	$P2_1/a$	11.904	6.832	12.095		106.99		17
	13l	$[(UO_2)(Sb_2O_4)]$	*C*2/*m*	13.490	4.0034	5.1419		104.164		18

References: (1) Loopstra & Cordfunke (1966), (2) Taylor (1971), (3) Koster *et al.* (1975), (4) Mijlhoff *et al.* (1993), (5) Loopstra & Rietveld (1969), (6) Fujino *et al.* (1977), (7) Yamashita *et al.* (1981), (8) Kovba *et al.* (1958), (9) Jove *et al.* (1988), (10) Finch *et al.* (1999b), (11) Loopstra & Brandenburg (1978), (12) Obbade *et al.* (2003c), (13) Krivovichev & Burns (2003i), (14) Gasperin (1987e), (15) Chevalier & Gasperin (1969), (16) Chevalier & Gasperin (1968), (17) Duribreux *et al.* (1999), (18) Sykora *et al.* (2004a).

$[(UO_2)(OH)_2]$, sheets of uranyl hexagonal bipyramids are connected through H bonds that extend through the interlayer region. Eight additional structures are based upon sheets of hexagonal bipyramids, with linkages provided by low-valence cations in the interlayers (Table 8).

Rutherfordine anion-topology: The rutherfordine anion-topology is composed of hexagons and triangles (Fig. 13c). It contains chains of edge-sharing hexagons that are identical to those of the α-UO_3 anion-topology (Fig. 13a), but these chains are now connected in the second dimension only by the sharing of vertices rather than edges, and adjacent chains are separated by triangles. The sheet in the structure of rutherfordine has all of the hexagons of the anion topology populated by uranyl ions, and half of the triangles correspond to CO_3 groups, whereas the remaining triangles are vacant (Fig. 13d). Note that all of the CO_3 triangles are in the same orientation. The structure of $[(UO_2)(SeO_3)]$ contains sheets that are topologically identical to those in rutherfordine, but the triangles of the topology are populated by $Se^{4+}O_3$ polyhedra that are distorted owing to the lone-electron pairs on the Se^{4+} cations. Neither rutherfordine or $[(UO_2)(SeO_3)]$ have interlayer constituents.

$K_2[(UO_2)(W_2O_8]$ anion-topology: Four structures have recently been reported (Table 8) that contain the anion topology shown in Figure 13e. The corresponding sheet contains chains of edge-sharing uranyl pentagonal bipyramids. Two equatorial edges of the bipyramids are shared with tungstate octahedra, such that octahedra are attached to either side of the chain (Fig. 13f). Adjacent uranyl tungstate chains are connected by the sharing of vertices between the tungstate octahedra. Low-valence cations provide linkages between the sheets, and each of these structures is anhydrous.

$[(UO_2)(BO_3)O]$ anion-topology: The uranyl borate sheet in the structure of $[(UO_2)(B_2O_3)O]$ (Fig. 13h) contains uranyl hexagonal bipyramids and borate triangles. The anion topology of the corresponding sheet (Fig. 13g) is similar to that of rutherfordine (Fig. 13c) in the presence of chains of edge-sharing hexagons that are separated by triangles, but in this case the chains are not directly linked, but rather are separated by chains of edge-sharing triangles that are two triangles wide. The uranyl borate sheets are linked through van der Waals forces only.

$[(UO_2)Nb_3O_8]$ anion-topology: Two uranyl niobates and one uranyl vanadate contain the sheet shown in Figure 13j (Table 8), which is based upon the anion topology in Figure 13i. The squares in the anion topology are populated by NbO_6 octahedra in $[(UO_2)Nb_3O_8]$, by both NbO_6 and TiO_6 octahedra in $[(UO_2)TiNb_2O_8]$, and by VO_5 square pyramids in $CsUV_3O_{11}$. In all three structures, the sheets are directly linked, with the O_{Ur} atoms of one sheet being the apical ligands of the octahedra or square pyramids of the adjacent sheet.

$[(UO_2)(Sb_2O_4)]$ anion-topology: The compound $[(UO_2)(Sb_2O_4)]$ possesses a novel sheet of uranyl hexagonal bipyramids and SbO_4 square pyramids (Fig. 13l), with the sheet anion-topology shown in Figure 13k. The sheet contains chains of edge-sharing bipyramids similar to those in rutherfordine (Fig. 13d) and $[(UO_2)(B_2O_3)O]$ (Fig. 13h). Unlike the case of rutherfordine, these chains are not directly linked, but rather are connected through zigzag chains of edge-sharing SbO_4 square pyramids. Note that the SbO_4 polyhedra are distorted because of the presence of a stereoactive lone-electron pair, and are geometrically similar to the $Te^{4+}O_4$ polyhedra in the structure of schmitterite (Fig. 10l).

Miscellaneous topologies

The compounds listed in Table 9 are based upon a variety of sheets with miscellaneous topologies. Each sheet is shown in Figure 14. The structure of the uranyl carbonate bijvoetite is unusual in that it contains uranyl carbonate sheets (Fig. 14a), whereas the majority of uranyl carbonates contain isolated uranyl tricarbonate clusters. The sheet contains both uranyl pentagonal and hexagonal bipyramids, and there are dimers of each that result from the sharing of equatorial edges. The dimers of hexagonal bipyramids are oriented perpendicular to the length of chains of uranyl polyhedra, and are connected through the dimers of uranyl pentagonal bipyramids, which extend along the length of the chains. As such, each of the equatorial vertices of the pentagonal bipyramids are shared with other uranyl polyhedra, but two of the equatorial vertices of each hexagonal bipyramid are bonded to only one U^{6+} cation. The resulting chain of polyhedra is unique in uranyl compounds. Carbonate groups are attached to the sides of the chains by sharing edges with the hexagonal bipyramids, such that each bipyramid is linked to two carbonate triangles. The chains are linked into sheets through irregular coordination-polyhedra about trivalent cations, which correspond to Y and various rare-earth elements, especially Dy. The sheets are linked through H bonds to H_2O groups located in the interlayer of the structure.

The structure of haiweeite contains sheets of uranyl pentagonal bipyramids and silicate tetrahedra (Fig. 14b). The bipyramids share edges, giving a chain that is one bipyramid wide, and silicate tetrahedra share equatorial edges of the bipyramids along both sides of the chain. The resulting uranyl silicate chain has the same anion-topology as that found in the uranyl silicates of the uranophane group (Fig. 10). However, the way these chains are connected into sheets distinguishes haiweeite from the uranophane group. The chains are directly linked in the uranophane group, as silicate tetrahedra bridge between adjacent chains of bipyramids. In the haiweeite sheet, the uranyl silicate chains are linked through a complex crankshaft-like chain of silicate tetrahedra, and two such chains in different orientations are superimposed in the long-range structure, which may

be consistent with a domain structure or true disorder of the chain orientations. The resulting complex sheets are linked by Ca cations in the interlayer, as well as through H bonds to interlayer H_2O groups.

The structure of $Ag_4[(UO_2)_4(IO_3)_2(IO_4)_2O_2]$ contains a sheet of uranyl pentagonal and hexagonal bipyramids, as well as both $I^{5+}O_4$ and $I^{5+}O_3$ polyhedra. The hexagonal bipyramids share an edge, forming a chain one polyhedron wide that is identical to that found in rutherfordine and other structures shown in Figure 13. However, unlike the structures in Figure 13, pentagonal bipyramids are attached to each side of this chain by sharing two of their equatorial edges with two different hexagonal bipyramids. The resulting chain is unique

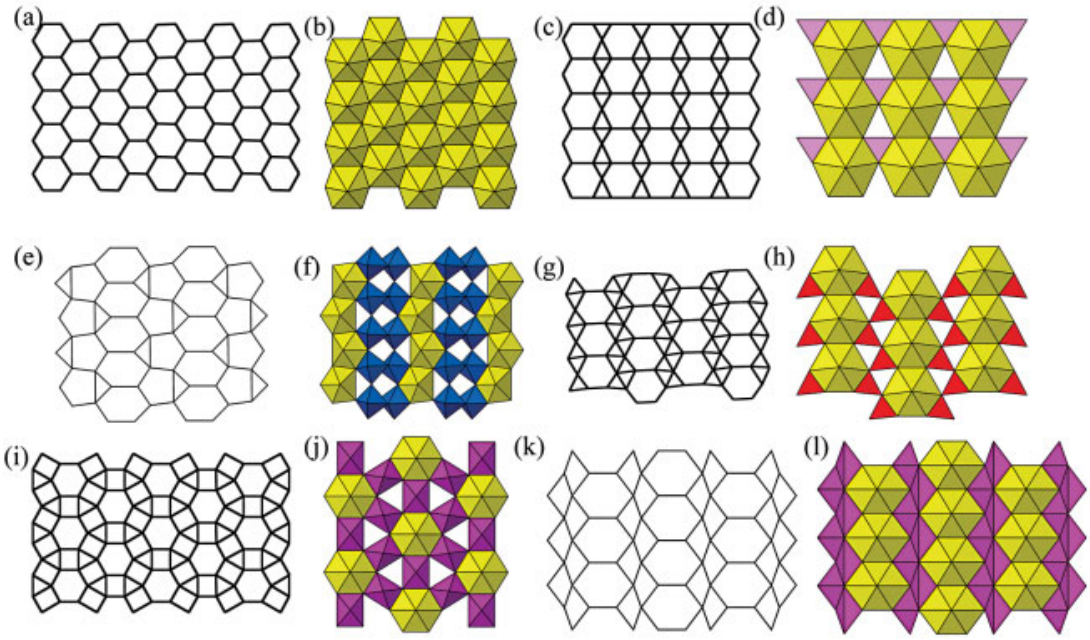

FIG. 13. Miscellaneous sheets of uranyl polyhedra and other polyhedra containing higher-valence cations that contain hexagons. The corresponding compounds are listed in Table 8.

TABLE 9. STRUCTURES BASED UPON MISCELLANEOUS SHEET-TOPOLOGIES

Name	Fig.	Formula	S. G.	*a* (Å)	*b* (Å)	*c* (Å)	β (°)	Ref.
Bijvoetite	14a	$[M^{3+}(H_2O)_{25}(UO_2)_{16}O_8(OH)_8(CO_3)_{16}](H_2O)_{14}$						
			$B12_11$	21.234	12.958	4.4911	90.00	1
Haiweeite	14b	$Ca[(UO_2)_2Si_5O_{12}(OH)_2](H_2O)_3$	*Cmcm*	7.125	17.937	18.342		2
	14c	$Ag_4(UO_2)_4(IO_3)_2(IO_4)_2O_2$	$P2_1/n$	15.040	8.051	18.332	100.738	3
	14d	$Ag_6[(UO_2)_3O(MoO_4)_5]$	*C*2/*c*	16.4508	11.3236	12.4718	100.014	4
	14e	$K[UO_2Te_2O_5(OH)]$	*Cmcm*	7.9993	8.7416	11.4413		5
	14f	$Cs_4[(UO_2)_2(V_2O_7)O_2]$	*Pmmn*	8.4828	13.426	7.1366		6
	14g	$Tl_3\{(UO_2)_2[Te_2O_5(OH)](Te_2O_6)\}\cdot 2H_2O$	*Pbam*	10.0623	23.024	7.9389		5
	14h	$Cs_6(UO_2)_4(W_5O_{21})(OH)_2(H_2O)_2$	*I*4*cm*	15.959		14.215		7

References: (1) Li *et al.* (2000), (2) Burns (2001b), (3) Bean *et al.* (2001c), (4) Krivovichev & Burns (2002d), (5) Almond & Albrecht-Schmitt (2002b), (6) Obbade *et al.* (2004b), (7) Sykora & Albrecht-Schmitt (2004).

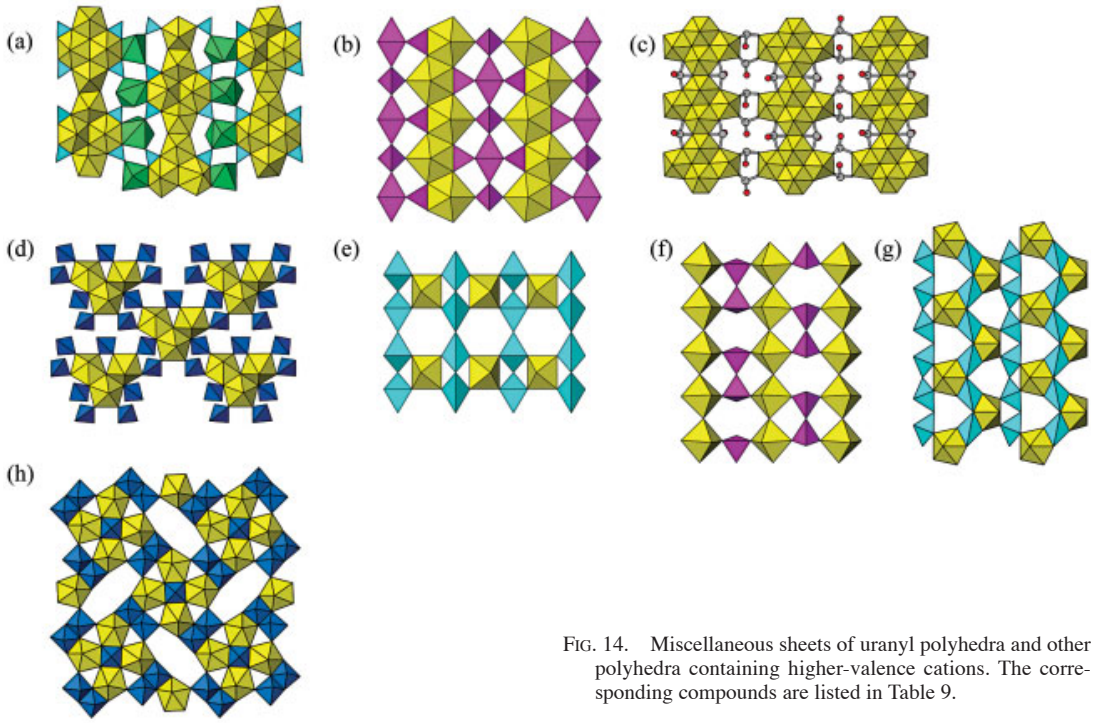

FIG. 14. Miscellaneous sheets of uranyl polyhedra and other polyhedra containing higher-valence cations. The corresponding compounds are listed in Table 9.

amongst uranyl compounds. Distorted $I^{4+}O_4$ pyramids are attached to both sides of the chains of uranyl polyhedra by sharing three of their vertices with uranyl polyhedra. The $I^{4+}O_4$ pyramids, which were described for the first time from this structure, are strongly distorted by the presence of a stereoactive lone-electron pair. The complex chains are linked through $I^{5+}O_3$ pyramids that also are distorted because of a stereoactive lone-electron pair, and these pyramids share one vertex with the chain on either side. The sheets are linked through interlayer Ag cations.

The structure of $Ag_6[(UO_2)_3O(MoO_4)_5]$ contains unusual sheets of uranyl pentagonal bipyramids and molybdate tetrahedra (Fig. 14d). Trimers of uranyl pentagonal bipyramids result from the sharing of edges, and these polyhedra share one common O atom. The trimers are connected by sharing vertices with molybdate tetrahedra that share one ligand with each of two such trimers. There is also a molybdate tetrahedron that bridges between two uranyl polyhedra of the same trimer. This sheet is unusual in that it has the only occurrence of an isolated trimer of uranyl polyhedra. Similar trimers exist in other sheets, but in all other cases they are linked directly by the sharing of vertices and edges between the uranyl polyhedra. The sheets are connected through bonds to interlayer Ag cations.

The structure of $K[UO_2Te_2O_5(OH)]$ contains the sheets of uranyl square bipyramids and distorted $Te^{4+}O_4$ pyramids shown in Figure 14e. The $Te^{4+}O_4$ pyramids, which are distorted because of a stereoactive lone-electron pair, share vertices to form a chain. These chains are linked by the sharing of equatorial vertices of the bipyramids with the $Te^{4+}O_4$ pyramids. The sheets are linked through bonds to the K cations, which are located within the voids in the sheets.

The structure of $Cs_4[(UO_2)_2(V_2O_7)O_2]$ contains the sheets of uranyl square bipyramids and vanadate tetrahedra shown in Figure 14f. The uranyl square bipyramids share equatorial vertices, resulting in a chain one polyhedron wide that is identical to those found isolated as chains in several anhydrous compounds (Fig. 5a). The chains are linked into sheets by sharing equatorial vertices with vanadate tetrahedra of pyrovanadate groups. Sheets are linked through Cs cations in the interlayer.

The structure of $Tl_3\{(UO_2)_2[Te_2O_5(OH)](Te_2O_6)\}\cdot 2H_2O$ has the sheets of uranyl pentagonal bipyramids and $Te^{4+}O_4$ pyramids shown in Figure 14g. The distorted $Te^{4+}O_4$ pyramids share vertices, resulting in chains similar to those in $K[UO_2Te_2O_5(OH)]$ (Fig. 14e). The chains of $Te^{4+}O_4$ pyramids are linked by sharing equatorial vertices of the uranyl pentagonal bipyramids, and sheets are linked through the Tl cations in the interlayer.

The structure of $Cs_6[(UO_2)_4(W_5O_{21})(OH)_2(H_2O)_2]$ contains unusual sheets of uranyl pentagonal bipyra-

mids, tungstate octahedra, and tungstate square pyramids (Fig. 14h). Four pentagonal bipyramids share vertices, forming a ring, with a tungstate square pyramid located at the center of the ring, such that its equatorial edges are also equatorial edges of the uranyl polyhedra. The resulting clusters are linked to four identical clusters through sharing edges and vertices with dimers of tungstate octahedra that are formed by sharing an edge.

Structures Containing Infinite Frameworks of Polyhedra

Burns *et al*. (1996) included only 26 structures in their hierarchy that contained frameworks with uranyl polyhedra. Through the detailed work of several groups in synthesizing new structures, this structural class has now ballooned to 56 (Table 10).

Frameworks of uranium polyhedra

Seven framework structures are based solely on uranium polyhedra. Four of these are polymorphs of UO_3 (Figs. 15a–d). These structures involve a range of U^{6+} coordination polyhedra, and two (β-UO_3 and δ-UO_3) do not contain uranyl ions. The structure of $(UO_2)Cl_2$ does contain a uranyl ion, but four of the equatorial vertices of the pentagonal bipyramids in the structure are Cl atoms. The bipyramids are linked by the sharing of edges, resulting in chains that are one polyhedron wide (Fig. 15e). Identical chains are known from the structures of moctezumite and $(UO_2)Cl_2(H_2O)$. Linkage of the chains is through a cation–cation interaction in which some of the O atoms of the uranyl ion also are equatorial ligands of the bipyramids of adjacent chains.

The structure of $(NH_4)_3(H_2O)_2\{[(UO_2)_{10}O_{10}(OH)][(UO_4)(H_2O)_2]\}$ is an infinite framework of uranium polyhedra (Fig. 15f), five of which are uranyl square or pentagonal bipyramids, whereas the sixth is better described as a distorted octahedron. Uranyl square and pentagonal bipyramids are linked by sharing vertices, resulting in a sheet based upon the β-U_3O_8 anion-topology that is topologically identical to those in ianthinite and spriggite (Fig. 11d). The square sites of the β-U_3O_8 anion-topology contain both the uranyl square bipyramids and the distorted $U^{6+}\phi_6$ octahedra. Two additional uranyl pentagonal bipyramids share an equatorial edge, giving a dimer. The sheets are stacked along [001], and are connected into a framework by linkages to the dimer of bipyramids located between the sheets. The NH_4 and H_2O groups are located within channels that extend parallel to the sheets of polyhedra.

The compound $Pb_2(H_2O)[(UO_2)_{10}UO_{12}(OH)_6(H_2O)_6]$ is the first Pb uranyl oxide hydrate reported to possess a framework structure (Fig. 15g). It has both uranyl square and pentagonal bipyramids, as well as one U^{6+} site that is in somewhat distorted octahedral coordination. The structure contains complex chains

TABLE 10. INFINITE FRAMEWORK STRUCTURES

Name	Fig.	Formula	S. G.	*a* (Å)	*b* (Å)	*c* (Å)	β (°)	Ref.
	15a	γ-UO_3	$I4_1/amd$	6.9013		19.9754		1
	15b	β-UO_3	$P2_1$	10.34	14.33	3.910	99.03	2
	15c	UO_3 HP	$P2_12_12_1$	7.511	5.466	5.224		3
	15d	δ-UO_3	$Pm\bar{3}m$	4.165				4
	15e	$(UO_2)Cl_2$	$Pnma$	5.725	8.409	8.720		5
	15f	$(NH_4)_3(H_2O)_2\{[(UO_2)_{10}O_{10}(OH)][(UO_4)(H_2O)_2]\}$						
			$C2/c$	11.627	21.161	14.706		6
	15g	$Pb_2(H_2O)[(UO_2)_{10}UO_{12}(OH)_6(H_2O)_6]$	$C2/c$	13.281	10.223	26.10	103.20	7
	15h	$KNa_3(UO_2)_2(Si_4O_{10})_2(H_2O)_4$	$C2$	12.782	13.654	8.268	119.24	8
	15h	$Na_4(UO_2)_2(Si_4O_{10})_2(H_2O)_4$	$C2/m$	12.770	13.610	8.2440	119.248	9
Soddyite	15i	$(UO_2)_2(SiO_4)(H_2O)_2$	$Fddd$	8.334	11.212	18.668		10
	15i	$(UO_2)_2(GeO_4)(H_2O)_2$	$Fddd$	8.179	11.515	19.397		11
Weeksite	15j	$K_{1.26}Ba_{0.25}Ca_{0.12}[(UO_2)_2(Si_5O_{13})]H_2O$	$Cmmb$	14.209	14.248	35.869		12
	15k	$Na_2(UO_2)(SiO_4)$	$I4_1/acd$	12.718		13.376		13
	15l	$RbNa(UO_2)(Si_2O_6)\cdot H_2O$	$P\bar{1}$	7.3668	7.8691	8.1766		14
	15m	$(UO_2)_3(PO_4)_2(H_2O)_4$	$Pnma$	7.063	17.022	13.172		15
	15n	$(UO_2)[(UO_2)(AsO_4)]_2(H_2O)_4$	$P2_1/c$	11.238	7.152	21.941	104.576	16
	15o	$(UO_2)[(UO_2)(AsO_4)]_2(H_2O)_5$	$Pca2_1$	20.133	11.695	7.154		17
		$(UO_2)[(UO_2)(VO_4)]_2(H_2O)_5$	$Cmcm$	17.978	13.561	7.163		17

TABLE 10. INFINITE FRAMEWORK STRUCTURES

Name	Fig.	Formula	S. G.	*a* (Å)	*b* (Å)	*c* (Å)	β (°)	Ref.
	15p	$Cs_2(UO_2)[(UO_2)(PO_4)]_4(H_2O)_2$	$Cmc2_1$	14.854	13.879	12.987		18
	15p	$Cs_2(UO_2)[(UO_2)(AsO_4)]_4(H_2O)$	$Cmc2_1$	15.157	14.079	13.439		19
	15p	$Rb_2(UO_2)[(UO_2)(PO_4)]_4(H_2O)_2$	Fm	15.72	13.84	13.05	90.39	18
	15p	$Rb_2(UO_2)[(UO_2)(AsO_4)]_4(H_2O)_{4.5}$	$C2/m$	13.4619	15.8463	14.0068	92.311	19
	15p	$K_2(UO_2)[(UO_2)(PO_4)]_4(H_2O)_2$	Fm	15.257	13.831	13.007	91.760	18
	15q	$(UO_2)_2V_2O_7$	$P2_1/c$	5.646	13.178	7.282	119.74	20
	15r	$Na(UO_2)_4(VO_4)_3$	$I4_1/amd$	7.2267		34.079		21
	15s	$Cs_2[(UO_2)_6(MoO_4)_7(H_2O)_2]$	$Pbcm$	13.990	10.808	25.671		22
	15s	$(NH_4)_2[(UO_2)_6(MoO_4)_7(H_2O)_2]$	$Pbcm$	13.970	10.747	25.607		23
	15s	$Rb_2[(UO_2)_6(MoO_4)_7(H_2O)_2]$	$Pbcm$	13.961	10.752	25.579		24
	15t	α-$Cs_2(UO_2)_2(MoO_4)_3$	$Pna2_1$	20.4302	8.5552	9.8549		25
	15t	$Rb_2[(UO_2)_2(MoO_4)_3]$	$Pna2_1$	20.214	8.3744	9.7464		26
	15t	$Tl_2[(UO_2)_2(MoO_4)_3]$	$Pna2_1$	20.1296	8.2811	9.7045		27
	15u	$Ba(UO_2)_3(MoO_4)_4(H_2O)_4$	$Pbca$	17.797	11.975	23.33		28
	15v	α-$(UO_2)(MoO_4)(H_2O)_2$	$P2_1/c$	13.612	11.005	10.854	113.05	29
	15w	$Sr(UO_2)_6(MoO_4)_7(H_2O)_{19}$	$C222_1$	11.166	20.281	24.061		30
	15w	$Ca[(UO_2)_6(MoO_4)_7(H_2O)_2](H_2O)_n$	$C222_1$	11.3691	20.0311	23.8333		31
	15x	$Mg(UO_2)_3(MoO_4)_4(H_2O)_8$	$Cmc2_1$	17.105	13.786	10.908		32
	15y	$(NH_4)_4[(UO_2)_5(MoO_4)_7](H_2O)_5$	$P6_1$	11.4067		70.659		33
	15z	$Na_3(UO_2)(P_2O_7)$	$Pna2_1$	13.259	8.127	6.973		34
	15aa	α-$(UO_2)(SeO_4)$	$P2_1/c$	6.909	5.525	13.318	103.79	35
	15aa	β-$(UO_2)(SO_4)$	$P2_1/c$	6.760	5.711	12.824	102.91	35
	15aa	$(UO_2)(MoO_4)$	$P2_1/c$	7.202	5.484	13.599	104.54	36
	15ab	$[(UO_2)_3(PO_4)O(OH)(H_2O)_2](H_2O)$	$P4_2/mbc$	14.105		13.083		37
	15ac	$Pb_2(UO_2)(TeO_3)_3$	$P2_1/n$	11.605	13.389	6.981	91.23	38
Cliffordite	15ad	$(UO_2)(Te_3O_7)$	$Pa\bar{3}$	11.335				38
	15ae	$Na_6[(UO_2)_6(TeO_3)_{10}]$	$I2_13$	14.633				39
	15af	$K_2[(UO_2)_2(VO)_2(IO_6)_2O]\cdot H_2O$	$Pba2$	9.984	16.763	4.977		40
	15ag	$Li(UO_2)(WO_4)_2$	$Pbcn$	7.9372	12.786	7.4249		41
	15ah	$Li_2(UO_2)_4(WO_4)_4O$	$C2/c$	14.019	6.3116	22.296	98.86	42
	15ai	Ba_2MgUO_6	$Fm\bar{3}m$	8.379				43
	15aj	$K_9BiU_6O_{24}$	$Pm\bar{3}m$	8.631				44
	15ak	β-$Cd(UO_2)O_2$	$Cmmm$	7.023	6.849	3.514		45
	15al	UCr_2O_6	$P\bar{3}1m$	4.988		4.620		46
	----	$Cu(UO_2)O_2$	$P2_1/m$	5.475	4.957	6.569	118.87	47
	----	$Mn(UO_2)O_2$	$Imma$	6.647	6.984	6.750		48
	15am	$U^{4+}(UO_2)(PO_4)_2$	$P\bar{1}$	8.8212	9.2173	5.4772	97.75	49
	15an	$Cs[(UO_2)_3(HIO_6)(OH)(O)(H_2O)](H_2O)_{15}$	Cc	13.0960	10.0714	11.0398	102.064	50

References: (1) Loopstra *et al.* (1977), (2) Debets (1966), (3) Siegel *et al.* (1966), (4) Weller *et al.* (1988), (5) Taylor & Wilson (1974), (6) Li *et al.* (2001b), (7) Li & Burns (2000c), (8) Burns *et al.* (2000), (9) Li & Burns (2001a), (10) Demartin *et al.* (1992), (11) Legros & Jeannin (1975), (12) Jackson & Burns (2001), (13) Shashkin *et al.* (1974), (14) Wang *et al.* (2002), (15) Locock & Burns (2002a), (16) Locock & Burns (2003f), (17) Saadi *et al.* (2000), (18) Locock & Burns (2002b), (19) Locock & Burns (2003e), (20) Tancret *et al.* (1995), (21) Obbade *et al.* (2004a), (22) Krivovichev & Burns (2001b), (23) Krivovichev & Burns (2001b), (24) Krivovichev & Burns (2002a), (25) Krivovichev *et al.* (2002a), (26) Krivovichev & Burns (2002a), (27) Nazarchuk *et al.* (2005a), (28) Tabachenko *et al.* (1984a), (29) Serezhkin *et al.* (1980b), (30) Tabachenko *et al.* (1984b), (31) Nazarchuk *et al.* (2005b), (32) Tabachenko *et al.* (1983), (33) Krivovichev *et al.* (2003), (34) Linde *et al.* (1984), (35) Brandenburg & Loopstra (1978), (36) Serezhkin *et al.* (1980a), (37) Burns *et al.* (2004b), (38) Branstätter (1981), (39) Almond *et al.* (2002a), (40) Sykora & Albrecht-Schmitt (2003), (41) Obbade *et al.* (2004c), (42) Obbade *et al.* (2004c), (43) Padel *et al.* (1972), (44) Gasperin *et al.* (1991), (45) Yamashita *et al.* (1981), (46) Hoekstra & Siegel (1971), (47) Siegel & Hoekstra (1968), (48) Bacmann & Bertaut (1966), (49) Bénard *et al.* (1994), (50) Sullens *et al.* (2004).

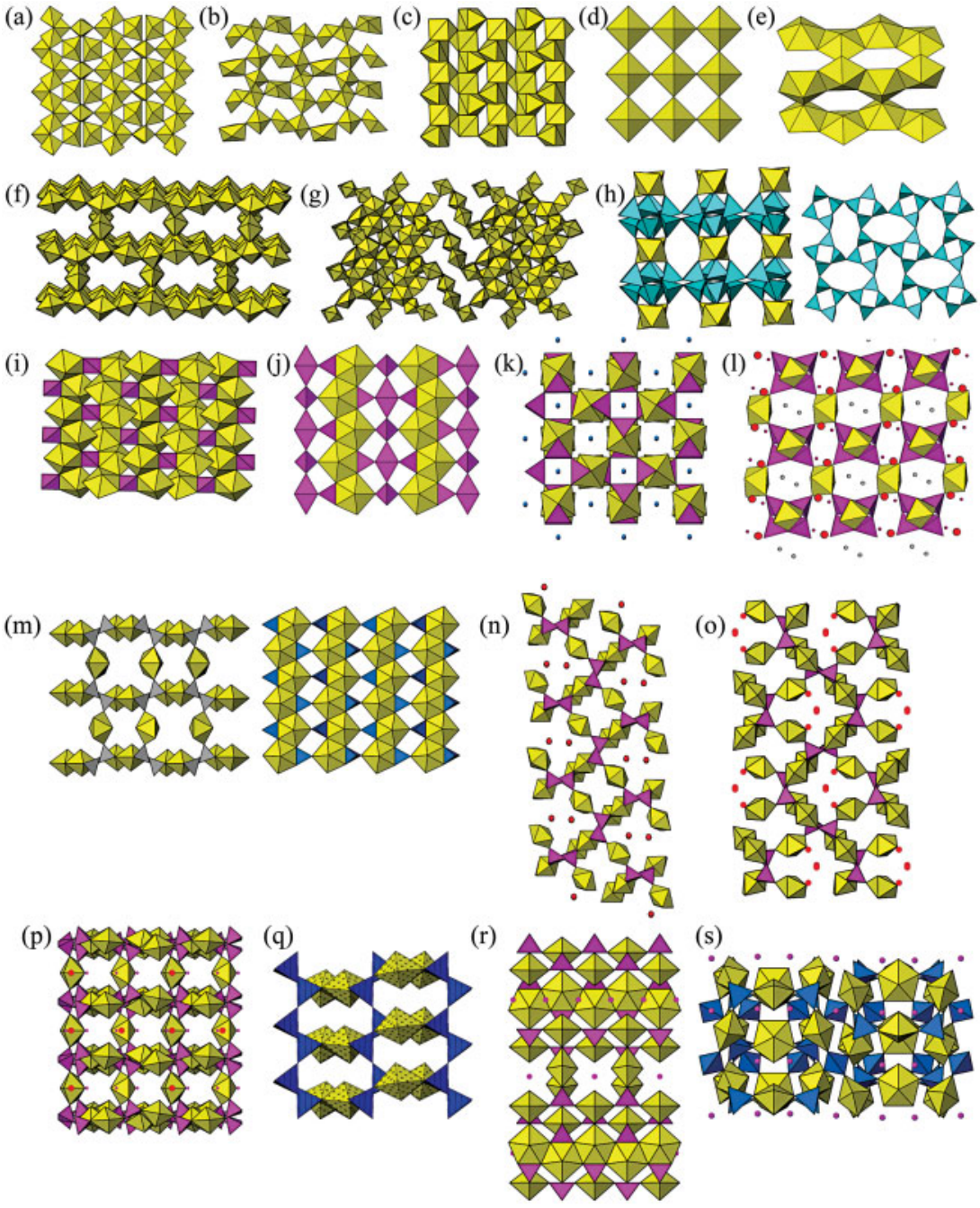

FIG. 15. Frameworks of uranyl polyhedra and other polyhedra containing higher-valence cations. The corresponding compounds are listed in Table 10.

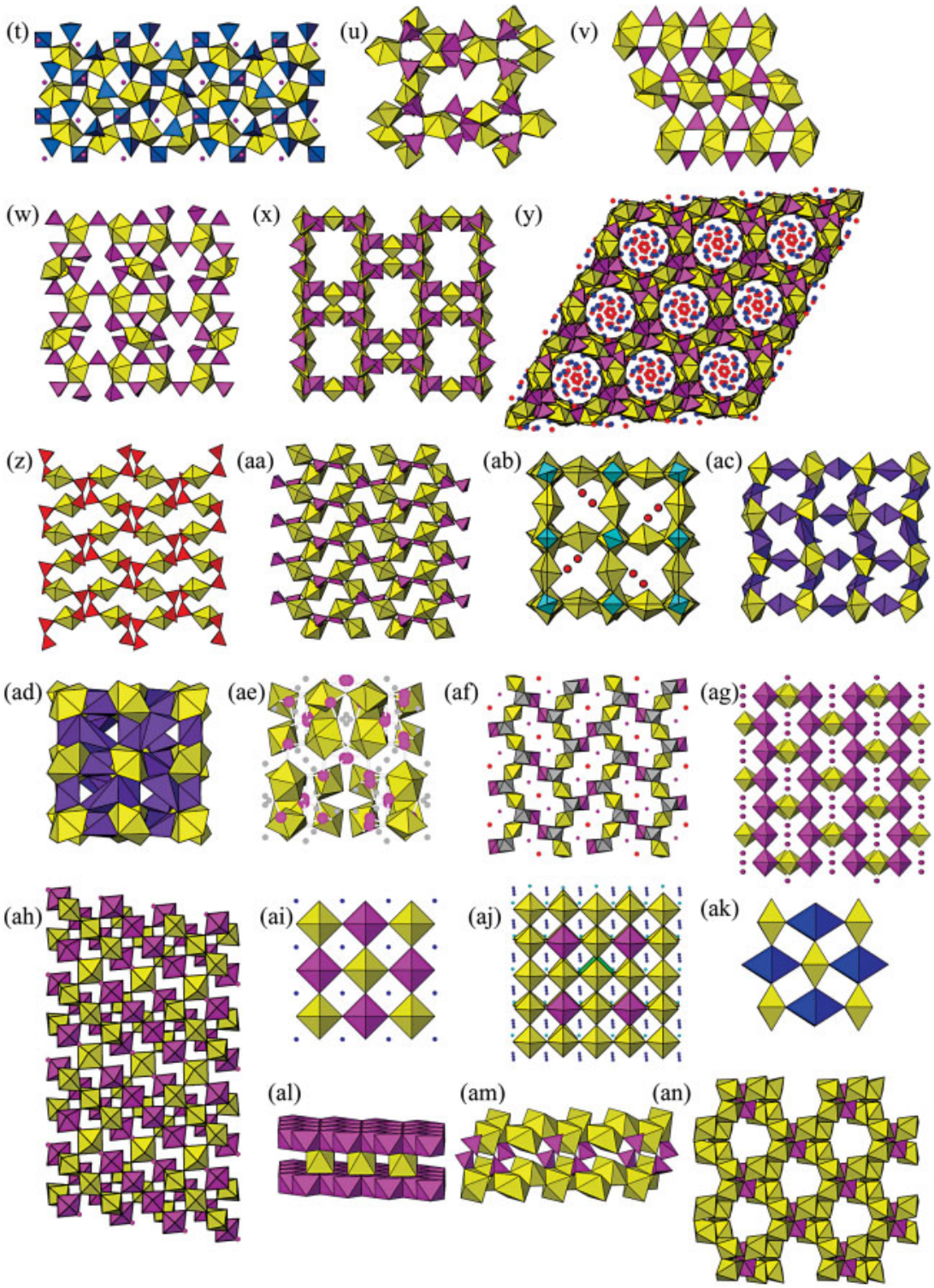
(t)
(u)
(v)
(w)
(x)
(y)
(z)
(aa)
(ab)
(ac)
(ad)
(ae)
(af)
(ag)
(ah)
(ai)
(aj)
(ak)
(al)
(am)
(an)

of vertex- and edge-sharing uranium polyhedra that are closely related to the chains of polyhedra that make up the curite sheet (Fig. 11l). The Pb^{2+} cations are located in channels extending through the framework of polyhedra.

Frameworks of uranium polyhedra and silicate tetrahedra

The structures of six framework uranyl silicates, two of which are minerals, and one uranyl germanate, have been described. In each structure, uranyl polyhedra share vertices or edges with silicate (or germanate) tetrahedra, and the frameworks are composed entirely of uranyl polyhedra and silicate (or germanate) tetrahedra.

The compound $KNa_3[(UO_2)_2(Si_4O_{10})_2](H_2O)_4$ was first found as an alteration phase of actinide-bearing borosilicate glass under consideration as a containment material for nuclear waste (Burns *et al*. 2000). The structure contains sheets of vertex-sharing silicate tetrahedra involving both four- and eight-membered rings of tetrahedra (Fig. 15h). Adjacent silicate sheets are connected through uranyl square bipyramids, such that apical ligands of the silicate tetrahedra correspond to all four of the equatorial vertices of the bipyramid (Fig. 15h). $Na_4[(UO_2)_2(Si_4O_{10})_2](H_2O)_4$ was later synthesized, and has an identical uranyl silicate framework (Li & Burns 2001a).

Soddyite and the isostructural compound $[(UO_2)_2(GeO_4)(H_2O)_2]$ contain uranyl pentagonal bipyramids that form chains by sharing equatorial edges (Fig. 15i). Each bipyramid also shares an edge with a tetrahedron, and the single unshared equatorial vertex of the bipyramid is occupied by H_2O. Adjacent uranyl silicate (germanate) chains are directly linked as each tetrahedron shares two edges with bipyramids from two different chains. Additional linkages arise through H bonds.

The structure of weeksite (Fig. 15j) contains sheets of uranyl pentagonal bipyramids and silicate tetrahedra that are topologically identically to those found in haiweeite. In the case of haiweeite, adjacent sheets are connected through bonds to Ca cations located in the interlayer. In weeksite, the sheets are connected into a framework through the apical O atoms of the silicate tetrahedra, which provides for channels extending parallel to the sheets that contain lower-valence cations and H_2O.

The structure of $Na_2[(UO_2)(SiO_4)]$ contains U^{6+} in distorted octahedral coordination, with four short (~2 Å) and two longer (~2.3 Å) U^{6+}–O bonds. Each $U^{6+}O_6$ octahedron shares four of its vertices with silicate tetrahedra, and Na cations are located in channels in the framework (Fig. 15k).

The compound $RbNa[(UO_2)(Si_2O_6)](H_2O)$ contains rings of four silicate tetrahedra formed by the sharing of tetrahedral vertices (Fig. 15l). Identical rings of tetrahedra are linked into sheets that are parallel to (001) by sharing vertices with uranyl square bipyramids, such that each of the equatorial ligands of the square bipyramid is shared with a tetrahedron from a different ring. The sheets are linked into a framework through additional uranyl square bipyramids, such that the four vertices of the silicate tetrahedra are shared with two tetrahedra within the ring, and two bipyramids. Note that similar four-membered rings of silicate tetrahedra occur in $KNa_3[(UO_2)_2(Si_4O_{10})_2](H_2O)_4$, in which they are linked directly to form silicate sheets (Fig. 15h).

Frameworks of uranyl pentagonal bipyramids and phosphate, arsenate, or vanadate tetrahedra

The compounds $[(UO_2)_3(PO_4)_2](H_2O)_4$, $(UO_2)[(UO_2)(AsO_4)]_2(H_2O)_4$, $(UO_2)[(UO_2)(AsO_4)]_2(H_2O)_5$, and $(UO_2)[(UO_2)(VO_4)]_2(H_2O)_5$ each contain topologically identical sheets of uranyl pentagonal bipyramids and tetrahedra, as shown in Figure 15m. The sheet is based upon the uranophane anion-topology (Fig. 10a), but is a novel graphical isomer. Note that all of the tetrahedra that share edges with bipyramids of any given chain of bipyramids are oriented in the same direction, in contrast to the uranyl silicate sheets shown in Figure 10. In all four structures, adjacent sheets are connected through uranyl pentagonal bipyramids located between the sheets, resulting in frameworks. Each of the bipyramids between the sheets shares one of its equatorial vertices with a tetrahedron in the sheet on either side, and the remaining three equatorial vertices are H_2O. In the cases of $[(UO_2)_3(PO_4)_2](H_2O)_4$ (Fig. 15m), $(UO_2)[(UO_2)(VO_4)]_2(H_2O)_5$, and $(UO_2)[(UO_2)(AsO_4)]_2(H_2O)_4$ (Fig. 15n), the sheets of polyhedra are relatively flat. In the case of $(UO_2)[(UO_2)(AsO_4)]_2(H_2O)_5$, the sheets are strongly corrugated (Fig. 15o).

The compounds $Cs_2(UO_2)[(UO_2)(PO_4)]_4(H_2O)_2$, $Rb_2(UO_2)[(UO_2)(PO_4)]_4(H_2O)_2$, $K_2(UO_2)[(UO_2)(PO_4)]_4(H_2O)_2$, $Cs_2(UO_2)[(UO_2)(AsO_4)]_4(H_2O)_2$, and $Rb_2(UO_2)[(UO_2)(AsO_4)]_4(H_2O)_{4.5}$ possess homeotypic framework structures (Fig. 15p). Each has sheets of uranyl pentagonal bipyramids and tetrahedra that are based upon the underlying uranophane anion-topology (Fig. 10a). In each structure, the sheet is the same graphical isomer as found in β-uranophane. Adjacent sheets are connected into a framework by sharing vertices with uranyl pentagonal bipyramids located between the sheets. Each interlayer bipyramid shares four of its equatorial vertices with tetrahedra, two from each of the adjacent sheets. The remaining equatorial vertex of the bipyramid is H_2O. The low-valence cations and additional H_2O are located in channels extending through the framework.

The structure of $[(UO_2)_2V_2O_7]$ (Fig. 15q) is a framework of uranyl pentagonal bipyramids and vanadate tetrahedra. It contains sheets that are based upon the uranophane anion-topology, with the same graphical isomer as found for $[(UO_2)_3(PO_4)_2](H_2O)_4$, $(UO_2)[(UO_2)(AsO_4)]_2(H_2O)_4$, $(UO_2)[(UO_2)(AsO_4)]_2(H_2O)_5$,

and $(UO_2)[(UO_2)(VO_4)]_2(H_2O)_5$ (Fig. 15m). However, in the structure of $[(UO_2)_2V_2O_7]$, there are no uranyl ions located between the sheets; rather, direct sharing of apical ligands of the vanadate tetrahedra connects the sheets into a framework.

The structure of $Na[(UO_2)_4(VO_4)_3]$ is an unusually complex framework composed of uranyl pentagonal bipyramids and vanadate tetrahedra (Fig. 15r). The bipyramids are linked by sharing edges into chains that are one bipyramid wide. Vanadate tetrahedra share equatorial edges of the bipyramids on either side of the chain, in the same fashion as occurs in sheets based upon the uranophane anion-topology. However, the uranyl vanadate chains in $Na[(UO_2)_4(VO_4)_3]$ are not aligned to form sheets, but rather occur in the structure in two mutually perpendicular orientations, and are linked into a framework with channels that accommodate the Na cations.

Frameworks of uranyl polyhedra and molybdate tetrahedra

Twelve uranyl molybdate compounds, corresponding to seven distinct crystal structures, are frameworks of uranyl pentagonal bipyramids and molybdate tetrahedra. The considerable diversity of this chemical group is related to the flexibility of the linkage between the bipyramids and tetrahedra, which show a range of U–O–Mo bond angles (*e.g.*, Krivovichev & Burns 2003b).

The compounds $Cs_2[(UO_2)_6(MoO_4)_7(H_2O)_2]$, $(NH_4)_2[(UO_2)_6(MoO_4)_7(H_2O)_2]$, and $Rb_2[(UO_2)_6(MoO_4)_7(H_2O)_2]$ are isostructural (Fig. 15s). There are two types of uranyl pentagonal bipyramids, those that share each of their equatorial vertices with molybdate tetrahedra, and those that share only four of their equatorial vertices with molybdate tetrahedra, with the fifth vertex corresponding to H_2O. All of the molybdate tetrahedra link to four different bipyramids. The lower-valence cations are located in irregular voids within the framework of polyhedra.

The compounds α-$Cs_2[(UO_2)_2(MoO_4)_3]$, $Rb_2[(UO_2)_2(MoO_4)_3]$ and $Tl_2[(UO_2)_2(MoO_4)_3]$ are isostructural (Fig. 15t). Each bipyramid shares all five of its equatorial vertices with molybdate tetrahedra, and the tetrahedra are either linked to three or four bipyramids. The structure contains unusually large channels that extend along [001] and [100], with dimensions 3.5 $\times$ 10.5 Å and 4.8 $\times$ 4.8 Å, respectively. The Cs and Rb cations are located within the channels through the framework.

The structures of $Ba(UO_2)_3(MoO_4)_4(H_2O)_4$ (Fig. 15u), α-$(UO_2)(MoO_4)(H_2O)_2$ (Fig. 15v), $Sr(UO_2)_6(MoO_4)_7(H_2O)_{19}$ (Fig. 15w), $Mg(UO_2)_3(MoO_4)_4(H_2O)_8$ (Fig. 15x) and $Ca[(UO_2)_6(MoO_4)_7(H_2O)_2](H_2O)_n$ (Fig. 15w) further illustrate the flexibility of the linkage between uranyl pentagonal bipyramids and molybdate tetrahedra. Each involves only vertex-sharing between these two types of polyhedra, yet the structural connectivities are remarkably diverse. In $Ba(UO_2)_3(MoO_4)_4(H_2O)_4$ and $Mg(UO_2)_3(MoO_4)_4(H_2O)_8$, only four of the equatorial vertices of the bipyramids are shared with tetrahedra, with the fifth position occupied by H_2O. In α-$(UO_2)(MoO_4)(H_2O)_2$ and $Sr(UO_2)_6(MoO_4)_7(H_2O)_{19}$, all of the equatorial vertices of the bipyramids are shared with tetrahedra. The ratios of bipyramids to tetrahedra range considerably in these four structures; in those with more tetrahedra relative to bipyramids, fewer of the vertices of the tetrahedra are linked to bipyramids. In $Mg(UO_2)_3(MoO_4)_4(H_2O)_8$ and $Ba(UO_2)_3(MoO_4)_4(H_2O)_4$, channels through the framework are bounded by O atoms of the uranyl ions, as well as by some apical (unshared) ligands of the tetrahedra. In $Sr(UO_2)_6(MoO_4)_7(H_2O)_{19}$ and $Ca[(UO_2)_6(MoO_4)_7(H_2O)_2](H_2O)_n$, channels in the framework are delineated by apical O atoms of tetrahedra.

The structure of $(NH_4)_2[(UO_2)_5(MoO_4)_7](H_2O)_5$ warrants special attention owing to the presence of large channels through the framework of uranyl pentagonal bipyramids and molybdate tetrahedra (Fig. 15y). Each of the five symmetrically distinct uranyl pentagonal bipyramids share all five of their equatorial vertices with tetrahedra, whereas four of the seven distinct tetrahedra share each of their vertices with bipyramids, and the remaining are each connected to three bipyramids. The considerable range of U–O–Mo bond angles in the structure, from 123.7 to 166.7°, permits the unprecedented connectivity observed in this structure (Krivovichev *et al.* 2003). The structure contains strips of bipyramids and tetrahedra that spiral about the tubular openings along [001], with a primitive repeat-distance of 70.6 Å. The resulting framework contains several channels, the largest of which extends along [001] with a cross-section of 7.5 by 7.5 Å. The (NH_4) cations and H_2O groups are located within the various channels.

Miscellaneous frameworks

Pyrophosphate P_2O_7 groups link uranyl pentagonal bipyramids into a framework in the structure of $Na_2[(UO_2)(P_2O_7)]$ (Fig. 15z). One phosphate tetrahedron of the pyrophosphate group shares an equatorial edge of a bipyramid, a vertex with another adjacent bipyramid, and one vertex with the other tetrahedron of the pyrophosphate group. The other phosphate tetrahedron shares a vertex with one bipyramid, and the remaining two vertices are unshared within the framework. The Na cations are located within voids in the framework.

The compounds α-$(UO_2)(SeO_4)$, β-$(UO_2)(SO_4)$, and $(UO_2)(MoO_4)$ have unusual frameworks that include cation–cation interactions (Fig. 15aa). Uranyl pentagonal bipyramids are linked into single-width chains extending along [010]. Each linkage between the bipyramids occurs through a cation–cation interaction,

meaning that one of the uranyl ion O atoms of each bipyramid is also an equatorial vertex of an adjacent bipyramid within the chain. The chains of bipyramids are linked through tetrahedra, and each of the tetrahedra shares all four of its vertices with bipyramids of the chains. In the case of the bipyramids, one of the equatorial positions corresponds to the cation–cation interaction, and each of the others is linked to tetrahedra.

The structure of $[(UO_2)_3(PO_4)O(OH)(H_2O)_2](H_2O)$ has structural elements in common with the phosphuranylite group of minerals (Fig. 15ab). The framework contains uranyl pentagonal and hexagonal bipyramids, as well as phosphate tetrahedra. Pentagonal bipyramids share an equatorial edge, forming a dimer. The dimers are linked into chains by sharing edges with hexagonal bipyramids, such that four of the equatorial edges of the hexagonal bipyramids are shared with pentagonal bipyramids, two on either side. The two equatorial edges of the hexagonal bipyramids that are not shared with pentagonal bipyramids are shared with phosphate tetrahedra, resulting in uranyl phosphate chains that are topologically identical to those found as parts of sheets in the phosphuranylite group of minerals. The H_2O groups are located at the non-chain equatorial vertices of the uranyl pentagonal bipyramids. The uranyl phosphate chains are in two mutually perpendicular orientations, and are linked directly through the phosphate tetrahedra, as each tetrahedron shares one edge with each of two different chains (Fig. 15ab). The resulting framework has channels along [001] that are delineated by uranyl phosphate chains on either side. The framework is electroneutral, with only H_2O groups located in the channels.

The compounds $Pb_2[(UO_2)(TeO_3)_3]$ (Fig. 15ad), $Na_8[(UO_2)_6(TeO_3)_{10}]$ (Fig. 15ae) and cliffordite (Fig. 15ad) all contain Te^{4+} cations that have stereoactive lone-electron pairs. Typically, the Te^{4+} cation is strongly bonded to three atoms of O with bond lengths of ~1.9 Å, as well as some additional anions located about 2.5 to 3.0 Å from the cation. The three short bonds about the cation are on one side, and the coordination polyhedron is a pyramid that is capped by the cation. The structures of $Pb_2(UO_2)(TeO_3)_3$ and $Na_8[(UO_2)_6(TeO_3)_{10}]$ each contain uranyl pentagonal bipyramids that share equatorial vertices and edges with TeO_3 pyramids to form the framework. Cliffordite is unusual in that it is the only framework structure for which all of the U is in hexagonal bipyramidal coordination.

The structure of $K_2[(UO_2)_2(VO)_2(IO_6)_2O](H_2O)$ is a rather open framework of uranyl square bipyramids and distorted VO_6 and IO_6 octahedra (Fig. 15af). The octahedra share edges, forming a chain that extends along [001]. The chains are linked into ribbons by sharing polyhedron vertices, and these ribbons are linked into the framework through the equatorial vertices of the uranyl square bipyramids. The K cations and H_2O groups are located in channels that extend through the framework (Fig. 15af).

The lithium uranyl tungstates $Li(UO_2)(WO_4)_2$ and $Li_2(UO_2)_4(WO_4)_4O$ both contain distorted WO_6 octahedra and uranyl pentagonal bipyramids, and $Li_2(UO_2)_4(WO_4)_4O$ also has uranyl square bipyramids. The structure of $Li(UO_2)(WO_4)_2$ contains sheets of vertex-sharing WO_6 octahedra that are linked through vertex-sharing with the uranyl polyhedra (Fig. 15ag). Note that uranyl polyhedra are linked into chains by vertex-sharing. These chains are identical to those found in sheets based upon the uranophane anion-topology (Fig. 10). As noted by Obbade *et al*. (2004c), insertion of additional chains of uranyl pentagonal bipyramids in the voids occupied by Li cations would result in uranyl tungstate sheets with the uranophane anion-topology. The structure of $Li_2(UO_2)_4(WO_4)_4O$ is composed of slabs of uranyl pentagonal bipyramids and WO_6 octahedra that are based upon the uranophane anion-topology (Fig. 15ah). These slabs are linked into a framework by sharing vertices with uranyl square bipyramids.

The perovskite-like structures of Ba_2MgUO_6 and $K_9BiU_6O_{24}$ (Figs. 15ai, aj) can be described as derivatives of the δ-UO_3 structure-type (Fig. 15d). In both cases, the U^{6+} cations are in holosymmetric octahedral coordination, with no uranyl ion present. These structures are derived from that of δ-UO_3 by doubling the unit-cell edges, replacing some of the UO_6 octahedra with either MgO_6, BiO_6 or KO_6 octahedra, and with Ba or K cations inserted into the 12-coordinated sites of the channels.

The structures of β-$Cd(UO_2)O_2$, $Cu(UO_2)O_2$, and $Mn(UO_2)O_2$ (Fig. 15ak) are closely related, although they are not strictly isostructural, as they crystallize in different space-groups. Each contains uranyl square bipyramids and octahedra that are occupied by the divalent cations. The O_{Ur} atoms are part of the octahedral coordination of the divalent cations, and as a result the U^{6+}–O bond lengths are longer than usual.

The structure of UCr_2O_6 involves a framework of uranyl square bipyramids and chromate octahedra (Fig. 15al). The chromate octahedra share edges, resulting in brucite-like sheets, but one-third of the octahedral sites are vacant. The uranyl square bipyramids are located between the chromate sheets, in correspondence with the vacant sites of the sheets of octahedra.

The compound $U^{4+}(UO_2)(PO_4)_2$ contains both U^{4+} coordinated by seven O atoms, and U^{6+} present as the typical uranyl pentagonal bipyramid. The uranium polyhedra share edges, giving chains that are cross-linked into a framework by sharing edges and corners with PO_4 tetrahedra (Fig. 15am).

The compound $Cs[(UO_2)_3(HIO_6)(OH)(O)(H_2O)](H_2O)_{15}$, as well as the isostructural Li, Na, K and Rb compounds, have the unusual framework of uranyl pentagonal bipyramids and periodate octahedra shown in Figure 15an. The most unusual aspect of this relatively open framework is that some of the linkages between uranyl pentagonal bipyramids are through

cation–cation interactions, making this one of the few uranyl compounds to show this type of connectivity. Sullens *et al*. (2004) suggested that the chelation of the U(3) cation, which is involved in the cation–cation interaction, by the HIO_6^{4-} ion results in transfer of significant electron-density from the HIO_6^{4-} ion to the uranyl ion, thus stabilizing the cation–cation interaction.

Nanostructure Materials

Nanostructure materials exhibit important properties with promise for many potential applications. Such materials also provide unique opportunities to study fundamental structure–property relationships, and the properties of many nanoscale materials are measurably particle-size dependent. Self-assembling small clusters have been reported based on main-group elements, most notably C-60-buckminsterfullerene (Kroto *et al*. 1985), and transition-metal oxide clusters, including a wide variety of polyoxometalates built on WO, MoO, and NbO framework structures (Müller *et al*. 1998). Following the discovery of carbon nanotubes, considerable attention has also been devoted to synthesizing a range of oxidic nanotubular materials, which also have

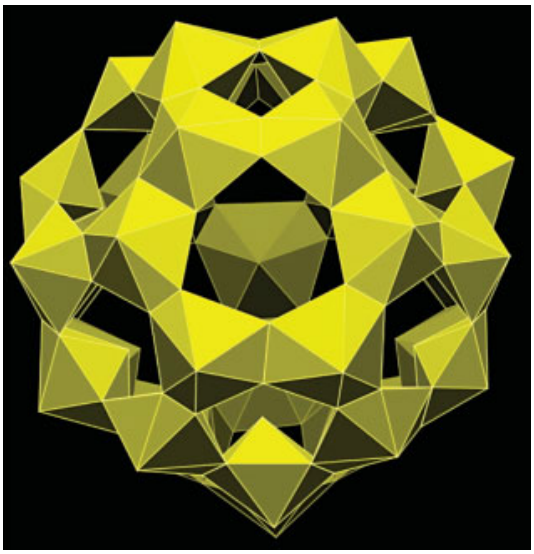

FIG. 16. U–32 uranyl peroxide nanosphere formed by the linkage of 32 chemically identical uranyl peroxide polyhedra. From Burns *et al*. (2005).

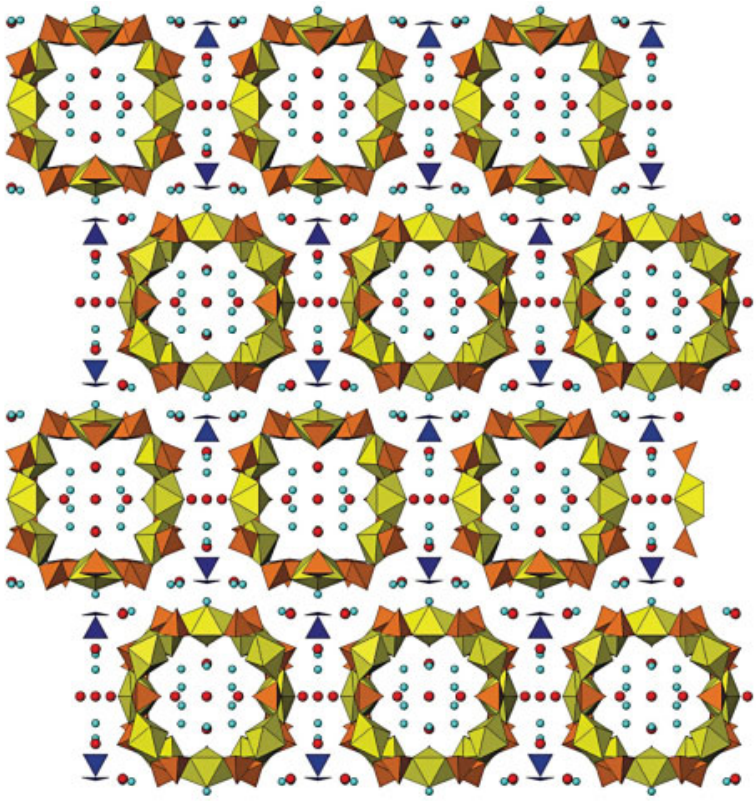

FIG. 17. Nanoscale tubules in a uranyl selenate. From Krivovichev *et al*. (2005a).

tremendous potential in materials applications. Prior to 2005, no materials have been reported with nanoscale aggregates or tubules of higher-valence actinide ions.

Burns *et al*. (2005) described an unprecedented family of actinyl peroxide nanoclusters. These chemically and structurally elegant spherical clusters were obtained from alkaline solutions containing peroxide under ambient conditions. The clusters are assembled from topologically identical uranyl peroxide polyhedra, and contain 24, 28 or 32 uranyl peroxide polyhedra within the clusters (*e.g*., Fig. 16). Burns *et al*. (2005) provided evidence for the self-assembly and persistence of the some of these clusters in alkaline solutions, prior to crystallization in complex molecular crystals. The assembly and persistence of these nanoclusters in solution suggest that they may influence the mobility of actinides in the environment, such as where highly alkaline nuclear wastes leak into the vadose zone. The complexity of the clusters, which constitute a new class of polyoxometalates, is in sharp contrast to other clusters of cation polyhedra of higher bond-valence in uranyl compounds that are illustrated in Figure 4.

Krivovichev *et al*. (2005a, b) reported the synthesis and structures of two remarkable new uranyl selenate compounds that contain nanoscale tubules (Fig. 17). In each case, uranyl pentagonal bipyramids share vertices with selenate tetrahedra, resulting in open sheets that are rolled into single-walled tubes, with external diameters of 17 and 25 Å, and inner crystallographically free diameters of 4.7 and 12.6 Å. This discovery presents the fascinating possibility that many of the myriad of sheets containing uranyl polyhedra may be able to form nanoscale tubules. The range of sheet topologies and compositions suggests many potential applications of such materials.

Summary and Future Outlook

The convergence of greatly enhanced technologies for detection of X-rays in single-crystal experiments with a renewed interest in the crystal chemistry of U^{6+} has resulted in an explosion of new structures containing U^{6+}. During the past decade, known structures of uranyl compounds has more than doubled. These studies have further revealed the tremendous structural elegance, beauty, and complexity of uranyl compounds, which are reflected in the many Figures of this manuscript.

Of the 368 structures covered in this structural hierarchy, 204 (55.4%) are based upon sheets of polyhedra containing cations of higher valence, and of the 89 minerals, 69 (77.5%) contain sheets. Structures based upon infinite chains and frameworks of polyhedra are about equally abundant, and correspond to 57 (15.5%) and 56 structures, respectively. Ten uranyl minerals are classed as infinite-chain structures, whereas only three have frameworks of polyhedra. There are 43 uranyl compounds with structures based upon isolated clusters of polyhedra, of which seven are minerals. Eight structures contain isolated uranyl polyhedra. In 1996, Burns *et al*. placed 180 structures in their hierarchy, of which 56 are minerals, 106 contain sheets, 19 contain chains, 22 contain clusters, 26 are frameworks, and seven contain isolated uranyl polyhedra. Structures discovered since 1996 have revealed many novel topological arrangements of uranyl polyhedra and other polyhedra containing higher-valence cations. Many of the new structures also correspond to topological arrangements that were known in 1996, and they expand the range of compositions known to adopt a given topology.

Tremendous advances have been made in understanding the crystal chemistry of uranyl compounds, including the structures of uranyl minerals. The structures of virtually all of the common uranyl minerals have been resolved, but the structures are still either unknown or unrefined for about half of the known uranyl minerals, many of which are extremely rare. There has been extensive exploration of many of the chemical classes of inorganic uranyl compounds, and much of the recent work has been focused on uranyl compounds containing tetrahedrally coordinated hexavalent cations such as Mo, S, and Cr, as well as cations that contain stereoactive lone-electron pairs such as Te^{4+} and Se^{4+}. Despite the considerable effort expended on structural studies of such chemical classes of uranyl compounds, new structural units and topologies continue to be found on a regular basis, which suggests that many more novel structural connectivities await discovery.

In developing the current structural hierarchy, I have attempted to provide a cohesive framework for the discussion and understanding of the structures of inorganic uranyl compounds. I consider this step to be essential toward application of knowledge of these structures to mineralogical, geological, environmental and technological issues. Just one example of the importance of understanding the structures and chemical composition of uranyl minerals and compounds lies in the area of nuclear waste disposal. Alteration of nuclear waste forms such as spent nuclear fuel and actinide-bearing waste glasses in a geological repository under moist oxidizing conditions will obviously result in complex suites of uranyl compounds. Some of these alteration phases will incorporate radionuclides into their structures, which is important for the long-term performance of the repository. Theoretical predictions of such incorporation mechanisms, as well as experimental verification of incorporation require a detailed understanding of the crystal structures. Determination of the thermodynamic stabilities and solubilities of uranyl compounds relies heavily on the structural formulae derived from crystallographic studies, as the compositions of many of these phases were incorrectly assigned in the absence of knowledge of their structures. Synthesis and structural analysis have permitted the discovery of many new uranyl compounds that may be relevant to repository performance. The ultimate prediction of thermodynamic properties and occurrences

of uranyl compounds on the basis of their structural connectivities is a tantalizing prospect, but this goal requires a detailed understanding of the crystal chemistry of uranium.

Reports of both nanoscale clusters containing uranyl polyhedra and nanotubular uranyl compounds appeared in the spring of 2005, and represent a new direction in the crystal chemistry of uranium and actinides in general. Discovery of these novel materials occurred after many years of research concerning uranyl crystal chemistry, at a time when the casual observer might have considered studies of uranium crystal chemistry to be a relatively mature field. Now, there are many research opportunities concerning nanoscale uranium-based materials, including their importance for understanding chemical processes involving actinides, the potential for novel materials applications, and the impact of such materials on transport of actinides in the environment.

Unlike U^{6+}, relatively few crystal structures have been analyzed that contain neptunium or plutonium in higher oxidation states (5+ or 6+). The degree to which the considerable knowledge concerning U^{6+} crystal chemistry may be transferable to Np and Pu compounds is unclear. The few structures of Np^{5+}, Np^{6+}, Pu^{5+} and Pu^{6+} compounds that are known do contain the same types of coordination polyhedra as U^{6+}, actinyl ions in square, pentagonal and hexagonal bipyramidal polyhedra. As such, one might expect that Np and Pu structures will in many ways be similar to those already known from uranyl compounds. This may largely be the case for Np^{6+} and Pu^{6+}, although their slightly longer bond-lengths, as compared with U^{6+}, may lead to some novel structural connectivities in structures where the sharing of edges between actinyl polyhedra and polyhedra containing higher-valence cations is important. In the cases of Np^{5+} and Pu^{5+}, the actinyl ion has a formal valence of 1+, and the bond strengths within the actinyl ions are likely to be somewhat lower than in the case where a hexavalent cation is present. As such, the O atoms of the actinyl ions containing Np^{5+} and Pu^{5+} will be more readily shared with other actinyl polyhedra, thus cation–cation interactions are likely to be much more important than in uranyl structures. The few structures of Np^{5+} compounds that are in the literature, as well as about a dozen structures my group and I have recently determined, commonly do contain cation–cation interactions, which results in dramatically different structures as compared to uranyl compounds with similar chemical compositions.

Acknowledgements

I acknowledge the Mineralogical Association of Canada for support and encouragement throughout my ongoing education and career. I am grateful to Prof. Rodney Ewing and Dr. Mark Miller for their tremendous contributions in the development of our original hierarchy of uranyl structures that was published in 1996. My research group at the University of Notre Dame has contributed in many ways to my understanding of uranyl crystal chemistry; I am grateful to all members of my group, past and present: post-doctoral fellows Sergey Krivovichev, Christopher Cahill, Robert Shuvalov, Francis Hill, Philip Almond, Oksana Kurmakova, graduate students Yaping Li, Andrew Locock, Karrie-Ann Hughes, Jennifer Jackson, Tori Ziemann, Paul Giesting, Amanda Klingensmith, Cara Alexopoulos, Bridget McCollam, undergraduates Erin Keppel, Alex Garza, Rebecca Glatz, Kara Tholen, Andrew Irvine, Aaron Martin, Kathryn Deely, Leslie Hayden, Jessica Callahan, Theodore Flynn, Lauren Sturm, Peter Hotchkiss, Virginia Kelly, Nathan Porter, Patrick Horan, Karen Carlaccini, Ginger Sigmon, Maha Jain, Jinalee Almes, and Erin Diminick. Leslie Hayden prepared many preliminary versions of the figures of uranyl compounds used in this manuscript.

I thank Prof. Thomas Albrecht-Schmitt and Prof. Sergey Krivovichev for their reviews of this manuscript, and Prof. Krivovichev for providing preprints of several of his papers. Thanks also to Prof. Frank C. Hawthorne and Prof. Robert F. Martin for editing the manuscript.

I acknowledge financial support for several years of study of uranyl crystal chemistry from the Environmental Management Sciences Program of the United States Department of Energy (DE–FG07–97ER14820), the National Science Foundation for my studies of Pb uranyl oxide hydrate minerals (EAR98–04723), and the National Science Foundation for the Environmental Molecular Science Institute at the University of Notre Dame (EAR02–21966). I also acknowledge current funding from the Office of Science, Technology and International of the United States Department of Energy that will permit the continuation of this line of research.

References

Åberg, M. (1969): The crystal structure of $[(UO_2)_2(OH)_2Cl_2(H_2O)_4]$. *Acta Chem. Scand.* **23**, 791-810.

_____ (1976): The crystal structure of $[(UO_2)_4Cl_2O_2(OH)_2(H_2O)_6]\bullet 4H_2O$ a compound containing a tetranuclear aquachlorohydroxooxo complex of uranyl(VI). *Acta Chem. Scand.* **A30**, 507-514.

_____ (1978) The crystal structure of hexaaqua-tri-μ-hydroxo-μ_3-oxo-triuranyl(VI) nitrate tetrahydrate, $[(UO_2)_3O(OH)_3(H_2O)_6]NO_3\bullet 4H_2O$. *Acta Chem. Scand.* **A32**, 101-107.

Alcock, N.W., Roberts, M.M. & Brown, D. (1982): Actinide structural studies. 3. The crystal and molecular structures of $UO_2SO_4\bullet H_2SO_4\bullet 5H_2O$ and $(NpO_2SO_4)_2\bullet H_2SO_4\bullet 4H_2O$. *J. Chem. Soc., Dalton Trans.*, 869-873.

ALLPRESS, J.G. & WADSLEY, A.D. (1964): The crystal structure of caesium uranyl oxychloride $Cs_x(UO_2)OCl_x$ (*x* approximately 0.9). *Acta Crystallogr.* **17**, 41-46.

ALMOND, P.M. & ALBRECHT-SCHMITT, T.E. (2002a): Hydrothermal syntheses, structures, and properties of the new uranyl selenites $Ag_2(UO_2)(SeO_3)_2$, $M[(UO_2)(HSeO_3)(SeO_3)]$ (M = K, Rb, Cs, Tl) and $Pb(UO_2)(SeO_3)_2$. *Inorg. Chem.* **41**, 1177-1183.

_____ & _____ (2002b): Expanding the remarkable structural diversity of uranyl tellurites: hydrothermal preparation and structures of $K[UO_2Te_2O_5(OH)]$, $Tl_3\{(UO_2)_2[Te_2O_5(OH)](Te_2O_6)\}\bullet 2H_2O$, β-$Tl_2[UO_2(TeO_3)_2]$, and $Sr_3[UO_2(TeO_3)_2](TeO_3)_2$. *Inorg. Chem.* **41**, 5495-5501.

_____ & _____ (2004): Hydrothermal synthesis and crystal chemistry of the new strontium uranyl selenites, $Sr[(UO_2)_3(SeO_3)_2O_2]\bullet 4H_2O$ and $Sr[UO_2(SeO_3)_2]$. *Am. Mineral.* **89**, 976-980.

_____, MCKEE, M.K. & ALBRECHT-SCHMITT, T.E. (2002a): Unusual uranyl tellurites containing $[Te_2O_6]^{4-}$ ions and three-dimensional networks. *Angew. Chem. Int. Ed.* **41**, 3426-3429.

_____, PEPER, S.M., BAKKER, E. & ALBRECHT-SCHMITT, T.E. (2002b): Variable dimensionality and new uranium oxide topologies in the alkaline-earth metal uranyl selenites $AE[(UO_2)(SeO_3)_2]$ (*AE* = Ca, Ba) and $Sr[(UO_2)(SeO_3)_2]\bullet 2H_2O$. *J. Solid State Chem.* **168**, 358-366.

APPLEMAN, D.E. & EVANS, H.T., JR. (1965): The crystal structures of synthetic anhydrous carnotite, $K_2(UO_2)_2V_2O_8$, and its cesium analogue, $Cs_2(UO_2)_2VO_8$. *Am. Mineral.* **50**, 825-842.

ATENCIO, D., NEUMANN, R., SILVA, A.J.G.C. & MASCARENHAS, Y.P. (1991): Phurcalite from Perus, São Paulo, Brazil, and redetermination of its crystal structure. *Can. Mineral.* **29**, 95-105.

BACHET, B., BRASSY, C. & COUSSON, A. (1991): Structure de $Mg[(UO_2)(AsO_4)]_2\bullet 4H_2O$. *Acta Crystallogr.* **C47**, 2013-2015.

BACMANN, M. & BERTAUT, E.F. (1966): Paramètres atomiques et structure magnétique de $MnUO_4$. *J. Physique* **27**, 726-734.

BEAN, A.C. & ALBRECHT-SCHMITT, T.E. (2001): Cation effects of the formation of the one-dimensional uranyl iodates $A_2[(UO_2)_3(IO_3)_4O_2]$ (A = K, Rb, Tl) and $AE[(UO_2)_2(IO_3)_2O_2](H_2O)$ (AE = Sr, Ba, Pb). *J. Solid State Chem.* **161**, 416-423.

_____, CAMPANA, C.F., KWON, O. & ALBRECHT-SCHMITT, T.E. (2001c): A new oxoanion: $[IO_4]^{3-}$ containing I(V) with a stereochemically active lone-pair in the silver uranyl iodate tetraoxoiodate(V), $Ag_4(UO_2)_4(IO_3)_2(IO_4)_2O_2$. *J. Am. Chem. Soc.* **123**, 8806-8810.

_____, PEPER, S.M. & ALBRECHT-SCHMITT, T.E. (2001a): Structural relationships, interconversion, and optical properties of the uranyl iodates, $UO_2(IO_3)_2$ and $UO_2(IO_3)_2(H_2O)$: a comparison of reactions under mild and supercritical conditions. *Chem. Mater.* **13**, 1266-1272.

_____, RUF, M. & ALBRECHT-SCHMITT, T.E. (2001b): Excision of uranium oxide chains and ribbons in the novel one-dimensional uranyl iodates $K_2[(UO_2)_3(IO_3)_4O_2]$ and $Ba[(UO_2)_2(IO_3)_2O_2](H_2O)$. *Inorg. Chem.* **40**, 3959-3963.

BEHM, H. (1985): Hexpotassium(*cyclo*-octahydroxotetracosaoxohexadecaborato) dioxouranate(VI) dodecahyrate, $K_6[UO_2\{B_{16}O_{24}(OH)_8\}]\bullet 12H_2O$. *Acta Crystallogr.* **C41**, 642-645.

BÉNARD, P., LOUËR, D., DACHEUX, N., BRANDEL, V. & GENET, M. (1994): $U(UO_2)(PO_4)_2$, a new mixed-valence uranium orthophosphate: *ab initio* structure determination from powder diffraction data and optical and X-ray photoelectron spectra. *Chem. Mater.* **6**, 1049-1058.

BLATOV, V.A., SEREZHKINA, L.B., SEREZKHIN, V.N. & TRUNOV, V.K. (1989): Crystal-structure of $NH_4UO_2SeO_4F\bullet H_2O$. *Zh. Neorg. Khim.* **34**, 162-164 (in Russ.).

BORÈNE, J. & CESBRON, F. (1970): Structure cristalline de l'uranyl-vanadate de nickel tetrahydraté $Ni(UO_2)_2(VO_4)_2\bullet 4H_2O$. *Bull. Soç. fr. Minéral. Cristallogr.* **93**, 426-432.

_____ & _____ (1971): Structure cristalline de la curiénite $Pb(UO_2)_2(VO_4)_2\bullet 5H_2O$. *Bull. Soç. fr. Minéral. Cristallogr.* **94**, 8-14.

BRANDENBURG, N.P. & LOOPSTRA, B.O. (1973): Uranyl sulphate hydrate, $UO_2SO_4\bullet 3½H_2O$. *Cryst. Struct. Commun.* **2**, 243-246.

_____ & _____ (1978): β-uranyl sulphate and uranyl selenate. *Acta Crystallogr.* **B34**, 3734-3736.

BRANSTÄTTER, F. (1981): Non-stoichiometric, hydrothermally synthesized cliffordite. *Tschermaks Mineral. Petrogr. Mitt.* **29**, 1-8.

BRUGGER, J., BURNS, P.C. & MEISSER, N. (2003): Contribution to the mineralogy of acid drainage of uranium minerals: marecottite and the zippeite-group. *Am. Mineral.* **88**, 676-685.

_____, KRIVOVICHEV, S.V., BERLEPSCH, P., MEISSER, N., ANSERMET, S. & ARMBRUSTER, T. (2004): Spriggite, $Pb_3[(UO_2)_6O_8(OH)_2](H_2O)_3$, a new mineral with β-$U_3O_8$-type sheets: description and crystal structure. *Am. Mineral.* **89**, 339-347.

BUCK, E.C., BROWN, N.R. & DIETZ, N.L. (1996): Contaminant uranium phases and leaching at the Fernald site in Ohio. *Env. Sci. Technol.* **30**, 81-88.

BURNS, P.C. (1997): A new uranyl oxide hydrate sheet in the structure of vandendriesscheite: implications for mineral paragenesis and the corrosion of spent nuclear fuel. *Am. Mineral.* **82**, 1176-1186.

_____ (1998a): CCD area detector of X-rays applied to the analysis of mineral structures. *Can. Mineral.* **36**, 847-853.

_____ (1998b): The structure of richetite, a rare lead uranyl oxide hydrate. *Can. Mineral.* **36**, 187-199.

_____ (1998c): The structure of compreignacite, $K_2[(UO_2)_3O_2(OH)_3]_2(H_2O)_7$. *Can. Mineral.* **36**, 1061-1067.

_____ (1998d): The structure of boltwoodite and implications of solid-solution toward sodium boltwoodite. *Can. Mineral.* **36**, 1069-1075.

_____ (1999a): The crystal chemistry of uranium. *In* Uranium: Mineralogy, Geochemistry and the Environment (P.C. Burns & R. Finch, eds.). *Rev. Mineral.* **38**, 23-90.

_____ (1999b): A new sheet complex sheet of uranyl polyhedra in the structure of wölsendorfite. *Am. Mineral.* **84**, 1661-1673.

_____ (1999c): Cs boltwoodite obtained by ion exchange from single crystals: implications for radionuclide release in a nuclear repository. *J. Nucl. Mater.* **265**, 218-223.

_____ (2000): A new uranyl phosphate chain in the structure of parsonsite. *Am. Mineral.* **85**, 801-805.

_____ (2001a): A new uranyl sulfate chain in the structure of uranopilite. *Can. Mineral.* **39**, 1139-1146.

_____ (2001b): A new uranyl silicate sheet in the structure of haiweeite and comparison to other uranyl silicates. *Can. Mineral.* **39**, 1153-1160.

_____, ALEXOPOULOS, C.M., HOTCHKISS, P.J. & LOCOCK, A.J. (2004b): An unprecedented uranyl phosphate framework in the structure of $[(UO_2)_3(PO_4)O(OH)(H_2O)_2](H_2O)$. *Inorg. Chem.* **43**, 1816-1818.

_____ & DEELY, K.M. (2002): A topologically novel sheet of uranyl pentagonal bipyramids in the structure of $Na[(UO_2)_4O_2(OH)_5](H_2O)_2$. *Can. Mineral.* **40**, 1579-1586.

_____, _____ & HAYDEN, L.A. (2003): The crystal chemistry of the zippeite group. *Can. Mineral.* **41**, 687-706.

_____, _____ & SKANTHAKUMAR, S. (2004a): Neptunium incorporation into uranyl compounds that form as alteration products of spent nuclear fuel: implications for geologic repository performance. *Radiochim. Acta* **92**, 151-160.

_____, EWING, R.C. & HAWTHORNE, F.C. (1997a): The crystal chemistry of hexavalent uranium: polyhedron geometries, bond-valence parameters, and polymerization of polyhedra. *Can. Mineral.* **35**, 1551-1570.

_____, _____ & MILLER, M.L. (1997b): Incorporation mechanisms of actinide elements into the structures of U^{6+} phases formed during the oxidation of spent nuclear fuel. *J. Nucl. Mater.* **245**, 1-9.

_____ & FINCH, R.J. (1999): Wyartite: crystallographic evidence for the first pentavalent-uranium mineral. *Am. Mineral.* **84**, 1456-1460.

_____, _____, HAWTHORNE, F.C., MILLER, M.L. & EWING, R.C. (1997c): The crystal structure of ianthinite, $[U^{4+}_2(UO_2)_4O_6(OH)_4(H_2O)_4](H_2O)_5$: a possible phase for Pu^{4+} incorporation during the oxidation of spent nuclear fuel. *J. Nucl. Mater.* **249**, 199-206.

_____ & HANCHAR, J.M. (1999): The structure of masuyite, $Pb[(UO_2)_3O_3(OH)_2](H_2O)_3$, and its relationship to protasite. *Can. Mineral.* **37**, 1483-1491.

_____ & HAYDEN, L.A. (2002): A uranyl sulfate cluster in $Na_{10}[(UO_2)(SO_4)_4](SO_4)_2 \bullet 3H_2O$. *Acta Crystallogr.* **C58**, i121-i123.

_____ & HILL, F.C. (2000a): Implications of the synthesis and structure of the Sr analogue of curite. *Can. Mineral.* **38**, 175-182.

_____ & _____ (2000b): A new uranyl sheet in $K_5[(UO_2)_{10}O_8(OH)_9](H_2O)$: new insight into sheet anion-topologies. *Can. Mineral.* **38**, 163-174.

_____ & HUGHES, K.-A. (2003): Studtite, $[(UO_2)(O_2)(H_2O)_2](H_2O)_2$: the first structure of a peroxide mineral. *Am. Mineral.* **88**, 1165-1168.

_____, HUGHES KUBATKO, K.-A., SIGMON, G., FRYER, B.J., GAGNON, J.E., ANTONIO, M.R. & SODERHOLM, L. (2005): Actinyl peroxide nanospheres. *Angewandte Chemie International Edition* **44**, 2135-2139.

_____ & LI, YAPING (2002): The structures of becquerelite and Sr-exchanged becquerelite. *Am. Mineral.* **87**, 550-557.

_____, MILLER, M.L. & EWING, R.C. (1996): U^{6+} minerals and inorganic phases: a comparison and hierarchy of structures. *Can. Mineral.* **34**, 845-880.

_____, OLSON, R.A., FINCH, R.J., HANCHAR, J.M. & THIBAULT, Y. (2000): $KNa_3(UO_2)_2(Si_4O_{10})_2(H_2O)_4$, a new compound formed during vapor hydration of an actinide-bearing borosilicate waste glass. *J. Nucl. Mater.* **278**, 290-300.

CAHILL, C.L. & BURNS, P.C. (2000): The structure of agrinierite: a Sr-containing uranyl oxide hydrate mineral. *Am. Mineral.* **85**, 1294-1297.

CHEVALIER, R. & GASPERIN, M. (1968): Structure cristalline de l'oxyde double UNb_3O_{10}. *C.R. Acad. Sci.* **C267**, 481-483.

_____ & _____ (1969): Synthèse en monocristaux et structure cristalline de l'oxyde $UTiNb_2O_{10}$. *C.R. Acad. Sci.* **C268**, 1426-1428.

CHUKANOV, N.V., PUSHCHAROVSKY, D.Y., PASERO, M., MERLINO, S., BARINOVA, A.V., MOCKEL, S., PEKOV, I.V., ZADOV, A.E. & DUBINCHUK, V.T. (2004): Larisaite, $Na(H_3O)(UO_2)_3(SeO_3)_2O_2{\bullet}4H_2O$, a new uranyl selenite mineral from Repete mine, San Juan County, Utah, USA. *Eur. J. Mineral.* **16**, 367-374.

COOPER, M.A. & HAWTHORNE, F.C. (1995): The crystal structure of guilleminite, a hydrated Ba–U–Se sheet structure. *Can. Mineral.* **33**, 1103-1109.

_____ & _____ (2001): Structure topology and hydrogen bonding in marthozite, $Cu^{2+}[(UO_2)_3(SeO_3)_2O_2](H_2O)_8$, a comparison with guilleminite, $Ba[(UO_2)_3(SeO_3)_2O_2](H_2O)_3$. *Can. Mineral.* **39**, 797-807.

CORDFUNKE, E.H.P., VAN VLAANDEREEN, P., ONINK, M. & IJDO, D.J.W. (1991): $Sr_3U_{11}O_{36}$: crystal structure and thermal stability. *J. Solid State Chem.* **94**, 12-18.

CREMERS, T.L., ELLER, P.G., LARSON, E.M. & ROSENZWEIG, A. (1986): Single-crystal structure of lead uranate(VI). *Acta Crystallogr.* **C42**, 1684-1685.

DEBETS, P.C. (1966): The structure of β-UO_3. *Acta Crystallogr.* **21**, 589-593.

_____ (1968): The structures of uranyl chloride and its hydrates. *Acta Crystallogr.* **B24**, 400-402.

DEMARTIN, F., DIELLA, V., DONZELLI, S., GRAMACCIOLI, C.M. & PILATI, T. (1991): The importance of accurate crystal structure determination of uranium minerals. I. Phosphuranylite $KCa(H_3O)_3(UO_2)_7(PO_4)_4O_4{\bullet}8H_2O$. *Acta Crystallogr.* **B47**, 439-446.

_____, GRAMACCIOLI, C.M. & PILATI, T. (1992): The importance of accurate crystal structure determination of uranium minerals. II. Soddyite $(UO_2)_2(SiO_4){\bullet}2H_2O$. *Acta Crystallogr.* **C48**, 1-4.

DICKENS, P.G., STUTTARD, G.P., BALL, R.G.J., POWELL, A.V., HULL, S. & PATAT, S. (1992): Powder neutron diffraction study of the mixed uranium–vanadium oxides $Cs_2(UO_2)_2(V_2O_8)$ and UVO_5. *J. Mater. Chem.* **2**, 161-166.

_____, _____ & PATAT, S. (1993): Structure of CuU_3O_{10}. *J. Mater. Chem.* **3**, 339-341.

DION, C., OBBADE, S., RAEKELBOOM, E., ABRAHAM, F. & SAADI, M. (2000): Synthesis, crystal structure, and comparison of two new uranyl vanadate layered compounds: $M_6(UO_2)_5(VO_4)_2O_5$ with *M* = Na, K. *J. Solid State Chem.* **155**, 342-353.

DURIBREUX, I., DION, C., ABRAHAM, F. & SAADI, M. (1999): $CsUV_3O_{11}$, a new uranyl vanadate with a layered structure. *J. Solid State Chem.* **146**, 258-265.

EVANS, H.T., JR. (1963): Uranyl ion coordination. *Science* **141**, 154-157.

FINCH, R.J., BUCK, E.C., FINN, P.A. & BATES, J.K. (1999a): Oxidative corrosion of spent UO_2 fuel in vapor and dripping groundwater at 90°C. *In* Scientific Basis for Nuclear Waste Management XXII (D.J. Wronkiewicz & J.H. Lee, eds.). *Mater. Res. Soc., Symp. Proc.* **556**, 431-438.

_____, COOPER, M.A., HAWTHORNE, F.C. & EWING, R.C. (1996): The crystal structure of schoepite, $[(UO_2)_8O_2(OH)_{12}](H_2O)_{12}$. *Can. Mineral.* **34**, 1071-1088.

_____, _____, _____ & _____ (1999b): Refinement of the crystal structure of rutherfordine. *Can. Mineral.* **37**, 929-938.

_____ & EWING, R.C. (1992): The corrosion of uraninite under oxidizing conditions. *J. Nucl. Mater.* **190**, 133-156.

FINN, P.A., HOH, J.C., WOLF, S.F., SLATER, S.A. & BATES, J.K. (1996): The release of uranium, plutonium, cesium, strontium, technetium and iodine from spent fuel under unsaturated conditions. *Radiochim. Acta* **74**, 65-71.

FISCHER, A. (2003): Competitive coordination of the uranyl ion by perchlorate and water – the crystal structures of $UO_2(ClO_4)_2{\bullet}3H_2O$, $UO_2(ClO_4)_2{\bullet}5H_2O$ and redetermination of $UO_2(ClO_4)_2{\bullet}7H_2O$. *Z. Anorg. Allg. Chem.* **629**, 1012-1016.

FITCH, A.N., BERNARD, L., HOWE, A.T., WRIGHT, A.F. & FENDER, B.E.F. (1983): The room-temperature structure of $DUO_2AsO_4{\bullet}4D_2O$ by powder neutron diffraction. *Acta Crystallogr.* **C39**, 159-162.

_____ & COLE, M. (1991): The structure of $KUO_2PO_4{\bullet}3D_2O$ refined from neutron and synchrotron-radiation powder diffraction data. *Mater. Res. Bull.* **26**, 407-414.

_____ & FENDER, B.E.F. (1983): The structure of deuterated ammonium uranyl phosphate trihydrate, $ND_4UO_2PO_4{\bullet}3D_2O$ by powder neutron diffraction. *Acta Crystallogr.* **C39**, 162-166.

_____, _____ & WRIGHT, A.F. (1982): The structure of deuterated lithium uranyl arsenate tetrahydrate $LiUO_2AsO_4{\bullet}4D_2O$ by powder neutron diffraction. *Acta Crystallogr.* **B38**, 1108-1112.

FRONDEL, C. (1958): Systematic mineralogy of uranium and thorium. *U.S. Geol. Surv., Bull.* **1064**.

FUJINO, T., MASAKI, N. & TAGAWA, H. (1977): The crystal structures of α and γ-$SrUO_4$. *Z. Kristallogr.* **145**, 299-309.

FULLER, C.C., BARGAR, J.R., DAVIS, J.A. & PIANA, M.J. (2002): Mechanisms of uranium interactions with hydroxyapatite: implications for groundwater remediation. *Env. Sci. Tech.* **36**, 158-165.

GASPERIN, M. (1987a): Synthèse et structure du diborouranate de magnésium, MgB_2UO_7. *Acta Crystallogr.* **C43**, 2264-2266.

_____ (1987b): Synthèse et structure de trois niobouranates d'ions monovalents: $TlNb_2U_2O_{11.5}$, $KNbUO_6$, et $RbNbUO_6$. *J. Solid State Chem.* **67**, 219-224.

_____ (1987c): Synthèse et structure du niobouranate de césium: $CsNbUO_6$. *Acta Crystallogr.* **C43**, 404-406.

_____ (1987d): Synthèse et structure du borouranate de calcium: $CaB_2U_2O_{10}$. *Acta Crystallogr.* **C43**, 1247-1250.

_____ (1987e): Structure du borate d'uranium UB_2O_6. *Acta Crystallogr.* **C43**, 2031-2033.

_____ (1988): Synthèse et structure du borouranate de sodium, $NaBUO_5$. *Acta Crystallogr.* **C44**, 415-416.

_____ (1990): Synthèse et structure du borouranate de lithium $LiBUO_5$. *Acta Crystallogr*. **C46**, 372-374.

_____, REBIZANT, J., DANCAUSSE, J.P., MEYER, D. & COUSSON, A. (1991): Structure de $K_9BiU_6O_{24}$. *Acta Crystallogr*. **C47**, 2278-2279.

GEBERT, E., HOEKSTRA, H.R., REIS, A.H., JR. & PETERSON, S.W. (1978): The crystal structure of lithium uranate. *J. Inorg. Nucl. Chem.* **40**, 65-68.

GESING, T. & RÜSCHER, C.H. (2000): Structure and properties of $UO_2(H_2AsO_4)_2•H_2O$. *Z. Anorg. Allg. Chem.* **626**, 1414-1420.

GINDEROW, D. (1988): Structure de l'uranophane alpha, $Ca(UO_2)_2(SiO_3OH)_2•5H_2O$. *Acta Crystallogr*. **C44**, 421-424.

_____ & CESBRON, F. (1983a): Structure de la derriksite, $Cu_4(UO_2)(SeO_3)_2(OH)_6$. *Acta Crystallogr.* **C39**, 1605-1607.

_____ & _____ (1983b): Structure de la demesmaekerite, $Pb_2Cu_5(SeO_3)_6(UO_2)_2(OH)_6•2H_2O$. *Acta Crystallogr*. **C39**, 824-827.

_____ & _____ (1985): Structure de la roubaultite, $Cu_2(UO_2)_3(CO_3)_2O_2(OH)_2•4H_2O$. *Acta Crystallogr*. **C41**, 654-657.

GLATZ, R.E., LI, YAPING, HUGHES, K.-A., CAHILL, C.L. & BURNS, P.C. (2002): Synthesis and structure of a new Ca uranyl oxide hydrate, $Ca[(UO_2)_4O_3(OH)_4](H_2O)_2$, and its relationship to becquerelite. *Can. Mineral.* **40**, 217-224.

GORBUNOVA, YU.E., LINDE, S.A., LAVROV, A.V. & POBEDINA, A.B. (1980): Synthesis and structure of $Na_{6-x}(UO_2)_3(H_xPO_4)(PO_4)_3$ ($x = 0.5$). *Dokl. Akad. Nauk SSSR* **251**, 385-389 (in Russ.).

GUESDON, A., CHARDON, J., PROVOST, J. & RAVEAU, B. (2002): A copper uranyl monophosphate built up from $[CuO_2]_{\infty}$ chains: $Cu_2UO_2(PO_4)_2$. *J. Solid State Chem.* **165**, 89-93.

HAYDEN, L.A. & BURNS, P.C. (2002a): A novel uranyl sulfate cluster in the structure of $Na_6(UO_2)(SO_4)_4(H_2O)_2$. *J. Solid State Chem*. **163**, 313-318.

_____ & _____ (2002b): The sharing of an edge between a uranyl pentagonal bipyramid and sulfate tetrahedron in the structure of $KNa_5[(UO_2)(SO_4)_4](H_2O)$. *Can. Mineral*. **40**, 211-216.

HILL, F.C. & BURNS, P.C. (1999): Structure of a synthetic Cs uranyl oxide hydrate and its relationship to compreignacite. *Can. Mineral*. **37**, 1283-1288.

HOEKSTRA, H.R. & SIEGEL, S. (1971): Preparation and properties of Cr_2UO_6. *J. Inorg. Nucl. Chem*. **33**, 2867-2873.

HUGHES, K.-A. & BURNS, P.C. (2003a): A new uranyl carbonate sheet in the crystal structure of fontanite, $Ca[(UO_2)_3(CO_3)_2O_2](H_2O)_6$. *Am. Mineral*. **88**, 962-966.

_____ & _____ (2003b): Uranyl nitrate trihydrate, $UO_2(NO_3)_2(H_2O)_3$. *Acta Crystallogr.* **C59**, i7-i8.

_____, _____ & KOLITSCH, U. (2003): The crystal structure and crystal chemistry of uranosphaerite, $Bi(UO_2)O_2OH$. *Can. Mineral*. **41**, 677-685.

HUGHES KUBATKO, K.-A. & BURNS, P.C. (2003): The Rb analogue of grimselite, $Rb_6Na_2[(UO_2)(CO_3)_3]_2(H_2O)$. *Acta Crystallogr.* **C60**, i25-i26.

_____ & _____ (2004): The crystal structure of a novel uranyl tricarbonate, $K_2Ca_3[(UO_2)(CO_3)_3]_2(H_2O)_6$. *Can. Mineral*. **42**, 997-1003.

_____, HELEAN, K.B., NAVROTSKY, A. & BURNS, P.C. (2003): Stability of peroxide-containing uranyl minerals. *Science* **302**, 1191-1193.

IJDO, D.J.W. (1993a): Redetermination of tristrontium uranate. VI. A Rietveld refinement of neutron powder diffraction data. *Acta Crystallogr.* **C49**, 650-652.

_____ (1993b): $Pb_3U_{11}O_{36}$, a Rietveld refinement of neutron powder diffraction data. *Acta Crystallogr*. **C49**, 654-656.

JACKSON, J.M. & BURNS, P.C. (2001): A re-evaluation of the structure of weeksite, a uranyl silicate framework mineral. *Can. Mineral*. **39**, 187-195.

JOVE, J., COUSSON, A. & GASPERIN, M. (1988): Synthesis and crystal structure of $K_2U_2O_7$ and Mössbauer (^{237}Np) studies of $K_2Np_2O_7$ and $CaNpO_4$. *J. Less-Common Metals* **139**, 345-350.

KAPSHUKOV, I.I., VOLKOV, Y.F., MOSKVITSEV, E.P., LEBEDEV, I.A. & YAKOVLEV, G.N. (1971): Crystalline-structure of uranyl tetranitrates. *Zh. Struct. Khim.* **12**, 94-98 (in Russ.).

KHOSRAWAN-SAZEDJ, F. (1982a): The crystal structure of meta-uranocircite II, $Ba(UO_2)_2(PO_4)_2•6H_2O$. *Tschermaks Mineral. Petrogr. Mitt.* **29**, 193-204.

_____ (1982b): On the space group of threadgoldite. *Tschermaks Mineral. Petrogr. Mitt.* **30**, 111-115.

KHRUSTALEV, V.N., ANDREEV, G.B., ANTIPIN, M.YU., FEDOSEEV, A.M., BUDANTSEVA, N.A. & SHIROKOVA, I.B. (2000):

Synthesis and crystal structure of rubidium uranyl dimolybdate $Rb_2UO_2(MoO_4)_2•(H_2O)$. *Zh. Neorg. Khim.* **45**, 1996-1998.

KOBATKO, K.-A. & BURNS, P.C. (2006): A novel arrangement of silicate tetrahedra in the uranyl silicate sheet of oursinite, $(Co_{0.8}Mg_{0.2})[(UO_2)(SiO_3OH)]_2(H_2O)_6$. *Am. Mineral.* **91** (in press).

KOLITSCH, U. & GIESTER, G. (2001): Revision of the crystal structure of ulrichite, $CaCu^{2+}(UO_2)(PO_4)_2•4(H_2O)$. *Mineral. Mag.* **65**, 717-724.

KOSKENLINNA, M, MUTIKAINEN, I., LESKELA, T. & LESKELA, M. (1997): Low-temperature structures and thermal decomposition of uranyl hydrogen selenite monohydrate, $UO_2(HSeO_3)_2•(H_2O)$ and diammonium uranyl selenite hemihydrate, $(NH_4)_2UO_2(SeO_3)_2•0.5(H_2O)$. *Acta Chem. Scand.* **51**, 264-269.

_____ & VALKONEN, J. (1996): Ammonium uranyl hydrogen selenite. *Acta Crystallogr.* **C52**, 1857-1859.

KOSTER, A.S., RENAUD, J.P.P. & RIECK, J.D. (1975): The crystal structures at 20 and 1000°C of bismuth uranate, Bi_2UO_6. *Acta Crystallogr.* **B31**, 127-131.

KOVBA, L.M. (1971): The crystal structure of potassium and sodium monouranates. *Radiokhimiya* **13**, 309-311 (in Russ.).

_____ (1972): Crystal structure of $K_2U_7O_{22}$. *J. Struct. Chem.* **13**, 235-238.

_____, IPPOLITOVA, E.A., SIMANOV, YU P. & SPITSYN, V.I. (1958): The X-ray investigation of uranates of alkali elements. *Dokl. Akad. Nauk. SSSR* **120**, 1042-1044 (in Russ.).

KRAUSE, W., EFFENBERGER, H. & BRANDSTÄTTER, F. (1995): Orthowalpurgite, $(UO_2)Bi_4O_4(AsO_4)_2•2H_2O$, a new mineral from the Black Forest, Germany. *Eur. J. Mineral.* **7**, 1313-1324.

KRIVOVICHEV, S.V. (2004): Combinatorial topology of salts of inorganic oxoacids: zero-, one- and two-dimensional units with corner-sharing between coordination polyhedra. *Crystallogr. Rev.* **10**, 185-232.

_____ & BURNS, P.C. (2000a): Crystal chemistry of uranyl molybdates. I. The structure and formula of umohoite. *Can. Mineral.* **38**, 717-726.

_____ & _____ (2000b): Crystal chemistry of uranyl molybdates. II. The crystal structure of iriginite. *Can. Mineral.* **38**, 847-851.

_____ & _____ (2001a): Crystal chemistry of uranyl molybdates. III. New structural themes in $Na_6[(UO_2)_2O(MoO_4)_4]$, $Na_6[(UO_2)(MoO_4)_4]$ and $K_6[(UO_2)_2O(MoO_4)_4]$. *Can. Mineral.* **39**, 197-206.

_____ & _____ (2001b): Crystal chemistry of uranyl molybdates. IV. The structures of $M_2[(UO_2)_6(MoO_4)_7(H_2O)_2]$ (M = Cs, NH_4). *Can. Mineral.* **39**, 207-214.

_____ & _____ (2002a): Crystal chemistry of rubidium uranyl molybdates: crystal structures of $Rb_6[(UO_2)(MoO_4)_4]$, $Rb_6[(UO_2)_2O(MoO_4)_4]$, $Rb_2[(UO_2)(MoO_4)_2]$, $Rb_2[(UO_2)_2(MoO_4)_3]$ and $Rb_2[(UO_2)_6(MoO_4)_7(H_2O)_2]$. *J. Solid State Chem.* **168**, 245-258.

_____ & _____ (2002b): Crystal chemistry of uranyl molybdates. VI. New uranyl molybdate units in the structures of $Cs_4[(UO_2)_3O(MoO_4)_2(MoO_5)]$ and $Cs_6[(UO_2)(MoO_4)_4]$. *Can. Mineral.* **40**, 201-209.

_____ & _____ (2002c): Crystal chemistry of uranyl molybdates. VII. An iriginite-type sheet of polyhedra in the structure of $[(UO_2)Mo_2O_7(H_2O)_2]$. *Can. Mineral.* **40**, 1571-1578.

_____ & _____ (2002d): Synthesis and structure of $Ag_6[(UO_2)_3O(MoO_4)_5]$: a novel sheet of triuranyl clusters and MoO_4 tetrahedra. *Inorg. Chem.* **41**, 4108-4110.

_____ & _____ (2003a): Geometrical isomerism in uranyl chromates II. Crystal structures of $Mg_2[(UO_2)_3(CrO_4)_5](H_2O)_{17}$ and $Ca_2[(UO_2)_3(CrO_4)_5](H_2O)_{19}$. *Z. Kristallogr.* **218**, 683-702.

_____ & _____ (2003b): Crystal chemistry of uranyl molybdates. VIII. Crystal structures $Na_3Tl_3[(UO_2)(MoO_4)_4]$, $Na_{13-x}Tl_{3+x}[(UO_2)(MoO_4)_3]_4(H_2O)_{6+x}$ (x = 0.1), $Na_3Tl_5[(UO_2)(MoO_4)_3]_2(H_2O)_3$ and $Na_2[(UO_2)(MoO_4)_2](H_2O)_4$. *Can. Mineral.* **41**, 707-719.

_____ & _____ (2003c): Structural topology of potassium uranyl chromates: crystal structures of $K_8[(UO_2)(CrO_4)_4](NO_3)_2$, $K_5[(UO_2)(CrO_4)_3](NO_3)(H_2O)_3$, $K_4[(UO_2)_3(CrO_4)_5](H_2O)_8$ and $K_2[(UO_2)_2(CrO_4)_3(H_2O)_2](H_2O)_4$. *Z. Kristallogr.* **218**, 725-752.

_____ & _____ (2003d): Synthesis and crystal structure of $Li_2[(UO_2)(MoO_4)_2]$, a uranyl molybdate with chains of corner-sharing uranyl square bipyramids and MoO_4 tetrahedra. *Solid State Sci.* **5**, 481-485.

_____ & _____ (2003e): The first sodium uranyl chromate, $Na_4[(UO_2)(CrO_4)_3]$: synthesis and crystal structure determination. *Z Anorg. Allg. Chem.* **629**, 1965-1968.

_____ & _____ (2003f): Geometrical isomerism in uranyl chromates. I. Crystal structures of $(UO_2)(CrO_4)(H_2O)_2$, $[(UO_2)(CrO_4)(H_2O)_2](H_2O)$ and $[(UO_2)(CrO_4)(H_2O)_2]_4(H_2O)_9$. *Z. Kristallogr.* **218**, 568-574.

_____ & _____ (2003g): Crystal chemistry of uranyl molybdates. IX. A novel uranyl molybdate sheet in the structure of $Tl_2[(UO_2)_2O(MoO_5)$. *Can. Mineral.* **41**, 1225-1231.

_____ & _____ (2003h): Crystal chemistry of uranyl molybdates. X. The crystal structure of $Ag_{10}[(UO_2)_8O_8(Mo_5O_{20})]$. *Can. Mineral.* **41**, 1455-1462.

_____ & _____ (2003i): A novel rigid uranyl tungstate sheet in the structures of $Na_2[(UO_2)W_2O_8]$ and α- and β-$Ag_2[(UO_2)W_2O_8]$. *Solid State Sci.* **5**, 373-381.

_____ & _____ (2003j): Combinatorial topology of uranyl molybdate sheets: synthesis and crystal structures of $(C_6H_{14}N_2)_3[(UO_2)_5(MoO_4)_8](H_2O)_4$ and $(C_2H_{10}N_2)[(UO_2)(MoO_4)_2]$. *J. Solid State Chem.* **170**, 106-117.

_____ & _____ (2004a): Synthesis and crystal structure of $Cs_4[UO_2(CO_3)_3]$. *Radiochem.* **46**, 12-15.

_____ & _____ (2004b): Crystal structure of $K[UO_2(NO_3)_3]$ and some features of compounds $M[UO_2(NO_3)_3]$ (M = K, Rb, and Cs). *Radiochem.* **46**, 16-19.

_____ & _____ (2004c): Crystal chemistry of uranyl molybdates. XI. Crystal structures of $Cs_2[(UO_2)(MoO_4)_2]$ and $Cs_2[(UO_2)(MoO_4)_2](H_2O)$. *Can. Mineral.* **43**, 713-720.

_____ & _____ (2004d): Synthesis and crystal structure of $Cu_2[(UO_2)_3((S,Cr)O_4)_5](H_2O)_{17}$. *Radiochem.* **46**, 408-411.

_____ & _____ (2006): The modular structure of the novel uranyl sulfate sheet in $[Co(H_2O)_6]_3[(UO_2)_5(SO_4)_8(H_2O)](H_2O)_5$. *Can. Mineral.* **44** (in press).

_____, Cahill, C.L. & Burns, P.C. (2002a): Syntheses and crystal structures of two topologically related modifications of $Cs_2[(UO_2)_2(MoO_4)_3]$. *Inorg. Chem.* **41**, 34-39.

_____, _____ & _____ (2003): A novel open framework uranyl molybdate: synthesis and structure of $(NH_4)_4[(UO_2)_5(MoO_4)_7](H_2O)_5$. *Inorg. Chem.* **42**, 2459-2464.

_____, Finch, R.J. & Burns, P.C. (2002b): Crystal chemistry of uranyl molybdates. V. Topologically distinct uranyl dimolybdate sheets in the structures of $Na_2[(UO_2)(MoO_4)_2]$ and $K_2[(UO_2)(MoO_4)_2](H_2O)$. *Can. Mineral.* **40**, 193-200.

_____ & Kahlenberg, V. (2005): Synthesis and crystal structure of $Zn_2[(UO_2)_3(SeO_4)_5](H_2O)_{17}$. *J. Alloys Comp.* **389**, 55-60.

_____, _____, Kaindl, R., Mersdorf, E., Tananaev, I.G. & Myasoedov, B.F. (2005b): Nanoscale tubules in uranyl selenates. *Angew. Chem. Int. Ed.* **44**, 1134-1136.

_____, _____, Tananaev, I.G., Kaindl, R., Mersdorf, E. & Myasoedov, B.F. (2005a): Highly porous uranyl selenate nanotubules. *J. Am. Chem. Soc.* **127**, 1072-1073.

_____, Locock, A.J. & Burns, P.C. (2005c): Lone electron pair stereoactivity, cation arrangements and distortion of heteropolyhedral sheets in the structures of $Tl_2[(UO_2)(AO_4)_2]$ (A = Cr, Mo). *Z. Kristallogr.* **220**, 1-9.

Krogh-Andersen, E., Krogh-Andersen, I.G. & Plough-Soerensen, G. (1985): Structure determination of a substance alleged to be hendecahydrogen diuranyl pentaphosphate. *Solid State Protonic Conduct. Fuel Cells Sens., Eur. Workshop on Solid State Mater. Low Medium Temp. Fuel Cells Monit., Spec. Emphasis Proton Conduct.* (J.B. Goodenough, J. Jensen & A. Potier, eds.). Odense University Press, Odense, Denmark (191-202).

Krot, N.N. & Grigoriev, M.S. (2004): Cation–cation interaction in crystalline actinide compounds. *Russ. Chem. Rev.* **73**, 89-100.

Kroto, H.W., Heath, J.R., O'Brien, S C., Curl, R.F. & Smalley, R.E. (1985): C-60-buckminsterfullerene. *Nature* **318**, 162-163.

Kubatko, K.-A. & Burns, P.C. (2006): A novel arrangement of silicate tetrahedra in the uranyl silicate sheet of oursinite, $(Co_{0.8}Mg_{0.2})[(UO_2)(Si_3OH)]_2(H_2O)_6$. *Am. Mineral.* **91** (in press).

_____, Helean, K.B., Navrotsky, A. & Burns, P.C. (2005): Thermodynamics of uranyl minerals: enthalpies of formation of rutherfordine, UO_2CO_3, andersonite, $Na_2CaUO_2(CO_3)_3(H_2O)_5$, and grimselite, $K_3NaUO_2(CO_3)_3H_2O$. *Am. Mineral.* **90**, 1284-1290.

Lee, M.R. & Jaulmes, S. (1987): Nouvelle série d'oxydes derivés de la structure de α-U_3O_8: M^{II} UMo_4O_{16}. *J. Solid State Chem.* **67**, 364-368.

Legros, J.P. & Jeannin, Y. (1975): Coordination de l'uranium par l'ion germanate. II. Structure du germanate d'uranyle dihydraté $(UO_2)_2GeO_4(H_2O)_2$. *Acta Crystallogr.* **B31**, 1140-1143.

Li, Yaping & Burns, P.C. (2000a): Investigations of crystal-chemical variation in lead uranyl oxide hydrates. II. Fourmarierite. *Can. Mineral.* **38**, 737-749.

_____ & _____ (2000b): Investigations of crystal-chemical variability in lead uranyl oxide hydrates. I. Curite. *Can. Mineral.* **38**, 727-735.

_____ & _____ (2000c): Synthesis and crystal structure of a new Pb uranyl oxide hydrate with a framework structure that contains channels. *Can. Mineral.* **38**, 1433-1441.

_____ & _____ (2001a): The structures of two sodium uranyl compounds relevant to nuclear waste disposal. *J. Nucl. Mater.* **299**, 219-226.

_____ & _____ (2001b): The crystal structure of synthetic grimselite, $K_3Na[(UO_2)(CO_3)_3](H_2O)$. *Can. Mineral.* **39**, 1147-1151.

_____ & _____ (2002): New structural arrangements in three Ca uranyl carbonate compounds with multiple anionic species. *J. Solid State Chem.* **166**, 219-228.

_____, _____ & Gault, R.A. (2000): A new rare-earth element uranyl carbonate sheet in the structure of bijvoetite-(Y). *Can. Mineral.* **38**, 153-162.

_____, CAHILL, C.L. & BURNS, P.C. (2001b): Synthesis, structural characterization, and topological rearrangement of a novel open framework U–O material: $(NH_4)_3(H_2O)_2\{[(UO_2)_{10}O_{10}(OH)][(UO_4)(H_2O)_2]\}$. *Chem. Mater.* **13**, 4026-4031.

_____, KRIVOVICHEV, S.V. & BURNS, P.C. (2001a): The crystal structure of $Na_4(UO_2)(CO_3)_3$ and its relationship to schröckingerite. *Mineral. Mag.* **65**, 297-304.

LINDE, S.A., GORBUNOVA, Y.E. & LAVROV, A.V. (1980): Formation of $K_4UO_2(PO_4)_2$ crystals. *Zh. Neorg. Khim.* **25**, 1992-1994 (in Russ.).

_____, _____, _____ & KUZNETSOV, V.G. (1978): Synthesis and structure of crystals of $CsUO_2(PO_3)_3$. *Dokl. Akad. Nauk SSSR* **242**, 1083-1085 (in Russ.).

_____, _____, _____ & POBEDINA, A.B. (1984): The synthesis and structure of crystals of $Na_2UO_2P_2O_7$, sodium uranyl phosphate. *Zh. Neorg. Khim.* **29**, 1533-1537 (in Russ.).

LOCOCK, A.J. & BURNS, P.C. (2002a): The crystal structure of triuranyl diphosphate tetrahydrate. *J. Solid State Chem.* **163**, 275-280.

_____ & _____ (2002b): Crystal structures of three framework alkali metal uranyl phosphate hydrates. *J. Solid State Chem.* **167**, 226-236.

_____ & _____ (2003a): The crystal structure of synthetic autunite, $Ca[(UO_2)(PO_4)]_2(H_2O)_{11}$. *Am. Mineral.* **88**, 240-244.

_____ & _____ (2003b): The structure of hügelite, an arsenate of the phosphuranylite group, and its relationship to dumontite. *Mineral. Mag.* **67**, 1109-1120.

_____ & _____ (2003c): The crystal structure of bergenite, a new geometrical isomer of the phosphuranylite group. *Can. Mineral.* **41**, 91-101.

_____ & _____ (2003d): Crystal structures and synthesis of the copper-dominant members of the autunite and meta-autunite groups: torbernite, zeunerite, metatorbernite and metazeunerite. *Can. Mineral.* **41**, 489-502.

_____ & _____ (2003e): Structures and synthesis of framework Rb and Cs uranyl arsenates and their relationships with their phosphate analogues. *J. Solid State Chem.* **175**, 372-379.

_____ & _____ (2003f): Structures and synthesis of framework triuranyl diarsenate hydrates. *J. Solid State Chem.* **176**, 18-26.

_____, _____ & FLYNN, T.M. (2005): The role of water in the structures of synthetic hallimondite, $Pb_2[(UO_2)(AsO_4)_2](H_2O)_n$ and synthetic parsonsite, $Pb_2[(UO_2)(PO_4)_2](H_2O)_n$, $0 \le n \le 0.5$. *Am. Mineral.* **90**, 240-246.

_____, SKANTHAKUMAR, S., BURNS, P.C. & SODERHOLM, L. (2004): Syntheses, structures, magnetic properties, and X-ray absorption spectra of carnotite-type uranyl chromium(V) oxides: $A[(UO_2)_2Cr_2O_8](H_2O)_n$ (A = K_2, Rb_2, Cs_2, Mg; n = 0, 4). *Chem. Mater.* **16**, 1384-1390.

LOOPSTRA, B.O. (1970): The structure of β-U_3O_8. *Acta Crystallogr.* **B26**, 656-657.

_____ (1977): On the crystal structure of α-U_3O_8. *J. Inorg. Nucl. Chem.* **39**, 1713-1714.

_____ & BRANDENBURG, N.P. (1978): Uranyl selenite and uranyl tellurite. *Acta Crystallogr.* **B34**, 1335-1337.

_____ & CORDFUNKE, E.H.P. (1966): On the structure of α-UO_3. *Rec. Trav. Chim. Pays-Bas* **85**, 135-142.

_____ & RIETVELD, H.M. (1969): The structure of some alkaline-earth metal uranates. *Acta Crystallogr.* **B25**, 787-791.

_____, TAYLOR, J.C. & WAUGH, A.B. (1977): Neutron powder profile studies of the gamma uranium trioxide phases. *J. Solid State Chem.* **20**, 9-19.

MACASKIE, L.E., BONTHRONE, K.M., YONG, PING & GODDARD, D.T. (2000): Enzymically mediated bioprecipitation of uranium by a *Citrobacter sp.*: a concerted role for exocellular lipopolysaccharide and associated phosphatase in biomineral formation. *Microbiology-UK* **146**, 1855-1867.

MAKAROV, E.S. & ANIKINA, L.I. (1963): Crystal structure of umohoite $[UMoO_6(H_2O)_2]\cdot 2H_2O$. *Geochemistry*, 14-21.

_____ & IVANOV, V.I. (1960): The crystal structure of meta-autunite, $Ca(UO_2)_2(PO_4)_2\cdot 6H_2O$. *Dokl. Acad. Sci. USSR* **132**, 601-603.

MARSH, R.E. (1988): On the structure of the series of oxides $M(II)UMo_4O_{16}$. *J. Solid State Chem.* **73**, 577-578.

MAYER, H. & MEREITER, K. (1986): Synthetic bayleyite, $Mg_2[UO_2(CO_3)_3]\cdot 18H_2O$: thermochemistry, crystallography and crystal structure. *Tschermaks Mineral. Petrogr. Mitt.* **35**, 133-146.

MEREITER, K. (1982a): The crystal structure of liebigite, $Ca_2UO_2(CO_3)_3\cdot$ë$11H_2O$. *Tschermaks Mineral. Petrogr. Mitt.* **30**, 277-288.

_____ (1982b): The crystal structure of walpurgite, $(UO_2)Bi_4O_4(AsO_4)_2\cdot 2H_2O$. *Tschermaks Mineral. Petrogr. Mitt.* **30**, 129-139.

_____ (1982c): Die Kristallstruktur des Johannits, $Cu(UO_2)_2(OH)_2(SO_4)_2\cdot 8H_2O$. *Tschermaks Mineral. Petrogr. Mitt.* **30**, 47-57.

_____ (1986a): Crystal structure and crystallographic properties of a schröckingerite from Joachimsthal. *Tschermaks Mineral. Petrogr. Mitt.* **35**, 1-18.

_____ (1986b): Synthetic swartzite, $CaMg[UO_2(CO_3)_3]\cdot 12H_2O$, and its strontium analogue, $SrMg[UO_2(CO_3)_3]\cdot$

$12H_2O$: crystallography and crystal-structures. *Neues Jahrb. Mineral., Monatsh.*, 481-492.

_____ (1986c): Neue kristallographische Daten ueber das Uranmineral Andersonit. *Anz. Oesterr. Akad. Wiss. Math.-Naturwiss. Kl.* **123**(3), 39-41.

_____ (1986d): Structure of strontium tricarbonatodiouranate(VI) octahydrate. *Acta Crystallogr.* **C42**, 1678-1681.

_____ (1986e): Crystal structure refinements of two francevillites, $(Ba,Pb)[(UO_2)_2V_2O_8]\bullet 5H_2O$. *Neues Jahrb. Mineral., Monatsh.*, 552-560.

_____ (1988): Structure of caesium tricarbonatodioxouranate(VI) hexahydrate. *Acta Crystallogr.* **C44**, 1175-1178.

MEUNIER, G. & GALY, J. (1973): Structure cristalline de la schmitterite synthétique $UTeO_5$. *Acta Crystallogr.* **B29**, 1251-1255.

MIJLHOFF, F.C., IJDO, D.J.W. & CORDFUNKE, E.H.P. (1993): The crystal structure of α- and β-$Cs_2U_2O_7$. *J. Solid State Chem.* **102**, 299-305.

MIKHAILOV, YU.N., GORBUNOVA, YU.E., BAEVA, E.E., SEREZHKINA, L.B. & SEREZHKIN, V.N. (2001b): Crystal structure of $Na_2(UO_2(SeO_4)_2)\bullet 4(H_2O)$. *Zh. Neorg. Khim.* **46**, 2017-2021.

_____, _____, KOKH, L.A., KUZNETSOV, V.G., GREVTSEVA, T.G., SOKOL, S.K. & ELLERT, G.V. (1977): Synthesis and crystal structure of potassium trisulfatouranylate $K_4(UO_2(SO_4)_3)$. *Koord. Khim.* **3**, 508-513.

_____, _____, SHISHKINA, O.V., SEREZHKINA, L.B. & SEREZHKIN, V.N. (2001a): Crystal structure of $Cs_2((UO_2)(SeO_4)_2(H_2O))(H_2O)$. *Zh. Neorg. Khim.* **46**, 1828-1832.

MILLER, M.L., FINCH, R.J., BURNS, P.C. & EWING, R.C. (1996): Description and classification of uranium oxide hydrate sheet anion topologies. *J. Mater. Res.* **11**, 3048-3056.

MILLER, S.A. & TAYLOR, J.C. (1986): The crystal structure of saleeite, $Mg[UO_2PO_4]_2\bullet 10H_2O$. *Z. Kristallogr.* **177**, 247-253.

MISTRYUKOV, V.E. & MIKHAILOV, Y.N. (1983): The characteristic properties of the structural function of the selenito-group in the uranyl complex with neutral ligands. *Koord. Khim.* **9**, 97-102 (in Russ.).

MOROSIN, B. (1978): Hydrogen uranyl tetrahydrate, a hydrogen ion solid electrolyte. *Acta Crystallogr.* **B34**, 3732-3734.

MUELLER, M.H., DALLEY, N.K. & SIMONSEN, S.H. (1971): Neutron diffraction study of uranyl nitrate dihydrate. *Inorg. Chem.* **10**, 323-328.

MÜLLER, A., PETERS, F., POPE, M.T. & GATTESCHI, D. (1998): Polyoxometalates: very large clusters – nanoscale magnets. *Chem. Rev.* **98**, 239-271.

MURAKAMI, T., OHNUKI, T., ISOBE, H & SATO, T. (1997): Mobility of uranium during weathering. *Am. Mineral.* **82**, 888-899.

NAZARCHUK, E.V., KRIVOVICHEV, S.V. & BURNS, P.C. (2005a): Crystal structure of $Tl_2[(UO_2)_2(MoO_4)_3]$ and crystal chemistry of the compounds with composition $M_2[(UO_2)_2(MoO_4)_3]$ (M = Tl, Rb, Cs). *Radiochem.* **47**, 447-451.

_____, _____ & _____ (2005b): Crystal structure and thermal transformations of $Ca[(UO_2)_6(MoO_4)_7(H_2O)_2](H_2O)_n$. *Zap. Vseross. Mineral. Obshchest.* (in press).

NIINISTÖ, L., TOIVONEN, J. & VALKONEN, J. (1978): Uranyl (VI) compounds. I. The crystal structure of ammonium uranyl sulfate dihydrate, $(NH_4)_2UO_2(SO_4)_2\bullet 2H_2O$. *Acta Chem. Scand.* **A32**, 647-651.

_____, _____ & _____ (1979): Uranyl (VI) compounds. II. The crystal structure of potassium uranyl sulfate dihydrate $K_2UO_2(SO_4)_2\bullet 2H_2O$. *Acta Chem. Scand.* **A33**, 621-624.

OBBADE, S., DION, C., BEKAERT, E., YAGOUBI, S., SAADI, M. & ABRAHAM, F. (2003c): Synthesis and crystal structure of new uranyl tungstates $M_2(UO_2)(W_2O_8)$ (M = Na, K), $M_2(UO_2)_2(WO_5)O$ (M = K, Rb), and $Na_{10}(UO_2)_8(W_5O_{20})O_8$. *J Solid State Chem.* **172**, 305-318.

_____, _____, DUVIEUBOURG, L., SAADI, M. & ABRAHAM, F. (2003a): Synthesis and crystal structure of α- and β-$Rb_6U_5V_2O_{23}$, a new layered compound. *J. Solid State Chem.* **173**, 1-12.

_____, _____, RIVENET, M., SAADI, M. & ABRAHAM, F. (2004a): A novel open-framework with non-crossing channels in the uranyl vanadates $A(UO_2)_4(VO_4)_3$ (A = Li, Na). *J. Solid State Chem.* **177**, 2058-2067.

_____, _____, SAADI, M. & ABRAHAM, F. (2004b): Synthesis, crystal structure and electrical characterization of $Cs_4[(UO_2)_2(V_2O_7)O_2]$, a uranyl divanadate with chains of corner-sharing uranyl square bipyramids. *J. Solid State Chem.* **177**, 1567-1574.

_____, YAGOUBI, S., DION, C., SAADI, M. & ABRAHAM, F. (2003b): Synthesis, crystal structure and electrical characterization of two new potassium uranyl molybdates $K_2(UO_2)_2(MoO_4)O_2$ and $K_8(UO_2)_8(MoO_5)_2O_6$. *J. Solid State Chem.* **174**, 19-31.

_____, _____, _____, _____ & _____ (2004c): Two new lithium uranyl tungstates $Li_2(UO_2)(WO_4)_2$ and $Li_2(UO_2)_4(WO_4)_4O$ with framework based on the uranophane sheet anion topology. *J. Solid State Chem.* **177**, 1681-1694.

ONDRUŠ, P., SKÁLA, R., VESELOVSKÝ, F., SEJKORA, J. & VITTI, C. (2003): Čejkaite, the triclinic polymorph of $Na_4(UO_2)(CO_3)_3$ – a new mineral from Jachymov, Czech Republic. *Am. Mineral.* **88**, 686-693.

PADEL, L., POIX, P. & MICHEL, A. (1972): Préparation et étude cristallographique du système $Ba_2(UMg)O_6$–$Ba_2(U_{2/3}Fe_{4/3})O_6$. *Rev. Chim. Minérale* **9**, 337-350.

PAGOAGA, M.K., APPLEMAN, D.E. & STEWART, J.M.(1987): Crystal structures and crystal chemistry of the uranyl oxide hydrates becquerelite, billietite, and protasite. *Am. Mineral.* **72**, 1230-1238.

PEARCY, E.C., PRIKRYL, J.D., MURPHY, W.M. & LESLIE, B.W. (1994): Alteration of uraninite from the Nopal I deposit, Peña Blanca District, Chihuahua, Mexico, compared to degradation of spent nuclear fuel in the proposed U.S. high-level nuclear waste repository at Yucca Mountain, Nevada. *Appl. Geochem.* **9**, 713-732.

PERRIN, A. (1976): Structure cristalline du nitrate de dihydroxo diuranyle tétrahydraté. *Acta Crystallogr.* **B32**, 1658-1661.

_____ (1977): Preparation, étude structurale et vibrationnelle des complexes $M_2U_2O_5Cl_4.2H_2O$ (M = Rb, Cs): mise en évidence d'un anion tétranucléaire $[(UO_2)_4O_2Cl_8(H_2O)_2]^{4-}$. *J. Inorg. Nucl. Chem.* **39**, 1169-1172.

_____ & LE MAROUILLE, J.-Y. (1977): Structure cristalline et moléculaire du complexe tétranucléaire $K_2(UO_2)_4O_2(OH)_2Cl_4(H_2O)_6$. *Acta Crystallogr.* **B33**, 2477-2481.

PIRET, P. (1985): Structure cristalline de la fourmariérite, $Pb(UO_2)_4O_3(OH)_4•4H_2O$. *Bull. Minéral.* **108**, 659-665.

_____ & DECLERCQ, J.-P. (1983): Structure cristalline de l'upalite $Al[(UO_2)_3O(OH)(PO_4)_2]•7H_2O$. Un exemple de macle mimétique. *Bull. Minéral.* **106**, 383-389.

_____, _____ & WAUTERS-STOOP, D. (1980): Structure cristalline de la sengiérite. *Bull. Minéral.* **103**, 176-178.

_____ & DELIENS, M. (1982): La vanmeersscheite $U(UO_2)_3(PO_4)_2(OH)_6•4H_2O$ et la méta-vanmeersscheite $U(UO_2)_3(PO_4)_2(OH)_6•2H_2O$, nouveaux minéraux. *Bull. Minéral.* **105**, 125-128.

_____ & _____ (1987): Les phosphates d'uranyle et d'aluminium de Kobokobo. IX. L'althupite $AlTh(UO_2)[(UO_2)_3O(OH)(PO_4)_2]_2(OH)_3•15H_2O$, nouveau minéral; propriétés et structure cristalline. *Bull. Minéral.* **110**, 65-72.

_____, _____ & PIRET-MEUNIER, J. (1988): La françoisite-(Nd), nouveau phosphate d'uranyle et de terres rares; propriétés et structure cristalline. *Bull. Minéral.* **111**, 443-449.

_____, _____, _____ & GERMAIN, G. (1983): La sayrite, $Pb_2[(UO_2)_5O_6(OH)_2]•4H_2O$, nouveau minéral; propriétés et structure cristalline. *Bull. Minéral.* **106**, 299-304.

_____ & PIRET-MEUNIER, J. (1988): Nouvelle détermination de la structure cristalline de la dumontite $Pb_2[(UO_2)_3O_2(PO_4)_2]•5H_2O$. *Bull. Minéral.* **111**, 439-442.

_____, _____ & DECLERCQ, J.-P. (1979): Structure of phuralumite. *Acta Crystallogr.* **B35**, 1880-1882.

_____, _____ & DELIENS, M. (1990): Composition chimique et structure cristalline de la dewindtite $Pb_3[H(UO_2)_3O_2(PO_4)_2]_2•12H_2O$. *Eur. J. Mineral.* **2**, 399-405.

PUSHCHAROVSKY, D. YU, RASTSVETAEVA, R.K. & SARP, H. (1996): Crystal structure of deloryite, $Cu_4(UO_2)[Mo_2O_8](OH)_6$. *J. Alloys Comp.* **239**, 23-26.

REIS, A.H., JR., HOEKSTRA, H.R., GEBERT, E. & PETERSON, S.W. (1976): Redetermination of the crystal structure of barium uranate. *J. Inorg. Nucl. Chem.* **38**, 1481-1485.

RESHETOV, K.V. & KOVBA, L.M. (1966): Structures of $SrUO_{(4-x)}$, $CdUO_{(4-x)}$ and Li_4UO_5. *J. Struct. Chem.* **7**, 589-590.

ROH, Y., LEE, S.R., CHOI, S.-K., ELLESS, M.P. & LEE, S.Y. (2000): Physicochemical and mineralogical characterization of uranium-contaminated soils. *Soil Sed. Contam.* **9**, 463-486.

ROSENZWEIG, A. & RYAN, R.R. (1975): Refinement of the crystal structure of cuprosklodowskite, $Cu[(UO_2)_2(SiO_3OH)_2]•6H_2O$. *Am. Mineral.* **60**, 448-453.

_____ & _____ (1977a): Kasolite, $Pb(UO_2)(SiO_4)•H_2O$. *Cryst. Struct. Commun.* **6**, 617-621.

_____ & _____ (1977b): Vandenbrandeite $CuUO_2(OH)_4$. *Cryst. Struct. Commun.* **6**, 53-56.

ROSS, M. & EVANS, H.T., JR. (1960): The crystal structure of cesium biuranyl trisulfate, $Cs_2(UO_2)_2(SO_4)_3$. *J. Inorg. Nucl. Chem.* **15**, 338-351.

_____ & _____ (1964): Studies of the torbernite minerals. I. The crystal structure of abernathyite and the structurally related compounds $NH_4(UO_2AsO_4)•3H_2O$ and $K(H_3O)(UO_2AsO_4)_2•6H_2O$. *Am. Mineral.* **49**, 1578-1602.

RYAN, R.R. & ROSENZWEIG, A. (1977): Sklodowskite, $MgO•2UO_3•2SiO_2•7H_2O$. *Cryst. Struct. Commun.* **6**, 611-615.

SAADI, M., DION, C. & ABRAHAM, F. (2000): Synthesis and crystal structure of the pentahydrated uranyl orthovanadate $(UO_2)_3(VO_4)_2•5H_2O$, precursor for the new $(UO_2)_3(VO_4)_2$ uranyl-vanadate. *J. Solid State Chem.* **150**, 72-80.

SADIKOV, G.G., KRASOVSKAYA, T.I., POLYAKOV, Y.A. & NIKOLAEV, V.P. (1988): Structural and spectral studies on potassium dimolybdatouranylate. *Inorg. Mater.* **24**, 91-96.

SAINE, M.-C. (1989): Synthèse et structure de KU_2O_7 monoclinique. *J. Less-Common Metals* **154**, 361-365.

SARIN, V.A., LINDE, S.A., FIKIN, L.E., DUDAREV, V.Y. & GORBUNOVA, Y.E. (1983): Neutronographic study of $UO_2H(PO_3)_3$ monocrystals. *Zh. Neorg. Khim.* **28**, 1538-1541 (in Russ.).

SEREZHKIN, V.N., BOIKO, N.V. & MAKAREVICH, L.G. (1980a): The refined crystal-structure of uranyl molybdate. *Kristallografiya* **25**, 858-860 (in Russ.).

_____, _____ & TRUNOV, V.K. (1982): Crystal structure of $Sr[UO_2(OH)CrO_4]_2 \bullet 8H_2O$. *J. Struct. Chem.* **23**, 270-273.

_____, EFREMOV, V.A. & TRUNOV, V.K. (1980b): Crystal structure of alpha-$UO_2MoO_4 \bullet 2H_2O$. *Kristallografiya* **25**, 861-865 (in Russ.).

_____, SOLDATKINA, M.A. & BOIKO, N.V. (1983): Refinement of the crystal-structure $(NH_4)_4[UO_2(CO_3)_3]$. *J. Struct. Chem.* **24**, 770-774.

_____, _____ & EFREMOV, V.A. (1981a): Crystal-structure of the uranyl selenate tetrahydrate. *J. Struct. Chem.* **22**, 451-454.

_____, _____ & _____ (1981b): Crystal-structure of $MgUO_2(SO_4)_2 \bullet 11H_2O$. *J. Struct. Chem.* **22**, 454-457.

_____ & TRUNOV, V.K. (1981): The crystal structure of $UO_2CrO_4 \bullet 5.5H_2O$. *Kristallografiya* **26**, 301-304 (in Russ.).

SEREZHKINA, L.B., TRUNOV, V.K., KHOLODKOVSKAYA, L.N. & KUCHUMOVA, N.V. (1990): Crystal structure of $KUO_2CrO_4(OH) \bullet 1.5(H_2O)$. *Koord. Khimiya* **16**, 1288-1291 (in Russ.).

SHASHKIN, D.P., LUR'E, E.A. & BELOV, N.V. (1974): Crystal-structure of $Na_2[(UO_2)SiO_4]$. *Kristallografiya* **19**, 958-963 (in Russ.).

SHUVALOV, R.R. & BURNS, P.C. (2003): A monoclinic polymorph of uranyl dinitrate trihydrate, $[(UO_2)(NO_3)_2(H_2O)_2] \bullet (H_2O)$. *Acta Crystallogr.* **C59**, i71-i73.

SIEGEL, S., HOEKSTRA, H. & SHERRY, E. (1966): The crystal structure of high-pressure UO_3. *Acta Crystallogr.* **20**, 292-295.

_____ & _____ (1968): The crystal structure of copper uranium tetroxide. *Acta Crystallogr.* **B24**, 967-970.

_____, _____ & GEBERT, E. (1972b): The structure of γ-uranyl dihydroxide, $UO_2(OH)_2$. *Acta Crystallogr.* **B28**, 3469-3473.

_____, VISTE, A., HOEKSTRA, H.R. & TANI, B.S. (1972a): The structure of hydrogen triuranate. *Acta Crystallogr.* **B28**, 117-121.

STERNS, M., PARISE, J.B. & HOWARD, C.J. (1986): Refinement of the structure of trilead(II) uranate(VI) from neutron powder diffraction data. *Acta Crystallogr.* **C42**, 1275-1277.

SULLENS, T.A., JENSEN, R.A., SHVAREVA, T.Y. & ALBRECHT-SCHMITT, T.E. (2004): Cation–cation interactions between uranyl cations in a polar open-framework uranyl periodate. *J. Am. Chem. Soc.* **126**, 2676-2677.

SWIHART, G.H., GUPTA, P.K.S., SCHLEMPER, E.O., BACK, M.E. & GAINES, R.V. (1993): The crystal structure of moctezumite $[PbUO_2](TeO_3)_2$. *Am. Mineral.* **78**, 835-839.

SYKORA, R.E. & ALBRECHT-SCHMITT, T.E. (2003): Self-assembly of a polar open-framework uranyl vanadyl hexaoxoiodate(VII) constructed entirely from distorted octahedral building units in the first uranium hexaoxoiodate: $K_2[(UO_2)_2(VO)_2(IO_6)_2O] \bullet H_2O$. *Inorg. Chem.* **42**, 2179-2181.

_____ & _____ (2004): Hydrothermal synthesis and crystal structure of $Cs_4[(UO_2)_4(W_5O_{21})(OH)_2(H_2O)_2]$: a new polar uranyl tungstate. *J. Solid State Chem.* **177**, 3729-3734.

_____, KING, J.E., ILLIES, A.J. & ALBRECHT-SCHMITT, T.E. (2004a): Hydrothermal synthesis, structure, and catalytic properties of $UO_2Sb_2O_4$. *J. Solid State Chem.* **177**, 1717-1722.

_____, MCDANIEL, S.M., WELLS, D.M. & ALBRECHT-SCHMITT, T.E. (2002a): Mixed-metal uranium(VI) iodates: hydrothermal syntheses, structures, and reactivity of $Rb[UO_2(CrO_4)(IO_3)(H_2O)]$, $A_2[UO_2(CrO_4)(IO_3)_2]$ (A = K, Rb, Cs), and $K_2[UO_2(MoO_4)(IO_3)_2]$. *Inorg. Chem.* **41**, 5126-5132.

_____, WELLS, D.M. & ALBRECHT-SCHMITT, T.E. (2002b): Hydrothermal synthesis and structure of a new one-dimensional, mixed–metal U(VI) iodate, $Cs_2[(UO_2)(CrO_4)(IO_3)_2]$. *Inorg. Chem.* **41**, 2304-2306.

TABACHENKO, V.V., BALASHOV, V.L., KOVBA, L.M. & SEREZHKIN, V.N. (1984a): Crystal-structure of barium molybdate-uranylate $Ba(UO_2)_3(MoO_4)_4.4H_2O$. *Koord. Khim.* **10**, 854-857 (in Russ.).

_____, KOVBA, L.M. & SEREZHKIN, V.N. (1979): Crystal structure of manganese sulfatouranylate $MnUO_2(SO_4)_2(H_2O)_5$. *Koord. Khim.* **5**, 1563-1568.

_____, _____ & _____ (1983): The crystal structure of molybdatouranylates of magnesium and zinc of composition $M(UO_2)_3(MoO_4)_4(H_2O)_8$ (M = Mg,Zn). *Koord. Khim.* **9**, 1568-1571 (in Russ.).

_____, _____ & _____ (1984b): Crystal structure of $Mg(UO_2)_6(MoO_4)_7 \bullet 18H_2O$ and $Sr(UO_2)_6(MoO_4)_7 \bullet 15H_2O$. *Koord. Khim.* **10**, 558-562 (in Russ.).

_____, SEREZHKIN, V.I., SEREZHKINA, L.B. & KOVBA, L.M. (1979): Crystal structure of manganese sulfatouranylate $MnUO_2(SO_4)_2 \bullet 5H_2O$. *Koord. Khim.* **5**, 1563-1568 (in Russ.).

TALI, R., TABACHENKO, V.V. & KOVBA, L.M. (1993): Crystal structure of $Cu_4UO_2(MoO_4)_2(OH)_6$. *Zh. Neorg. Khim.* **38**, 1450-1452 (in Russ.).

TANCRET, N., OBBADE, S. & ABRAHAM, F. (1995): Ab initio structure determination of uranyl divanadate $(UO_2)_2V_2O_7$ from powder X-ray diffraction data. *Eur. J. Solid State Inorg. Chem.* **32**, 195-207.

TAYLOR, J.C. (1971): The structure of the α form of uranyl hydroxide. *Acta Crystallogr*. **B27**, 1088-1091.

_____ & BANNISTER, M.J. (1972): A neutron diffraction study of the anisotropic thermal expansion of β-uranyl dihydroxide. *Acta Crystallogr*. **B28**, 2995-2999.

_____ & MUELLER, M.H. (1965): A neutron diffraction study of uranyl nitrate hexahydrate. *Acta Crystallogr.* **19**, 536-543.

_____ & WILSON, P.W. (1974): The structure of uranyl chloride monohydrate by neutron diffraction and the disorder of the water molecule. *Acta Crystallogr*. **B30**, 169-175.

TUTOV, A.G., PLAKHTII, V.P., USOV, O.A., BUBLYAEV, R.A. & CHERNENKOV, YU P. (1991): Neutron-diffraction refinement of the structure of a nonlinear optical-crystal of dicesiumuraniltetrachloride $Cs_2UO_2Cl_4$. *Kristallografiya* **36**, 1135-1138 (in Russ.).

VAN DER PUTTEN, N. & LOOPSTRA, B.O. (1974): Uranyl sulphate UO_2SO_4•2½H_2O. *Cryst. Struct. Commun.* **3**, 377-380.

VAN DUIVENBODEN, H.C. & IJDO, D.J.W. (1986): Redetermination of tricalcium uranate(VI). A Rietveld refinement of neutron powder diffraction data. *Acta Crystallogr.* **C42**, 523-525.

VAN EGMOND, A.B. (1976a): Investigations on cesium uranates. V. The crystal structures of Cs_2UO_4, $Cs_4U_5O_{17}$, $Cs_2U_7O_{22}$ and $Cs_2U_{15}O_{46}$. *J. Inorg. Nucl. Chem.* **38,** 1649-1651.

_____ (1976b): Investigations on cesium uranates. VI. The crystal structures of $Cs_2U_2O_7$. *J. Inorg. Nucl. Chem.* **38**, 2105-2107.

VISWANATHAN, K. & HARNEIT, O. (1986): Refined crystal structure of β-uranophane $Ca(UO_2)_2(SiO_3OH)_2$•$5H_2O$. *Am. Mineral.* **71**, 1489-1493.

VOCHTEN, R., VAN HAVERBEKE, L., VAN SPRINGEL, K., BLATON. N. & PEETERS, O.M. (1995): The structure and physicochemical characteristics of synthetic zippeite. *Can. Mineral.* **33**, 1091-1101.

WANG, XIQU, HUANG, JIN, LIU, LUMEI & JACOBSON, A.J. (2002): The novel open-framework uranium silicates $Na_2(UO_2)(Si_4O_{10})$•2.1(H_2O) (USH–1) and $RbNa(UO_2)(Si_2O_6)$•(H_2O) (USH–3). *J. Mater. Chem.* **12**, 406-410.

WELLER, M.T., DICKENS, P.G. & PENNY, D.J. (1988): The structure of δ-UO_3. *Polyhedron* **7**, 243-244.

_____, LIGHT, M.E. & GELBRICH, T. (2000): Structure of uranium(VI) oxide dihydrate, UO_3•$2H_2O$; synthetic meta-schoeptite $(UO_2)_4O(OH)_6$•$5H_2O$. *Acta Crystallogr.* **B56**, 577-583.

WOLF, R. & HOPPE, R. (1985): Neues über Oxouranate: über α-Li_6UO_6. Mit einer Bemerkung über β-Li_6UO_6. *Z. Anorg. Allg. Chem.* **528**, 129-137.

_____ & _____ (1986): Neues über Oxouranate (VI): Na_4UO_5 und K_4UO_5. *Rev. Chim. Minérale* **23**, 828-848.

_____ & _____ (1987): Ein neues Oxouranat (VI): $K_2Li_4[UO_6]$. Mit einer Bemerkung über $Rb_2Li_4[UO_6]$ und $Cs_2Li_4[UO_6]$. *Z. Anorg. Allg. Chem.* **554**, 34-42.

WRONKIEWICZ, D.J., BATES, J.K., GERDING, T.J., VELECKIS, E. & TANI, B.S. (1992): Uranium release and secondary phase formation during unsaturated testing of UO_2 at 90°C. *J. Nucl. Mater.* **190**, 107-127.

_____, _____, WOLF, S.F. & BUCK, E.C. (1996): Ten-year results from unsaturated drip tests with UO_2 at 90°C: implications for the corrosion of spent nuclear fuel. *J. Nucl. Mater.* **238**, 78-95.

YAMAKAWA, I. & TRAINA, S.J. (2001): Precipitation processes of uranium in highly alkaline solutions: possible chemical reactions occurring in the Hanford vadose zone. *Am. Chem. Soc.* **222**, 55-GEOC Part 1 (abstr.).

YAMASHITA, T., FUJINO, T., MASAKI, N. & TAGAWA, H. (1981): The crystal structures of α- and β-$CdUO_4$. *J. Solid State Chem.* **37**, 133-139.

ZALKIN, A., RUBEN, H. & TEMPLETON, D.H. (1978): Structure of a new uranyl sulfate hydrate, α-$2UO_2SO_4$•$7H_2O$. *Inorg. Chem.* **17**, 3701-3702.

_____, TEMPLETON, L.K. & TEMPLETON, D.H. (1989): Structure of rubidium uranyl(VI) trinitrate. *Acta Crystallogr*. **C45**, 810-811.

Received January 24, 2005, revised manuscript accepted June 7, 2005.